Distribution Agreement

In presenting this thesis or dissertation as a partial fulfillment of the requirements for an advanced degree from Emory University, I hereby grant to Emory University and its agents the non-exclusive license to archive, make accessible, and display my thesis or dissertation in whole or in part in all forms of media, now or hereafter known, including display on the world wide web. I understand that I may select some access restrictions as part of the online submission of this thesis or dissertation. I retain all ownership rights to the copyright of the thesis or dissertation. I also retain the right to use in future works (such as articles or books) all or part of this thesis or dissertation.

Signature:

DocuSigned by:
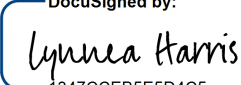
Lynnea Harris
1347CCEB5E5D4C5...

Lynnea Harris
Name

3/22/2023 | 11:17 AM EDT
Date

Title	GluN2B-Selective NMDA Receptor Negative Allosteric Modulation as a Treatment for Chronic Pain and Opioid Tolerance

Author	Lynnea Harris
Degree	Doctor of Philosophy

Program	Biological and Biomedical Sciences
	Molecular and Systems Pharmacology

Approved by the Committee

Dennis Liotta

Advisor

Gereau, Robert

Committee Member

Shannon Gourley

Committee Member

John Hepler

Committee Member

Stephen Traynelis

Committee Member

Accepted by the Laney Graduate School

Kimberly Jacob Arriola, PhD, MPH

Dean, James T. Laney School of Graduate Studies

GluN2B-Selective NMDA Receptor Negative Allosteric Modulation as a Treatment for Chronic Pain and Opioid Tolerance

By

Lynnea D. Harris

B.S., Furman University, 2016

Advisor: Dennis C. Liotta, Ph.D.

An abstract of

A dissertation submitted to the Faculty of the James T. Laney of Graduate Studies of Emory University in partial fulfillment of the requirements for the degree of Doctor of Philosophy in Molecular and Systems Pharmacology

2023

Abstract

GluN2B-Selective NMDA Receptor Negative Allosteric Modulation as a Treatment for Chronic Pain and Opioid Tolerance

By: Lynnea D. Harris

Drug overdose is the leading cause of accidental death in the US. From April 2021 to April 2022, there were over 100,000 new cases — an increase of nearly 30% compared to the previous year. The majority of these cases involved use of an opioid. Opioids are sought after for their profound analgesic properties, however their utility is significantly hindered by adverse off-target effects including addiction, physical dependence, and tolerance. Analgesic tolerance to opioids is characterized by a decrease in the efficacy of an opioid over time with repeated use. Tolerance requires increasingly higher doses of the opioid to maintain suitable analgesia and can lead to overdose. Persistent activation of NMDA receptors is a key mechanism in the development of tolerance. Additionally, the NMDA receptors which contain the GluN2B subunit are of particular interest in this mechanism. Here, we have introduced a novel GluN2B-selective negative allosteric modulator of the NMDA receptor, EU93-108, and evaluated its effects on pain and tolerance in mice. EU93-108 is potent and brain penetrant, and possesses analgesic properties in allodynia and thermal nociception rodent pain models. The compound also produces a significant enhancement effect whereby morphine, when combined with EU93-108, produces stronger thermal antinociception compared to that of morphine alone. These results suggest that GluN2B negative modulation has utility in the treatment of chronic pain and tolerance. Further structure-activity relationship work around this compound could give rise to compounds that can function as analgesic adjuvant therapeutics to diminish the onset of tolerance due to chronic opioid use.

GluN2B-Selective NMDA Receptor Negative Allosteric Modulation as a Treatment for Chronic Pain and Opioid Tolerance

By

Lynnea D. Harris

B.S., Furman University, 2016

Advisor: Dennis C. Liotta, Ph.D.

A dissertation submitted to the Faculty of the James T. Laney of Graduate Studies of Emory University in partial fulfillment of the requirements for the degree of Doctor of Philosophy in Molecular and Systems Pharmacology

2023

Table of Contents

List of Illustrations

      Figures

      Tables

      Schemes

      List of Abbreviations

Chapter 1: Background and Overview of Pathological Pain, Opioids, Analgesic Tolerance, and NMDAR Allosteric Modulation

Chapter 2: Novel GluN2B-Selective NMDA Receptor Negative Allosteric Modulator Possesses Intrinsic Analgesic Properties and Enhances Analgesia of Morphine in Rodent Pain Models

List of Illustrations   **Page**

List of Figures

List of Tables

List of Schemes

<u>Chapter 2:</u>

List of Abbreviations

IASP: International Association for the Study of Pain
TRP: transient receptor potential cation channel
ASIC: acid sensing channel
Nav: voltage-gated sodium channel
ATP: adenosine triphosphate
SA1: slowly adapting type 1 mechanoreceptor
GABA: gamma-aminobutyric acid
fMRI: functional magnetic resonance imaging
PAG: periaqueductal gray
NAc: nucleus accumbens
CBT: cognitive behavioral therapy
ACT: acceptance and commitment therapy
NSAIDs: non-steroidal anti-inflammatory drugs
TM: transmembrane domain
GPCR: G protein-coupled receptor
CNS: central nervous system
MOR: mu opioid receptor
KOR: kappa opioid receptor
DOR: delta opioid receptor
GDP: guanosine diphosphate
GTP: guanosine triphosphate
cAMP: cyclic adenosine monophosphate
GIRK: G protein-coupled inwardly rectifying potassium channel
DRG: dorsal root ganglion
GRK: G protein-coupled receptor kinase

DA: dopamine
VTA: ventral tegmental area
DAMGO: (D-Ala(2)-mephe(4)-gly-ol(5))enkephalin
AMPAR: α-amino-3-hydroxy-5-methyl-4-isoxazolepropionic acid
NMDAR: N-methyl-D-Aspartate receptor
KO: knockout
WT: wild type
CFA: complete Freund's adjuvant
PMA: phorbol 12-myristate 13-acetate
SNL: spinal nerve ligation
MAPK: mitogen-activated protein kinase
RVM: rostro ventromedial medulla
mIPSC: miniature inhibitory post-synaptic currents
RGS: regulator of G protein signaling
PKC: protein kinase C
JNK: c-Jun N-terminal kinase
ERK: extracellular signal-regulated kinase
iGluR: ionotropic glutamate receptor
ATD: amino terminal domain
LBD: ligand binding domain
TMD: transmembrane domain
CTD: C terminal domain
EC_{50}: effective concentration 50%
FDA: Food and Drug Administration
PCP: phencyclidine
IC_{50}: inhibitory concentration 50%
LTP: long-term potentiation
AP5: D-2-amino-5-phosphonopentanoate
NBQX: 2,3-dioxo-6-nitro-7-sulfamoyl-benzo[f]quinoxaline
CaMKII: calcium/calmodulin-dependent protein kinase 2
NAM: negative allosteric modulator
ER: endoplasmic reticulum
SEM: standard error of the mean
CI: confidence interval
ANOVA: analysis of variance
RMSD: root mean square deviation
PDB: protein data bank
DMSO: dimethyl sulfoxide
PEG: polyethylene glycol
DMA: dimethyl acetamide
TIT: tail immersion test
CYP: cytochrome P450 enzyme
UGT: uridine 5'-diphospho-glucuronosyltransferase
SAR: structure-activity relationship
LMNG: lauryl maltose neopentyl glycol
HEPES: 4-(2-hydroxyethyl)-1-piperazineethanesulfonic acid

K-EDTA: Potassium ethylenediaminetetraacetic acid
LC-MS/MS: liquid chromatography-mass spectrometry/mass spectrometry
NIMH: National Institute of Mental Health
PDSP: Psychoactive Drug Screening Program
MCAA: mechanical conflict aversion apparatus

Chapter 1: Background and Overview of Pathological Pain, Opioids, Analgesic Tolerance, and NMDAR Allosteric Modulation

1.1 Overview of Beneficial and Pathological Pain

The International Association for the Study of Pain (IASP) defines pain as "an unpleasant sensory and emotional experience associated with, or resembling that associated with, actual or potential tissue damage"[1]. The ability to perceive pain has always been necessary for human survival. Pain is beneficial for avoiding poisons and toxins, avoiding danger, and alerting us to damage or malfunction in our bodies. The sensation of pain in general is not harmful; however, unregulated, unrelenting or idiopathic pain does not serve a beneficial purpose. It is no longer a symptom of injury or disease, rather it is a pathological condition in its own right that diminishes quality of life and requires treatment[2]. There are many ways to conceptualize pain, but for this discussion we will describe pain in four main components: nociception, perception, suffering, and pain behavior. All four components have anatomical, physiological, and psychological substrates, and are useful for categorizing the many types of pain.

Nociception[3] is the process of detecting tissue damage. The damage is detected by nociceptors. These nociceptors transduce the stimulus into an electrical signal which then travels to the brain via Aδ- and C-type nerve fibers. Nociceptors can be specialized to detect chemical, thermal, or mechanical stimuli, or combinations of these.

Perception of pain[3] is most frequently generated by tissue damage or disease, but it can also be triggered by lesions to the central or peripheral nervous systems. In the latter case, the nerves themselves have suffered damage and this can happen in the absence of an external stimulus. In other words, perception of pain can occur with or without nociception. Stroke, spinal

cord injury or autoimmune diseases are a few examples of disease states that are associated with nerve damage. Unlike pain from tissue damage, pain associated with nerve lesions is not responsive to analgesics such as acetaminophen or morphine[4].

Suffering can be defined as the emotional or psychological aspect of pain sensation. It is the negative response elicited not only by the pain itself, but by the stress, anxiety and/or fear caused by the pain.

Pain behaviors[3] are all of the various ways humans express pain or discomfort. These behaviors can include verbalizing the pain (*e.g.,* saying "ouch"), laying down or staying home from work, facial grimacing, or seeking medical attention.

1.1.1 Neurocircuitry Underlying Pain

The IASP has provided a robust definition of pain which has been widely accepted since 1979 (see above section), but this definition does not convey the full biological complexity underlying pain and its circuitry.

Pain originates from a wide array of peripheral sensors that detect nociceptive input from peripheral tissues and from the outside world. These nociceptive stimuli can be inflammatory, neuropathic, or nociceptive in nature. These sensors then transmit nociceptive signals to a series of neural circuits in the spinal cord dorsal horn. Nociceptive neurons in the dorsal horn innervate several regions of the brain, which produces the landscape of emotions, behaviors, and sensations that we have come to associate with pain[5].

As mentioned briefly in the previous section, nociceptive primary sensory neurons are categorized as Aδ or C fibers. Aβ fibers are also involved, but to a lesser extent. Aδ fibers are

myelinated and mediate quick and sharp pain sensations, particularly mechanical or mechanothermal stimuli. C fibers are unmyelinated and mediate dull and radiating pain sensations. C fibers are classified as polymodal because they can respond to thermal, mechanical or chemical stimuli. Myelinated fibers possess a higher conduction velocity than unmyelinated fibers and are therefore able to transmit pain signals at a faster rate. These fibers innervate the skin, deep tissues, and internal organs, and they respond to noxious mechanical, chemical, or thermal stimuli through the activation of sensory transducers. These transducers are ion channels that facilitate the conversion of noxious stimuli to an electrochemical signal that can be transmitted to the brain in a process called transduction[6,7].

There are three main aspects of pain transduction: transmission, modulation, and perception[8]. Transmission is the process of relaying information from the noxious stimulus from the site of injury to the brain. Modulation is the "checks and balances" system which acts to reduce transmission. Finally, perception is referred to as the subjective awareness of pain. It is the end result of the brain synthesizing and making sense of all of the sensory input from the initial injury. Perception also includes several aspects involved in the subjective experience of pain, including attention, expectation, and interpretation[8].

Ion channels involved in transduction include families of transient receptor potential cation channels (TRP), particularly the heat-sensing transient receptor potential channel vanilloid 1 (TRPV1), and acid sensing ion channels (ASICs).

Transient receptor potential (TRP) channels are a broad class of ion channels composed of 28 isoforms divided into six subfamilies: canonical (TRPC), vanilloid (TRPV), ankyrin (TRPA), melastatin (TRPM), polycystin (TRPP), and mucolipin (TRPML)[9]. TRP channels are involved in many physiological processes ranging from taste or visual transduction to pheromone signaling to

muscle contraction[10–12]. The main isoforms involved in transduction are TRPV1, TRPV3, TRPA1, and TRPM8[13,14].

TRPV1 was discovered in 1997[15] and is the most well-characterized member of the TRPV family. TRPV1 is preferentially expressed within peripheral sensory neurons including laminae I and II of the spinal cord dorsal horn[16] as well as neurons in the dorsal root ganglia, trigeminal ganglia, and nodal ganglia[17]. It is also expressed at lower levels in nerve fibers that innervate the bladder[18], lungs[19], and upper respiratory tract[20]. TRPV1 is activated by noxious heat (>42C), acidity and molecules like the vallinoid capsaicin which is why it is also called the capsaicin receptor[21]. Following a skin lesion, a wide array of pro-inflammatory molecules are released including bradykinin, prostaglandins, substance P, leukotrienes, histamine, serotonin, thromboxanes, adenosine and ATP, platelet-activating factor, protons and free radicals[17]. All of these molecules sensitize TRPV1 channels, lowering the threshold for activation.

TRPV3 channels are expressed in keratinocytes[22] and in dorsal root ganglia and trigeminal ganglia neurons[23]. TRPV3 channels respond to warm heat as opposed to noxious heat (>33C)[21,22]. TRPV1 and TRV3 channels share significant homology, and both show increased activity in response to noxious heat. However, unlike TRPV1, TRPV3 does not respond to acidity or capsaicin[21]. TRPA1 channels are sensitive to thermal, mechanical and chemical stimuli[24]. Kremeyer *et al.* found that a gain-of-function mutation in TRPA1 produces a 5-fold increase in inward current at resting potential. This finding was subsequently shown to be the pathogenesis of Familial Episodic Pain syndrome, characterized by episodes of severe pain localized to the upper body[25]. TRPA1 channels are located on neurons and on non-neuronal cells such as keratinocytes[22], endothelial cells and fibroblasts, but their utility in these cell types is less understood. TRPM8

channels, expressed in cutaneous fibers, respond to noxious cold and are the principal receptors responsible for cold pain transduction[26–28].

Acid-sensing ion channels (ASICs) are proton-induced sodium channels that are expressed in free nerve endings and somatosensory organs[29,30]. ASICs respond to changes in pH[13] and are associated with various disease states such as epilepsy[31], migraine[32], depression[33], and neuropathic pain[34]. Only two isoforms, ASIC3 and ASIC1b, are involved in acidic nociception (*e.g,.* ischemia- or inflammation-related pain)[35].

Voltage-gated sodium (Nav) channels are primarily involved in the transition from pain transduction to transmission. Activation of TRP channels and ASICs generates a potential that is sufficient to depolarize Nav channels, leading to an action potential[13]. Nine isoforms have been identified (Nav1.1 – 1.9), but 1.3, 1.7, 1.8 and 1.9 are the isoforms most important for pain transduction[36,37]. Nav channels are expressed in the soma of dorsal root ganglion neurons[38] as well as free nerve endings in the periphery[39]. For example, 1.6, 1.7, 1.8 and 1.9 are expressed in epithelial nerve endings[39]. Other Nav channels are expressed in skeletal and cardiac muscle, the cerebellum, and the cerebral cortex[37].

Neurons are not the only cells involved in transduction of pain signals from the periphery. Certain epithelial cell types such as Merkel cells or keratinocytes interact with peripheral fibers and are implicated as sensory transduction modulators. For example, Merkel cells make up the epidermal end of slowly adapting type 1 (SA1) mechanoreceptors which facilitate the recognition of edges and textures. Depolarization of Merkel cells directly activates SA1 fibers[40]. Keratinocytes also directly contribute to nociceptive transduction. Activation of channelrhodopsin or TRPV1

channels ectopically expressed by keratinocytes in mice induced action potential firing in sensory neurons, neuronal activity in the spinal cord, and pain-like behaviors in mice[41,42].

Pain transduction is also regulated by a series of inhibitory mechanisms working in parallel with the excitatory mechanisms discussed. When an injury occurs, endogenous opioid peptides are released and interact with peripheral nociceptors that express opioid receptors[43,44] and/or other anti-inflammatory mediators[45]. Inhibition is mediated in the spinal cord via release of endogenous opioids or gamma-aminobutyric acid (GABA) from interneurons which reduce excitatory transmission by activating presynaptic opioid or GABA receptors expressed in nociceptors. Additionally, opioids and GABA can open postsynaptic K^+ or Cl^- channels, evoking inhibitory potentials in dorsal horn neurons[46–48]. If nociceptive stimulation continues, spinal interneurons increase opioid production by upregulating gene expression[49,50]. Other inhibitory (or descending) pathways, particularly serotonergic and noradrenergic pathways, are also activated.

The spinal cord dorsal horn is the primary locus for integration of peripheral sensory input and pain modulation[13,51–53]. The dorsal horn contains six Rexed laminae which are innervated by primary sensory neurons. Aδ and C mostly innervate outer laminae I and II which are activated by noxious stimuli. The inner laminae are more sensitive to innocuous touch. The dorsal horn also contains a large interneuron population that is primarily excitatory while approximately 25% are inhibitory[13]. Projection neurons, which are responsible for relaying information about pain to higher brain centers, are also located in the dorsal horn across laminae I, III, IV and V.
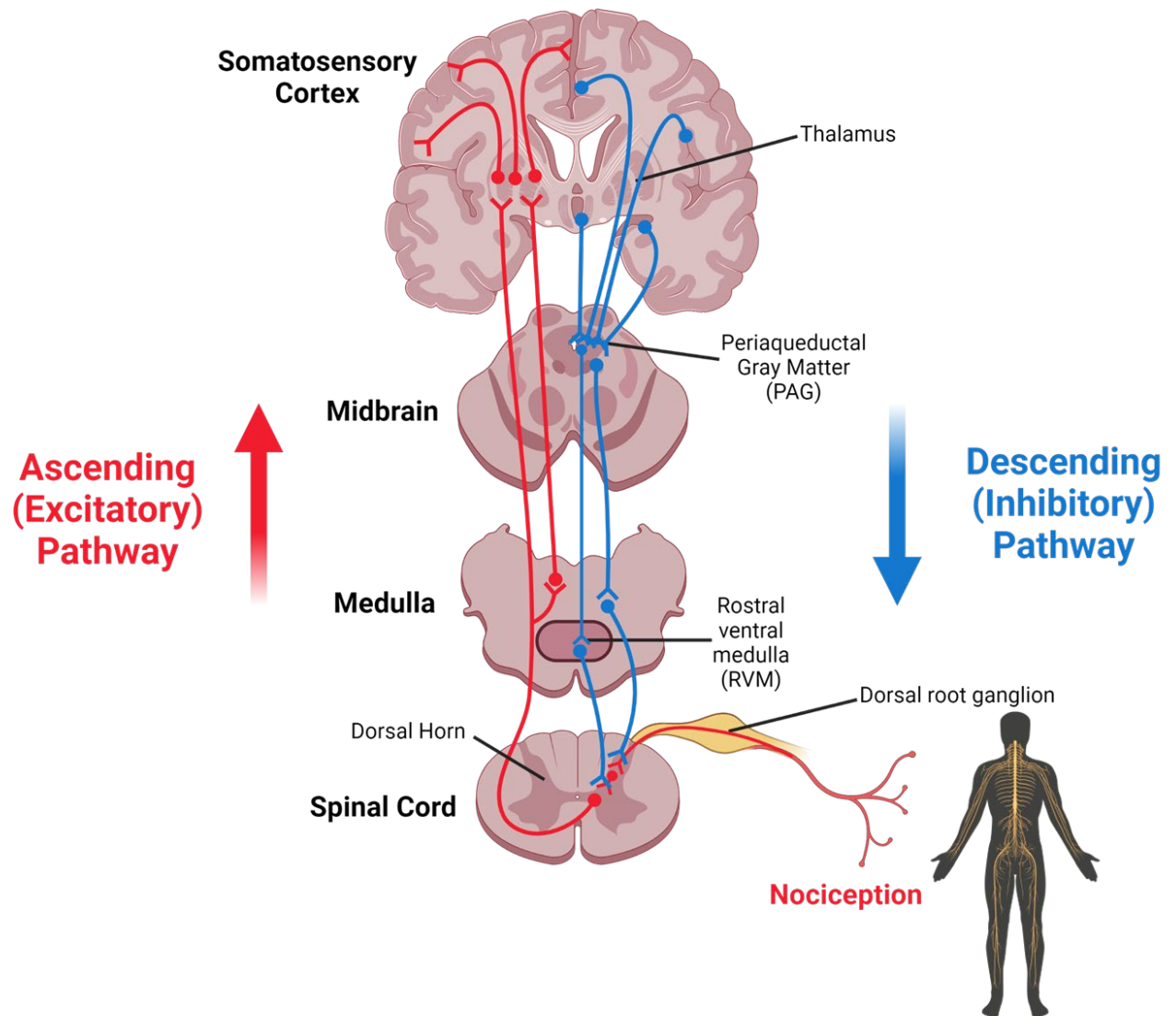
Figure 1. Brain regions involved in processing nociceptive input. The figure depicts the ascending and descending pain modulatory pathways. Ascending: Nociceptive input is transmitted from the site of injury to the dorsal horn of the spinal cord, then up the spinothalamic tract to the thalamus and somatosensory cortex. Descending: nociceptive input is transmitted from the thalamus and somatosensory cortex to the periaqueductal gray matter (PAG), then to the rostroventral medulla (RVM), then finally back to the dorsal horn.

Functional magnetic resonance imaging (fMRI) studies in humans have identified several brain regions **(Figure 1)** where coordinated activation occurs in response to noxious somatic and visceral stimuli. First, primary afferent neurons engage motor and autonomic spinal and brainstem circuits to trigger reflexive behaviors[54,55]. This works to limit exposure to the nociceptive stimuli. These afferent neurons also synapse onto second-order neurons in the trigeminal nucleus caudalis and the spinal cord dorsal horn. The second-order neurons then project onto the lateral parabrachial nucleus and the periaqueductal gray (PAG), which innervate the somatosensory, anterior cingulate, insular, and prefrontal cortices, nucleus accumbens (NAc), hypothalamus, medial thalamus, and amygdala[56–59]. The PAG also relays to rostral ventromedial medulla, which projects onto the dorsolateral funiculus to the dorsal horn[60].

This network of brain regions was previously thought of as a "pain matrix"[61–63] which is consistently engaged in response to any type of pain. However, we now understand that the pain matrix hypothesis was too simplified. Studies have demonstrated that all pain is not associated with activation of specific brain regions[64,65]. Rather, while some brain regions such as those listed above may be more consistently involved, additional brain regions that are involved in the surrounding aspects of the pain (i.e., emotion/mood, injury, cognition, etc.) may also be engaged[66,67]. The amygdala, basal ganglia, parabrachial complex, and supplementary motor area are a few examples of brain regions that are more context-dependent and therefore less consistently activated in response to pain[56].

1.1.2 Types of Pain

Acute pain occurs when there has been tissue injury or damage, but the damage is well managed by medical attention and/or pharmacological intervention. Examples of acute pain

include surgical pain which is mitigated by anesthesia, and post-operative pain which is managed by analgesics. Acute pain is defined as pain that lasts days to weeks[68].

Chronic pain is pain that lasts longer than 3 months[69]. It is defined as "a syndrome characterized by persistent physical pain, disability, emotional disturbance, and social withdrawal symptoms, existing together and influencing one another"[70]. This is the most complex form of pain, and the form that pain pathologies fall under. In this type of pain, the damage might have exceeded the body's ability to heal either because the trauma or scarring is too extensive, because the body part has been lost, or because the nervous system has been damaged. Chronic pain can be initially caused by severe injury or disease, such as lower back pain, fibromyalgia, or post-surgical pain. However, pathological chronic pain is that which persists after wound healing or exists in the absence of tissue damage[68,70]. This type of pain must be managed long-term using a combination of physical, psychological, and pharmacological approaches.

1.1.3 Interventions for Chronic Pain Management

Physical interventions for chronic pain management include physiotherapy and occupational therapy. With physiotherapy, the goal is to maintain the patient's functional abilities without exacerbating pain. The therapist places emphasis on remaining active via stretching and aerobics – paying special attention to muscle strength and range of motion. Therapy sessions may include MRI and physical exam results to help keep patients updated on their progress[71,72].

The goal of occupational therapy is to increase physical capability. This therapy discourages excessive resting to avoid pain, as this could make the pain worse. The therapist works with the patient to establish a baseline of daily activities that the patient can build on each day.

Occupational therapy could also include keeping a pain diary to keep track of which exercises/activities caused pain over time[73].

Either method could also involve a pain specialist nurse who can advise the patient on dose and timing of prescribed medications to limit side effects. Increasing communication around medication helps to alleviate confusion or fear and increases compliance[74].

Psychological interventions include cognitive-behavioral therapy (CBT) and acceptance and commitment therapy (ACT). CBT emphasizes autonomy and focuses on reframing or adjusting maladaptive thought processes and beliefs around pain[75]. The patient is not simply a passive responder to pain, rather he or she can actively process the pain and make the best decisions for themselves[76]. CBT has shown improvements in quality of life, decreases in anxiety and depression[77], and decreases in frequency of hospital visits and therefore a reduction in healthcare costs[78].

As opposed to CBT which focuses on thoughts and beliefs, ACT focuses on behavioral responses. This type of treatment emphasizes improvement, not eradication, of pain. Significant attention is also given to practicing mindfulness to foster acceptance, reduce focus on the pain, and increase focus on life goals and values[79,80].

Pharmacological interventions for chronic pain are typically analgesic medications, which can range from over-the-counter drugs to powerful opioids. Non-opioid drugs include aspirin, acetaminophen, steroids, or non-steroidal anti-inflammatory drugs (NSAIDs, *e.g.*, naproxen). As outlined in the World Health Organization analgesic ladder, these drugs are the first line of defense against any type of pain and are typically effective against light to moderate pain[81]. However, if the pain persists or becomes more severe, then a weak opioid such as codeine might be prescribed

in tandem with a non-opioid drug. As the pain continues to persist or increase, stronger opioids might be prescribed. These include morphine, oxycodone, and hydrocodone among others.

1.2 Overview of Opioids and Opioid Receptors

Opioids are a class of compounds that bind to opioid receptors to produce pain-relieving (analgesic) effects. The earliest opioid discovered was morphine, first isolated from opium plants in 1805. The highly addictive nature of morphine was soon recognized, and the pharmaceutical company Bayer began an initiative to develop an analog of morphine that was devoid of addictive liability while maintaining profound analgesic properties. This effort led to the development of heroin in 1898[82], which was initially marketed as a non-addictive painkiller, however, we now know that heroin is more addictive than morphine. These discoveries paved the way for many other opioid analogues to be developed.
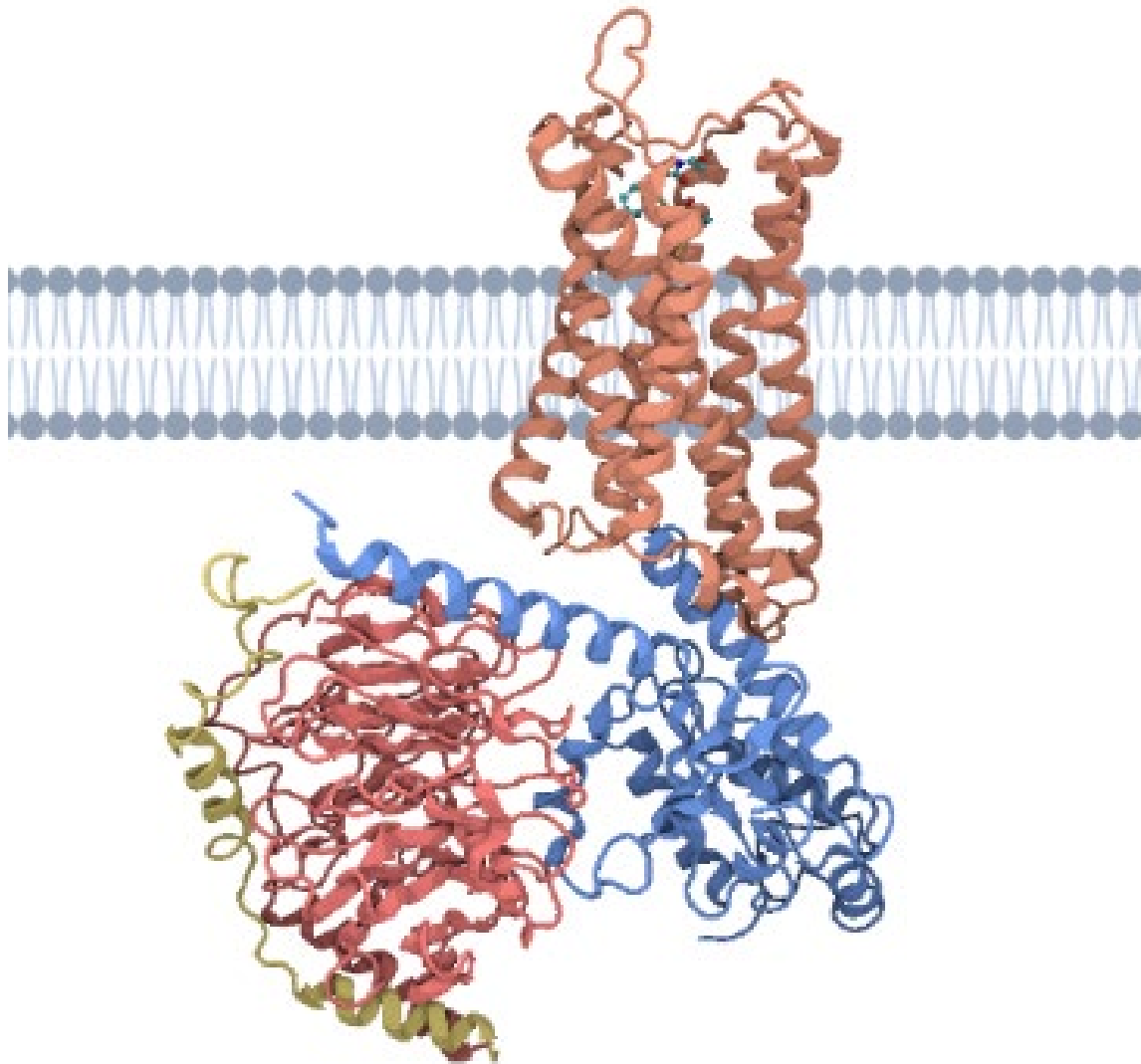
Figure 2. Structure of the mu-opioid receptor and G protein complex[83]. The mu-opioid receptor is shown in orange. The G-alpha subunit is shown in blue, G-beta in red, and G-gamma in gold.

1.2.1 Opioid Receptors

Opioid receptors **(Figure 2)** are G-protein coupled receptors (GPCRs) which are coupled to $G_{i/o}$ proteins and consist of an extracellular N-terminus, 7 transmembrane helices, 3 extracellular and 3 intracellular loops, and an intracellular C-terminus[84]. There are three subtypes of opioid

receptor – mu, delta, and kappa – each of which are encoded by distinct genes first discovered by Kieffer[85] and Evans[86] in 1992 (*OPRM1*, *OPRD1*, and *OPRK1* respectively)[82]. These receptors are found both in the CNS and in peripheral tissues, and are activated by endogenous peptides called β-endorphins, enkephalins, and dynorphins which were first isolated by Hughes and Kosterlitz in 1975[87].

The μ-opioid receptor (MOR) is primarily found in the brainstem, medial thalamus, and amygdala. MORs are also expressed in immune cells, ectodermal cells, and neuroendocrine cells such as the pituitary and adrenal glands[44,88]. This receptor subtype is responsible for supraspinal analgesia, euphoria, sedation, respiratory depression, decreased gastrointestinal motility, and physical dependence[84]. The κ-opioid receptor (KOR) is primarily located in the limbic brain regions, such as the hypothalamus and pituitary gland, along with the brainstem and spinal cord. Activation of this receptor subtype brings about spinal analgesia, dysphoria, sedation, and respiratory depression[84]. The final subtype is the δ-opioid receptor (DOR). This subtype is primarily responsible for the emotional response to the opioid, as opposed to the rewarding effects of opioids[89], as DOR activation has demonstrated anxiolytic and anti-depressive effects[90]. The following discussion will focus on the MOR, as nearly all clinically relevant actions of opioids are exerted through stimulation of this receptor subtype[82,91].

MORs are encoded by a single structural gene, *OPRM1*, and can form many splice variants[92]. While some of these variants do not possess any cellular activity, the active variants can differ in opioid binding affinity, potency and efficacy in mice[93] and humans[94]. The active variants can be divided into two groups: exon 1-associated variants, and exon 11-associated variants.

Exon 1-associated variants of the MOR all produce active and complete G-protein coupled receptors, and have identical binding pockets to the main variant, MOR1. These variants mainly

differ in the structure of the intracellular carboxy terminus. The carboxy terminus is known to be important for phosphorylation and signal transduction[95], thus differences in this region affect ligand potency and efficacy. Clinically, it is well known that opioid drugs can have differing effects from patient to patient[96,97], and these differences can be partially explained by the differences in the identities of the splice variants present in each individual. Exon 11-associated variants make up about 25% of the total level of mRNA and protein splice variants[98]. These variants produce receptors that are structurally identical to MOR1, but their expression levels differ regionally across the CNS[99,100].

Individual splice variants have also been associated with specific effects of opioid use. For example, a single nucleotide polymorphism (SNP) in the variant MOR1X has been associated with fentanyl-induced emesis in Chinese women undergoing gynecological surgery[101]. Additionally, Liu *et al.* reported that the variant MOR1D is required for morphine-induced scratching in mice, while MOR1, the major variant, is the only variant required for morphine-induced analgesia[102].

Upon binding of a ligand such as an opioid, conformational changes take place which allow for intracellular coupling of $G_{i/o}$ proteins to the C terminus of the MOR. GDP is displaced by GTP at the $G\alpha$ subunit, and the trimeric G protein dissociates into $G\alpha_i$ and $G\beta\gamma$ subunits. $G\alpha_i$ inhibits adenylyl cyclase and cAMP production while $G\beta\gamma$ interacts with membrane ion channels[103,104].

Once activated, MORs exert their antinociceptive effects via several mechanisms of action. MOR activation by opioids produces increased potassium conductance via $G\beta\gamma$-mediated activation of G protein-coupled inwardly rectifying K^+ (GIRK) channels[105]. GIRK channel activation prevents neuronal excitation and propagation of action potentials. Studies have demonstrated that mutant mice that lack or have dysfunctional GIRK channels show decreased opioid antinociception, highlighting that GIRK channel activation is important for the

antinociceptive effects of opioids[106–108]. In dorsal root ganglia (DRG) neurons, the Gβγ subunit also inhibit a number of ion channels such as Na^+ channels[109], Ih channels[110], and the TRPV1[111,112] and ASIC channels[113] mentioned in the ***Neurocircuitry of Pain*** section. This decreases presynaptic calcium-dependent fusion of synaptic vesicles with the membrane terminal, which leads to a reduction in neurotransmitter release.

Opioids also stimulate the descending, or inhibitory pain pathway. The descending pathway includes the periaqueductal gray (PAG), rostroventral medulla (RVM), the nucleus reticularis paragigantocellularis (NRPG), and the substantia gelatinosa of the dorsal horn, all of which contain high concentrations of MORs[114]. These regions contain both inhibitory GABAergic neurons and excitatory glutamatergic neurons. MOR activation by opioids inhibits the GABAergic neurons in these regions, allowing for increased glutamatergic activity. Increased excitatory input throughout the descending pathway leads to decreased nociceptive transmission from the periphery. Activation of MORs by opioids also increases neuronal traffic through the nucleus raphe magnus[115] leading to increased stimulation of serotonergic[116,117] and enkephalin-containing neurons which project onto the dorsal horn. This results in decreased nociceptive transmission from the peripheral site of injury to the thalamus[114]. Importantly, in the spinal cord opioids also block excitatory postsynaptic currents evoked by glutamate receptors in the ascending or excitatory pain modulatory pathway. The net result of these interactions is decreased transmission of nociceptive signals and decreased perception of pain[60].

Following stimulation of a GPCR by an agonist, the receptor undergoes several opposing mechanisms to maintain homeostasis. The most universal mechanism amongst GPCRs is a process called desensitization[118–120]. Activated receptors are recognized by GPCR kinases (GRKs) which phosphorylate the receptor either on the C-terminus or on any number of cytoplasmic loops. There

are 7 members of the GRK family, GRK 1-7. Expression of GRK 1 and 7 is restricted to visual rods and cones respectively. GRK 4 is expressed in few tissues, while the remaining GRKs, 2, 3, 5, and 6 are ubiquitously expressed[120]. MORs are primarily phosphorylated by GRKs 2 and 3[121–123].

Phosphorylation promotes recruitment and binding of arrestin proteins. Arrestins are a family of four proteins named arrestin 1-4. Expression of arrestins 1 and 4 (also known as visual arrestin and X arrestin respectively) is localized to visual rods and cones, while arrestins 2 and 3 (termed β-arrestin 1 and β-arrestin 2 respectively) have ubiquitous expression. MORs primarily interact with β-arrestin 2[124]. Visual arrestin was discovered by Kuhn *et al.* in 1987 which led to the discovery of the remaining members and eventual cloning of the proteins by the Bob Lefkowitz laboratory in the early 1990s[125–128]. Binding of arrestin proteins to the GPCR sterically blocks the receptor from interaction with its associated G protein, therefore decreasing signaling even in the continued presence of a stimulus. Desensitized GPCRs are then removed from the plasma membrane via clathrin-mediated endocytosis for degradation and recycling[119,129].

1.2.2 Opioids and the Dopamine Reward System

Emotions help us learn from our experiences. Negative emotions like fear or pain allow us to avoid detrimental actions in the future, whereas positive emotions like pleasure or reward increase the probability of continuing certain behaviors in the future. This concept is referred to as reinforcement[130,131].

Positive reinforcement – the process by which we learn to repeatedly seek out pleasurable or rewarding activities – is a hallmark of drugs of abuse such as opioids. As mentioned earlier, our endogenous opioid system consists of β-endorphins, enkephalins and dynorphins which signal

through MORs, DORs and KORs respectively[87,132]. This system modulates our mesolimbic dopamine reward system[133,134] and is involved, along with the dorsal medial prefrontal cortex, in the processes of assigning value to rewards and processing reward-related input to inform decision making and execution of goal-directed behaviors[135,136]. However, while endogenous opioids are beneficial, exogenous opioids, particularly those synthesized to be orders of magnitude more potent, have abuse liability and fall under the term "drugs of abuse".
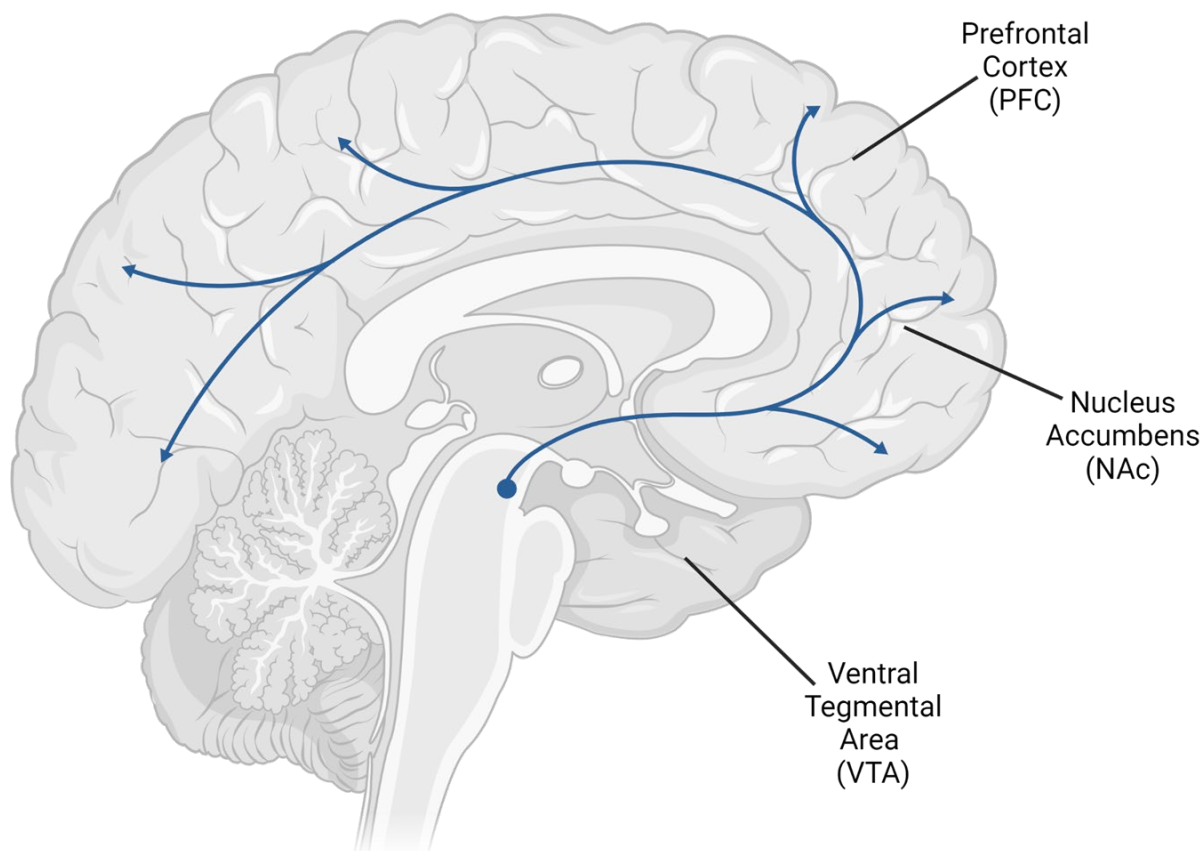
Figure 3. The dopamine reward pathway. Opioid-induced activation of the ventral tegmental area (VTA) stimulates dopamine release into the nucleus accumbens (NAc) and into the prefrontal cortex (PFC).

Every drug with abuse or addiction liability either directly or indirectly increases dopamine (DA) release. These drugs activate dopaminergic neurons in the ventral tegmental area (VTA) which causes DA release into the nucleus accumbens (NAc)[130,137–140]. These two regions, with influence from the amygdala and hypothalamus, make up the mesolimbic dopamine reward system[141–143] **(Figure 3)**. In 1981, Bozarth and Wise demonstrated using conditioned place preference that mice prefer to spend more time in an area where they previously received a drug of abuse[144]. Phillips *et al*. then demonstrated that this effect can be prevented if dopaminergic neurons in the VTA are destroyed[145,146], suggesting that DA release in the VTA is an important substrate for reinforcement of drugs of abuse[147]. Dopaminergic neurons in the substantia nigra project onto the dorsal striatum and are involved in the synthesis of repetitive reward signals into habitual actions. Sustaining this pathway leads to habit formation[148].

Opioids also contribute to reinforcement by modulating hedonic behaviors and inhibiting negative affective states[149]. Hedonic behaviors are those that are characterized by avoiding pain and seeking pleasure, and they form the basis of what we "like" and "want". The NAc, specifically the rostrodorsal quadrant of the medial shell, is known as the hedonic hotspot and plays a key role in modulating these behaviors[150–152]. In 2005, Smith *et al*. demonstrated in multiple studies that MOR activation by D-Ala(2)-MePhe(4)-Gly-ol(5))enkephalin (DAMGO) in this region increased the hedonic impact (or "liking") of sweet tastes[153–155], whereas MOR stimulation in other regions of the medial shell failed to have an effect[153].

Excessive and repeated DA stimulation from opioids and other drugs of abuse can induce neuroadaptations in many neurotransmitter systems including GABAergic[156], cholinergic[157,158],

endocannabinoid[132,149], noradrenergic[159], serotonergic[160,161], and importantly glutamatergic systems[162].

In the case of the glutamatergic system, these neuroadaptations involve glutamatergic input onto dopaminergic neurons in the VTA and onto medium spiny neurons in the NAc[163–165]. α-amino-3-hydroxy-5-methyl-4-isoxazolepropionic acid (AMPA) and N-methyl-D-aspartate (NMDA) receptors are glutamatergic receptors that play large roles in enhancing neuronal excitability and modulating neuroplasticity[132]. Some adaptations in this system are similar to the synaptic changes associated with learning, including NMDAR-and AMPAR-mediated long-term potentiation and long-term depression, and changes in dendritic morphology[151,163].

Neuroadaptations in glutamatergic systems are believed to be key substrates of drug use conditioning, including enhancement of incentive saliency (an increase in "wanting", and therefore an increase in drug-seeking behavior) and increased behavioral inflexibility[166–168]. Once conditioning is established, dopaminergic neurons begin to fire in response to drug-predictive cues, essentially anticipating the forthcoming reward[132]. Drug-predicted cues can include the primary emotion or mental state experienced during previous drug use, or people or places that are associated with drug use. Ultimately these cues can increase motivation to seek out the drug in the future.

1.3 The United States Opioid Epidemic

Opioids are sought after and widely used for their profound pain-relieving properties but continued use can also lead to misuse and eventually addiction and overdose. Increased prevalence of these factors can ultimately lead to an epidemic.

Drug overdose is the leading cause of accidental death in the United States[169,170]. 932,000 people have died from a drug overdose between 1999 and 2022, and there were over 100,000 deaths in 2022 alone[171]. Two-thirds of those deaths involved an opioid drug. Opioids are readily prescribed for treating chronic pain, which impacts 1 in 5 people in the US[172–174] and worldwide[175,176]. Although opioid medications are the most effective treatment for chronic pain, they are severely limited by many adverse effects—the most concerning of which is their highly addictive nature.

In the 19th century there was no formal regulation for the use of opioids and cocaine, which allowed for these drugs to be used for any number of conditions ranging from toothaches to diarrhea[177]. The Narcotics Tax act, which passed in 1914, regulated the importation, manufacture, and distribution of opioids and cocaine[178]. Addiction was becoming increasingly prevalent yet was not recognized as a disease the way it is today. Doctors who prescribed opioids to addicted patients during that time risked losing their licenses, making the treatment of addiction essentially illegal. This mishandling of addiction led to inadequate treatment of pain[177].

There are three driving forces that ushered in the current opioid epidemic: the belief that pain relief is a human right and therefore there is a moral obligation to treat pain, the response to the undertreatment of pain, and the influence of pharmaceutical companies[179].

On August 29, 2010, the 13th World Congress of Pain was held in Montréal, Canada. The Congress lasted until September 3, 2010, at which time the IASP hosted an International Pain Summit to address the prevalence of unrelieved pain. The conclusion of this summit yielded a document called the Declaration of Montréal, which stated among other things that access to pain management is a fundamental human right[180].

The Declaration was written in 2010, but this was not the first time the importance of adequate pain management was examined. In the 1990s, publications describing discrepancies in pain management based on sex and race began to surface[181–184]. Following these revelations, in 1999 the American Pain Society officially named pain the "fifth vital sign" and encouraged healthcare professionals to assess pain at every visit and treat it immediately[185]. In 2000, the Joint Commission officially approved pain as the fifth vital sign, making this the standard for how we think about pain. This approval was an overcorrection to make up for the lack of adequate treatment in the past[186].

Pharmaceutical companies began to think of pain as a symptom to be avoided at all costs, which led to the increase of opioid prescriptions, and many pharmaceutical companies played a leading role in this initiative. In 2001, Purdue Pharma developed the drug Oxycontin – oxycodone that was formulated using a sustained or "continuous" release delivery system. The pharmaceutical industry spent $200 million promoting this drug, which led to a 10-fold increase in sales the following year. Eventually 6.2 million prescriptions were written annually for Oxycontin. Sales representatives operated under a bonus system to incentivize the increase in sales and to encourage healthcare professionals to increase prescriptions for Oxycontin. Pharmaceutical companies also pushed sales by giving all-expenses paid trips to the 5000 healthcare providers who wrote the most prescriptions each year[187].

In addition to driving the increase of opioid use, pharmaceutical companies also intentionally understated the risk of addiction, stating that there was a less than 1% chance that patients could become addicted. Purdue was fined $634 million for misbranding, but this did not stop the increase in opioid prescriptions. Along with oxycontin, doses of morphine given in

hospital settings increased from 96 milligrams to 700 milligrams from 1997 to 2007 – an increase of 600%[188].

During the 1990s and early 2000s, opioids transitioned from exclusive use for palliative care or for cancer pain, to use for non-cancer pain, to use for pain that was not severe to begin with[179]. As of 2019, 25% of prescription drugs given for worker's compensation injuries were narcotics, and of those narcotics, 45% were formulations containing oxycodone[189]. Opioids and opioid-containing formulations are also consistently found on the 20 most prescribed drugs list[177].

The US Opioid Epidemic is defined as the overuse and/or misuse of addictive opioid drugs with significant medical, social and economic consequences, including overdose deaths. To date, the estimated economic burden of this epidemic is $200 billion per year. This cost includes healthcare, governmental assistance, lost productivity, and criminal justice intervention. The last two decades have ushered in two distinct waves of the opioid epidemic – the first being the rise in production of heroin and other "street drugs", and the second being the increase in synthetic analogs such as fentanyl. These drugs are even more addictive than those used in the clinic, and the majority of people who are using these drugs first abused prescribed opioids.

1.4 Strategies to Develop Safer Analgesic Therapeutics

The general role of opioid receptors is to regulate basic processes that are crucial for self and species survival, particularly regulating reward/aversion processing, coping with stress, and alleviating pain. Therefore, opioid receptors are key in pain treatment and neuropsychiatric disorders that involve these processes.

We know from the work of Matthes in 1996 and Kieffer in 2002 that MORs are primarily responsible for all *in vivo* morphine effects[91,190]. When MOR knockout (KO) mice are given

morphine, they do not experience analgesia, reward, constipation, respiratory depression, or any of the positive or adverse effects of morphine. MORs are also central to the reward processing of other drugs of abuse[191]. For example, when MOR KO mice are given rewarding drugs such as alcohol[192], cannabinoids[193], or nicotine[194], these drugs do not elicit reinforcing patterns even though they bind to their own receptors and do not have any direct interaction with the MOR itself. MORs are also critical for processing of natural rewards such as eating[195], maternal attachment[196], and social interaction[197], also demonstrated using MOR KO mice.

Since MORs mediate both positive and negative aspects of drugs of abuse, one persistent question in the field has emerged: how can we design an analgesic therapeutic that preferentially mediates the positive effects while avoiding the negative effects? Many strategies are currently being evaluated to address this longstanding hurdle.

One well-studied strategy is biased agonism or functional selectivity of opioid receptors. The goal is to design a therapeutic that targets a specific signaling pathway of the MOR, thereby tailoring the drug's action and limiting adverse effects. In 1999, Laura Bohn and colleagues discovered that morphine shows an improved therapeutic profile in β-arrestin KO mice compared to WT[198]. Morphine maintains its analgesic properties while limiting tolerance and respiratory depression[199–201]. Since this discovery, many $G_{i/o}$-biased therapeutics have been developed for clinical trials. Two examples are SR-17018[202] published by Schmid in 2017 and TRV130[203] (also known as oliceridine), published by DeWire in 2013. TRV130 completed phase III clinical trials and, under the tradename Olinvyk™, has been approved for short-term i.v. use in controlled settings such as hospitals[204].

Manglik *et al*. were among the first to utilize molecular docking technology to discover MOR biased agonists. Molecular docking facilitated evaluation of 3 million potential scaffolds

which were ranked according to probability of success. From there, the group chose a smaller number to synthesize and test *in vitro*. From this testing, PZM21 emerged as the lead compound[205]. This compound showed little to no respiratory depression in clinical trials.

Other strategies include designing peripherally restricted opioids, such as loperamide and NFEPP[206], published by Spahn in 2017. The ability for opioids to access the brain facilitates both positive and negative effects of opioids, so the goal is to develop a therapeutic that shows comparable analgesia, but only acts at peripheral MORs to limit the negative rewarding effects mediated by the reward circuitry in the brain.

Allosteric modulation is yet another strategy. Bristol Myers Squibb has developed two compounds[207], BMS 986122 and BMS 986187, that have been evaluated in clinical trials. Allosteric modulation has only shown modest efficacy to date. RB101 is an enkephalin degradation inhibitor designed to increase analgesia by increasing the concentration of endogenous opioid peptides[208]. Bivalent ligands, or opioid ligands that can bind two opioid receptor types, have also been developed. BU 08028 acts at MOR and the nociception opioid receptor[209], while CYM51010 acts at MOR and DOR[210].

1.5 Behavioral Paradigms to Assess Efficacy of Analgesic Therapeutics

Analgesic therapeutics have been evaluated for safety and efficacy in rodents using a number of experimental modalities. Below, I discuss thermal, mechanical, pharmacological and surgical methods of studying pain and analgesic tolerance in rodents.

Thermal Methods

The hot plate test[211,212] is one of the simplest measures of thermal heat nociception. Unrestrained mice or rats are placed on a hot plate typically set between 50-55°C, and the time to observe a pain-like response such as vocalization, moving off the plate, licking, jumping, etc is measured.

The tail flick or tail immersion test[213–215] was first described by D'Amour and Smith in 1941. In this paradigm, rodents are restrained either in a plastic tube or container or in a cloth. The tail remains free and is lowered into either hot or cold water. A stopwatch is used to measure the time to observe the pain-like response of removing (or flicking) the tail out of the water.

The Hargreaves test[216–218] was first published in 1988 and differs from the hot plate and tail flick tests in that a radiant light beam is used to evoke the pain-like response. The rodent is placed in a box with a transparent glass bottom. The rodent's hind paw is exposed to a light beam through the glass surface and the time to withdraw the paw is measured. The intensity of the light beam can also be adjusted or incrementally increased.

Mechanical Methods

Physiologist Max von Frey first reported the procedure for the von Frey mechanical nociception method in 1896. The von Frey filament test[219–221] is widely used to assess mechanical allodynia (pain perception in response to an innocuous stimulus) in rodents. The rodent is first placed on a wire mesh surface. Then a series of von Frey filaments which apply increasing force are applied to the rodent's hind paw. The amount of force required to evoke a pain-like response is recorded. This method lends itself well to internal controls as one hind paw could be neuropathic while the other is not. The force can also be applied manually or automatically by computer.

Another mechanical paradigm is the Randall Selitto test[222,223], first described by Randall and Selitto in 1957. Similar to the von Frey method, increasing force is applied to a rodent's hind paw and the amount of force required to evoke a pain-like response is recorded. This method was originally done manually, but electronic algesimeters have since become standard practice.

Pharmacological Methods

The formalin test[224–226], first described in 1977, is used to assess chemical nociception and is considered to be one of the most predictive models of acute pain in rodents[227]. Formalin is a saturated solution of formaldehyde in water. A dilute solution of formalin (typically 2-5%) is injected subcutaneously into a rodent's paw to elicit an inflammatory pain response. Interestingly, the pain response is consistently biphasic, where the rodent will have an immediate licking or biting response followed by a period of quiescence followed by a second interval of licking or biting. These two phases are thought to be driven by separate mechanisms, where phase 1 is primarily due to peripheral nociceptor activation via TRPA1 channels while phase 2 is due to inflammatory response and central sensitization[227].

Writhing tests[212,228,229] are used to evaluate visceral pain in rodents. Pain is induced by systemic administration (either oral or intraperitoneal) of an irritant such as acetic acid or phenylquinone. The time spent writhing or stretching or the number of observations of this behavior is recorded.

Complete Freund's Adjuvant or CFA is commonly used to develop pain hypersensitivity in rodents[230,231]. CFA contains heat-killed mycobacteria which when injected into a rodent's hind paw, elicits a strong immune response that causes inflammation and pain in the affected paw. Once

the inflammatory response takes place, other methods such as the von Frey test can be used to measure pain threshold.

Carrageenan is a red seaweed extract widely used as a food additive or preservative. Similar to CFA, it can also be used to induce an inflammatory response. A diluted solution is injected into the rodent's hind paw and evokes an inflammatory response that causes hyperalgesia[232–234] (enhanced pain perception in response to a moderately painful stimulus). Secondary methods like the von Frey or Hargreaves tests are then used to assess pain thresholds.

Capsaicin is a compound found in spicy peppers. As mentioned earlier, capsaicin activates TRPV1 channels and evokes a pain response followed by sustained desensitization to chemical pain[233,235–237]. A solution of capsaicin is injected subcutaneously into the rodent's hind paw and the rodent is observed for a period of time. The time spent licking or otherwise attending to the affected paw is measured.

Phorbol 12-myristate 13-acetate (PMA) is another strong immunogenic compound. It activates immune cells through activation of several kinases along the mitogen-activated protein kinase (MAPK) pathway such as protein kinase C, extracellular signal-regulated kinases 1 and 2, and c-Jun N-terminal kinase[238,239]. Similar to capsaicin, a solution of PMA is injected into the rodent's hind paw and the resulting pain-like behaviors are measured[233,240].

Surgical Methods

Finally, spinal nerve ligation is also commonly used to elicit inflammatory pain and allodynia and/or hyperalgesia[232,241,242]. This method was first described by Chung in 1992 and involves tightly ligating either the L5 and L6 spinal nerves, or just the L5 nerve, of an anesthetized

rodent (see Chapter 2 Methods). Secondary methods such as the von Frey test can then be used to evaluate pain thresholds.

1.6 Analgesic Tolerance to Opioids

An addition to the addictive nature of opioids, two other major adverse effects are physical dependence and analgesic tolerance. Physical dependence is a physiological state where the body can no longer maintain homeostasis in the absence of a drug[243]. Dependence typically manifests as a series of withdrawal symptoms following cessation of drug use. Withdrawal symptoms in humans include sweating, scratching, vomiting, and severe cramps, while symptoms in rodents include excessive jumping (escape jumps), wet dog shakes, and excessive salivation.

Tolerance is a multi-faceted phenomenon that can develop against any of the on-target or off-target effects of a drug at varying rates. Analgesic tolerance is defined as a decreased response to the analgesic effects of opioids. Over time, the initial dose given becomes ineffective in relieving pain, therefore increasingly higher doses must be used to maintain the desired level of analgesia [244,245]. Tolerance to the analgesic effects of opioids can develop within weeks, and continually increasing doses can result in overdose[245,246].

Although we have standard of care procedures for treatment of addiction and dependence[247], we do not have a method of preventing or prolonging the onset of tolerance. Preventing tolerance could drastically decrease the likelihood of physical dependence and addiction in patients who use opioids because they would not need to continually increase the dose of their prescribed opioid medications. The longer the patient is taking the drug, and the higher the concentration in the body, the higher the probability that physical dependence and addiction can

be developed. Tolerant patients are also more likely to have longer stays at hospitals, are more likely to be readmitted within 30 days, and have a higher likelihood of comorbidities[248]. If discharged from the hospital, tolerant patients show increased mortality if they have experienced a period of abstinence from the drug then resume drug use, especially at the same dose as before hospitalization.

There are several coordinated mechanisms that cause the cellular adaptions that contribute to the development of analgesic tolerance to opioids. For this discussion, it is useful to categorize the mechanisms as those at the neurotransmitter level and those at the receptor level. The first refers to changes in neuronal firing due to changes in neurotransmitter release, whereas the second refers to changes in receptor function due to interactions with molecules or signaling proteins.

For neurotransmitter-level mechanisms, we focus on the descending pain modulatory pathway, which includes the PAG, rostral ventromedial medulla (RVM), and spinal cord dorsal horn. MORs are highly expressed throughout this pathway, and these brain regions are well known to contribute to tolerance development[249–251]. The PAG contains both GABAergic and glutamatergic neurons and projects onto the RVM[251,252]. When MORs in the PAG are activated by opioids, GABAergic activity is decreased, leading to disinhibition of the excitatory glutamatergic projections to the RVM[253,254]. Bobeck *et al.* used electrophysiology to demonstrate that opioids reduce the probability of GABA release from the PAG, as indicated by a decrease in the frequency of spontaneous miniature inhibitory postsynaptic currents (mIPSCs)[254]. mIPSCs are a well-known property of GABAergic neurons, and mIPSC frequency is directly related to GABAergic transmission[254,255]. This mechanism was supported by *in vivo* data collected by Stiller *et al.* which demonstrated that administration of morphine into the PAG reduces extracellular GABA[253]. This increase in glutamate release into the RVM and throughout the pain modulatory pathway can

induce synaptic plasticity which strengthens the connections between neurons and makes them hypersensitive to future stimulus. Over time, this synaptic strengthening contributes to tolerance because the threshold for nociceptive signaling is lowered so that pain perception persists even in the presence of an opioid.

Chronic MOR activation by opioids induces several receptor-level adaptations which contribute to tolerance. Tolerance is ultimately caused by a reduction of functional MORs[82]. Mechanisms that contribute to this reduction include receptor desensitization and decoupling, impaired resensitization machinery, and enhanced kinase activity.

The first step in the process of desensitization is phosphorylation of MORs. Phosphorylation is carried out hierarchically where residue S375 is considered to be the main site of agonist-induced phosphorylation, followed by T370[256]. Other phosphorylation sites include T354, T357, S363, T376 and T379[257]. MORs are primarily phosphorylated by G protein-coupled receptor kinases[257–259] (GRKs), particularly GRKs 2, 3 and 5. Phosphorylation of MORs triggers the recruitment and binding of β-arrestin which leads to desensitization of the receptor. Binding of phosphate groups, β-arrestins, and other effector proteins, such as calmodulin, creates steric bulk that prevents G protein binding[82,118]. Uncoupled receptors are no longer functional and therefore are targeted for endocytosis and recycling[260]. Chronic morphine treatment was previously thought to enhance endocytosis, but subsequent studies have suggested that endocytosis is most likely not affected during the development of tolerance[261,262].

This process of desensitization and decoupling is accelerated during tolerance development. Dang *et al.* and Ingram *et al.* both reported that chronic exposure to morphine enhances desensitization[263,264]. Accelerated desensitization is also caused by a number of kinases

which will be discussed below, but upregulation of other proteins such as regulators of G protein signaling (RGS) proteins[265], spinophilin[266], or phospholipase D2[267] could play a role as well.

Dang *et al*. have also shown that chronic morphine administration impairs recovery from desensitization after withdrawal from morphine[268,269]. Impaired recovery is thought to be β-arrestin-dependent because β-arrestin knockout mice showed normal levels of desensitization compared to wildtype[261,269] and because β-arrestin knockout mice did not develop morphine-induced analgesic tolerance[270,271]. β-arrestin knockout mice showed attenuated tolerance to morphine, but not to fentanyl, methadone or oxycodone, suggesting that β-arrestin is required for tolerance to morphine[270–272].

Chronic morphine administration engages several kinases that work to decrease the number of functional MORs. GRK2 is one of the primary kinases that phosphorylate MORs, and chronic morphine administration has been shown to increase GRK2 protein levels by approximately 20% in the locus coeruleus. This phenomenon was only seen following chronic morphine, not acute[273,274]. Whistler *et al.* also demonstrated that increased GRK expression potentiates morphine-induced desensitization[275].

Protein kinase C (PKC) also plays a large role in tolerance development. Tolerance is reduced by PKC inhibitors[276] and is reduced in PKC knockdown[277,278] and knockout[279] mice. PKC activation is required for activation of c-Jun N-terminal kinase (JNK)[280]. JNK inhibitors can attenuate short-term tolerance to morphine and JNK-2 knockout mice did not develop short-term tolerance to morphine[280]. These effects were recapitulated with buprenorphine and morphine-6-glucuronide, a metabolite of morphine, but not in oxycodone or fentanyl[280]. Opioids like morphine

also activate extracellular signal-regulated kinases (ERK1/2). ERK1/2 inhibition has been shown to block MOR phosphorylation, desensitization, and internalization[281,282].

The work presented in this dissertation focuses on a third aspect – persistent activation of N-methyl-D-aspartate receptors (NMDARs) in the brain. The work in this dissertation originated from an interest in how persistent activation of NMDARs contributes to the mechanistic tapestry of opioid-induced tolerance.

1.7 The NMDA Receptor

Most excitatory transmission in the CNS is mediated by vesicular release of glutamate. Additionally, all primary afferents that transmit pain signals use glutamate[283]. Glutamate activates both pre- and post-synaptic metabotropic glutamate receptors, which are members of the GPCR family, and ionotropic glutamate receptors (iGluRs), which are members of the ion channel family. iGluRs are membrane proteins that are comprised of four subunits that create an ion channel pore. Each of these subunits contain four semi-autonomous domains connected by flexible linkers: the amino-terminal domain (ATD), the ligand-binding domain (LBD), the transmembrane domain (TMD), and the intracellular carboxyl-terminal domain (CTD)[284–286]. There are four major classes of iGluRs, each named for the synthetic glutamate mimetic that each receptor selectively binds: α-amino-3-hydroxy-5-methyl-4-isoxasolepropionic acid receptors (AMPARs), (2S,3S,4S)-3-(carboxymethyl)-4-prop-1-en-2-ylpyrrolidine-2-carboxylic acid (kainate) receptors, the less understood delta receptors, and N-methyl-D-aspartate receptors (NMDARs, **Figure 4**)[284].
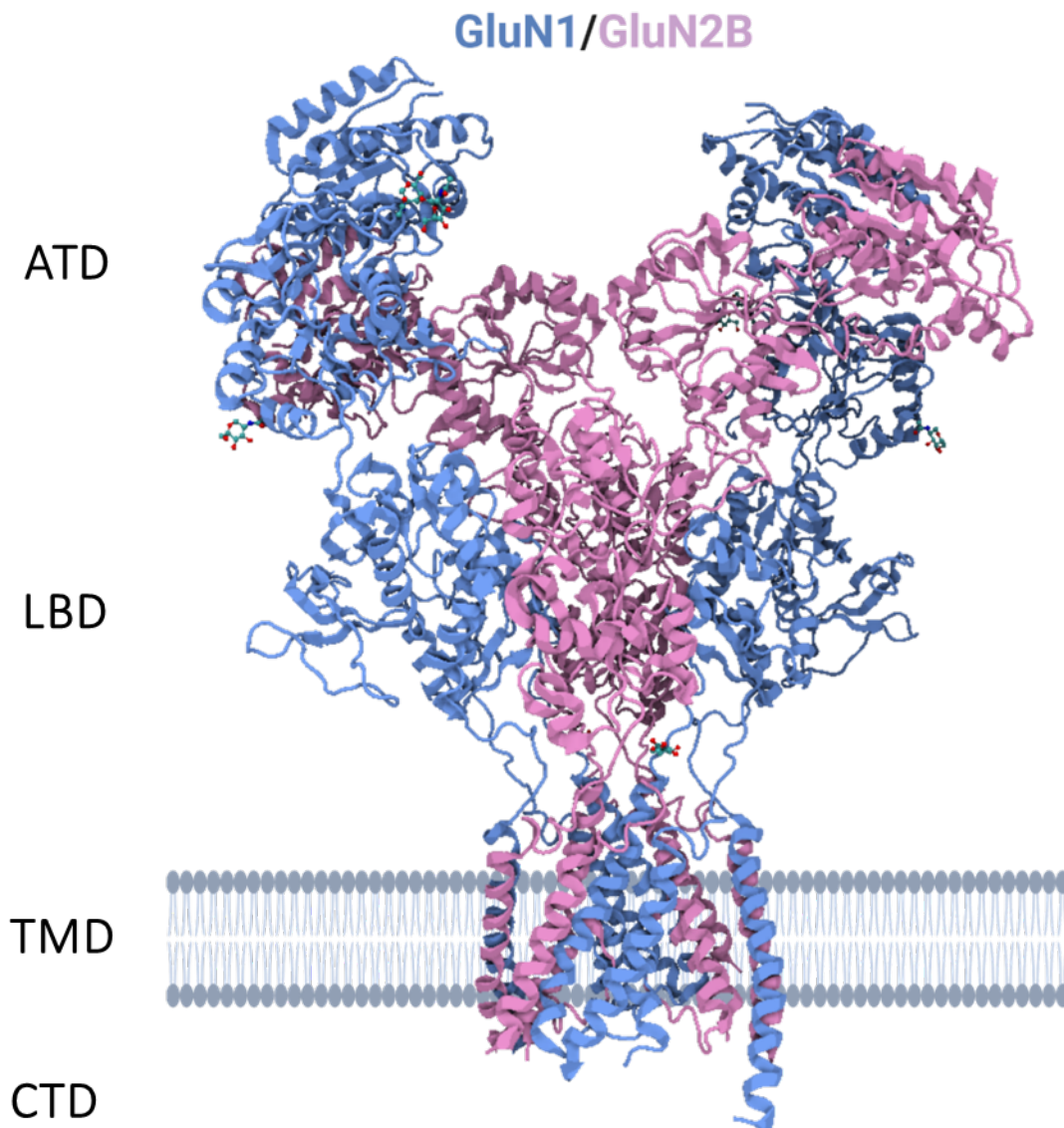
Figure 4. The NMDA receptor. The receptor is shown bound to the membrane, where GluN1 subunits are shown in blue and GluN2B subunits are shown in pink. The amino terminal domain (ATD), the ligand binding domain (LBD), the transmembrane domain (TMD), and the C-terminal domain (CTD) are labeled.

The NMDAR ATD consists of two halves, R1 and R2, which assemble as a clamshell structure. The cleft of the clamshell contains three parts: a hydrophilic pocket which contains two

residues involved in Zn^{2+} binding, His127 and Glu284[287,288], a hydrophobic pocket located in the core of the clamshell which contains residues that affect binding of ifenprodil and other GluN2B-selective inhibitors (binding site of ifenprodil discussed below)[289], and an ion-binding site located between the two pockets which binds Na^+ and Cl^- ions. This ion-binding site is present in both Zn^{2+}-bound and -unbound states[290].

The LBD also assembles as a clamshell and contains two halves, S1 and S2, each of which form one half of the clamshell, D1 and D2 respectively[291]. The LBD is highly conserved across all glutamate receptors and agonist binding interactions are conserved across all NMDAR subunits[292–296]. Upon binding of the co-agonists glutamate and glycine to the LBD, the D2 lobe is elevated towards D1, pulling the S2 section connected to the M3 helix in the TMD into an open arrangement and facilitating pore opening and ion flow[297–299].

The TMD forms the pore of the receptor and is highly conserved across all NMDARs. This domain contains residues that are important for voltage-dependent Mg^{2+} block[300] and binding of uncompetitive antagonists (also called channel blockers)[301,302]. The TMD consists of three transmembrane helices, M1, M3, and M4, and a reentrant loop, M2[285,286,303,304]. The M2 loop and the M3 helix make up the inner and outer portion of the pore respectively. The M1 and M4 helices assemble in relation to M2 and M3 and form the remainder of the pore, conferring 4-fold symmetry once the pore tetramer is fully assembled[284].

Finally, the M4 helix is attached to the CTD. This region is the least conserved across NMDARs and is not essential for receptor function. The CTD is suggested to have a regulatory role as it has been shown to be involved in post-translational modifications, protein degradation, and membrane targeting among others[284].

NMDARs are excitatory ionotropic glutamate receptors, expressed in neurons throughout the brain, which mediate CNS excitatory transmission, synaptic plasticity[305,306], learning[307,308], and memory[309]. NMDARs function via coincidence detection, or Hebbian plasticity. Many organisms use coincidence detection to quickly and appropriately respond to stimuli. The work of Cotman and Monaghan in 1988 suggested that NMDARs function as coincidence detectors because they are blocked by a Mg^{2+} ion at resting (hyperpolarized) states[310]. Additionally, NMDARs are highly calcium permeable and can initiate many intracellular signaling cascades as well as changes to the postsynaptic neuron[311–315]. Bliss and Collingridge noted that these properties are consistent with Hebbian properties[306]. Coincidence detection means that activation of the receptor requires several events to take place, which are sensed by the receptor. First, the co-agonist neurotransmitters glycine and glutamate must bind to the LBDs of GluN1 and GluN2, respectively[300,316–318]. Once the ligands are bound, the neuronal membrane must also be depolarized. This can happen via influx of Na^+ ions caused by activation of co-localized AMPARs[319]. Depolarization of the neuron releases the Mg^{+2} ion that sits in the inactive ion channel pore and facilitates opening of the channel, allowing the influx of Na^+ and Ca^{+2} and the efflux of K^{+}[320–325].

NMDARs are heterotetrameric in structure, exhibiting two obligatory glycine-binding GluN1 subunits, and either two glutamate-binding GluN2 subunits, two glycine-binding GluN3 subunits, or one of each[285,326–330]. The GluN1 subunit is encoded by a single gene, *Grin1*, and has eight splice variants, GluN1-1a – GluN1-4a and GluN1-1b – GluN1-4b. Four *Grin2* genes exist, giving rise to four GluN2 isoforms, GluN2A-D[327,331–334]. Two *Grin3* genes encode the GluN3 subunit yielding isoforms GluN3A-B[326,335–337]. NMDARs can exist as either diheteromeric receptors or triheteromeric receptors[338,339]. Both versions contain two GluN1 subunits, but diheteromeric assembly contains only one type of GluN2 or GluN3 subunit (*e.g.*, two GluN2B

subunits), and triheteromeric assembly contains two different GluN2 or GluN3 subunits (*e.g.,* one GluN2B subunit and one GluN3A subunit). GluN3 diheteromers are less understood than GluN2 diheteromers, but more research is being done to better understand their effects on receptor function.

Expression patterns of GluN2 subunits confer differential permeation and gating properties, such as open probability[340–343], Ca^{+2} permeability, Mg^{+2} block, single channel conductance[284,344,345], deactivation time[325], and agonist potency[292]. For example, GluN2A- and GluN2B-containing receptors have higher permeability to calcium, higher magnesium sensitivity and higher conductance compared to GluN2C- and 2D-containing receptors. Additionally, open probability decreases, deactivation time increases, and agonist potency increases in order from GluN2A- to GluN2D-containing receptors[284,326,344]. At GluN1/GluN2A, glutamate and glycine EC_{50} values are in the micromolar range, compared to GluN1/GluN2D where the EC_{50} values are submicromolar[292,346].

Each GluN2 subunit possesses unique spatiotemporal expression patterns which further impart each receptor assembly with unique pharmacological properties[324,347,348]. In young childhood, GluN2A expression is high and continues to increase across the lifespan. GluN2B, along with GluN2D, are the only subunits expressed in the pre-natal brain. GluN2B expression peaks at post-natal day 7 and is expressed primarily in the forebrain throughout the lifespan. GluN2D expression sees a sharp decline after birth, but remains widespread in interneurons and present in low levels in the diencephalon and mesencephalon in adulthood. The observation that GluN2B and GluN2D are the only subunits expressed in embryo suggests that these two subunits may play important roles in synapse formation and maturation[349], while the predominance of GluN2A and GluN2B in adulthood might suggest roles in synaptic plasticity and synaptic

function[324,347,350]. GluN2C expression is highest in the cerebellum and olfactory bulb, but is also present in the thalamus and in astrocytes and oligodendrocytes, among other locations.GluN2C appears later than the other subunits at post-natal day 10. In the spinal cord, there is considerable expression of GluN2A and GluN2B and low expression of GluN2C and GluN2D. GluN2A and GluN2B are both present in high levels at birth. GluN2A expression peaks during postnatal days 0 – 14, then declines to moderate levels in adulthood[351,352]. GluN2B expression declines during postnatal days 0 – 14, then increases into adulthood, primarily restricted to laminae I and II of the substantia gelatinosa[232,352].

Dysfunction of NMDARs are implicated in many neurological and psychiatric pathologies including cerebral ischemia[353] and traumatic brain injury[354,355], neuropathic pain[356,357], Alzheimer`s disease[358], Huntington`s disease[359], Parkinson`s disease[360], depression[361], white matter injury[362], autism spectrum disorders[363,364], and schizophrenia[365,366] among others, thus making the NMDAR an attractive target for many drug development initiatives.

1.7.1 NMDAR Uncompetitive Antagonists

Broad-spectrum uncompetitive antagonists, or ion channel blockers, were among the first compounds developed to treat NMDAR-related pathologies. These antagonists require NMDAR activation to bind in the ion pore[367]. The channel blocker class demonstrates broad chemical diversity, with ligands ranging from single ions such as Mg^{2+}, to polyamines, to "cage-like" adamantine analogs, such as memantine, to drug-like small molecules like ketamine. However, these compounds are characterized by adverse psychotomimetic effects due to global unselective blockade of NMDARs[326]. Despite this liability, several ion channel blockers – dextromethorphan, ketamine, esketamine, memantine and adamantine – are currently FDA-approved for clinical use in humans **(Figure 5)**.
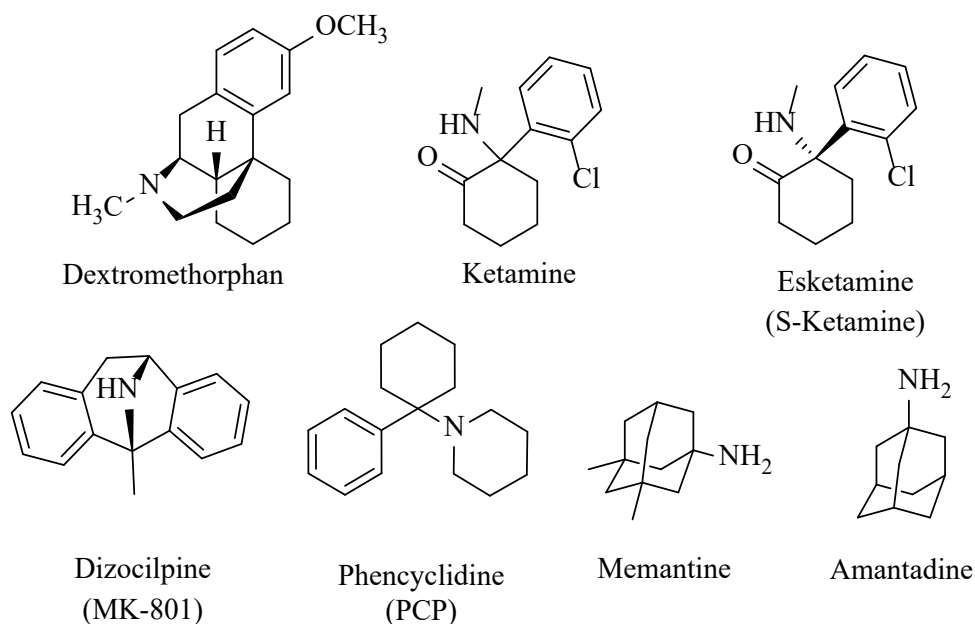
Figure 5. Uncompetitive NMDAR antagonists.

Dextromethorphan is a commonly used active ingredient in over-the-counter antitussive medications and has been in use for over 50 years[368]. It was also approved for the treatment of pseudobulbar affect when used in combination with quinidine[369]. In addition to NMDAR antagonism, dextromethorphan also exerts its pharmacological actions via sigma-1 receptor agonism, and serotonin and norepinephrine reuptake inhibition[362].

Ketamine is approved for use in general anesthesia and short-term procedural sedation. Ketamine possesses a short half-life and low potency, making it a more attractive alternative to comparable compounds, such as dizocilpine (MK-801) and phencyclidine (PCP) **(Figure 5)**[367,370]. Ketamine has also been shown to demonstrate a rapid and robust anti-depressant effect when administered at sub-anesthetic doses; however, recent data suggest that this anti-depressant effect is triggered by an NMDA receptor-inhibition independent mechanism[371]. However, the predominant mechanism underpinning ketamine's antidepressant effects remains unknown[372]. Ketamine is currently prescribed off-label for treatment-resistant depression and major depressive

disorder[373,374], and it has also been clinically evaluated for treatment of postoperative and neuropathic pain[375,376], post-traumatic stress disorder[377] and obsessive-compulsive disorder[378], although these mechanisms are not well understood. Esketamine (the S-enantiomer of ketamine) is approved for treatment-resistant depression when used in conjugation with other oral antidepressants.

Memantine is approved for treatment of moderate-to-severe Alzheimer's disease. Compared to ketamine, memantine is of similarly low affinity, has a faster off-rate, and was shown to exert preferential activity toward extrasynaptic NMDA receptors[379,380]. Amantadine is indicated for the treatment of dyskinesia associated with Parkinson's disease[381].

1.7.2 GluN2B-Selective Antagonists

To combat the adverse psychotomimetic effects associated with ion channel blockers, subunit-selective NMDA receptor therapeutics were developed. NMDA receptor subunits vary in regional expression and in their physiological functions[324,347,350]. This coupled with the high sequence variability of the ATD allows for the development of compounds that preferentially act on one subunit over the others[284,345]. This subunit selectivity decreases the prevalence of off-target effects and provides a more targeted approach to treatment.

As mentioned earlier, GluN2A and GluN2B are the two subunits primarily expressed in the adult forebrain[324,347]. GluN2A-containing receptors tend to be expressed at the synapse and have been proposed to function as neuronal survival promoters. Conversely, GluN2B-containing receptors can be synaptic or extrasynaptic in nature[382] and have been proposed as neuronal death promoters[383–385]. The elucidation of the preferential roles of GluN2A and GluN2B led to the conclusion that enhancement of GluN2A-containing receptors rather than GluN2B-containing

receptors is a more attractive strategy to treat neurodegeneration and other NMDAR-mediated pathologies[326,386]. The role of GluN2B enhancement in excitotoxicity and neuronal death sparked a global interest in designing GluN2B-selective antagonists[387,388].

Ifenprodil, a noncompetitive GluN2B-selective antagonist, was the first subunit-selective modulator developed, boasting an IC_{50} of 100 nanomolar[389] and 200-400-fold selectivity for GluN2B over 2A, 2C, and 2D[390]. Ifenprodil is thought to act via binding to GluN2B ATD to facilitate agonist binding, but it also significantly decreases open probability of the receptor, yielding a net antagonistic effect. Ifenprodil binds at the interface of GluN1 and GluN2B[391,392]. Interestingly, the residues that interact with ifenprodil in this pocket are conserved in GluN2A, but differences in the ATD of GluN2A restrict ligand access[393]. Ifenprodil is a unique compound because its effects differ based on glutamate concentration. For example, ifenprodil modulation increases glutamate affinity which reduces inhibition at sub-saturating agonist concentrations. At very low glutamate concentrations, ifenprodil can act as a potentiator[394]. Additionally, ifenprodil and similar modulators have pH-dependent mechanisms of action[395–398].

Ro25-6981 is another GluN2B-selective inhibitor that is more potent and more selective than ifenprodil, with an IC_{50} of 3 nanomolar and 5000-fold selectivity for GluN2B-containing receptors compared to that of GluN2A-containing receptors[399]. Ro25-6981 binds in the same pocket as ifenprodil and has a similar mode of action. Ro25-6891 also demonstrated more potent neuroprotection compared to ifenprodil in glutamate toxicity studies and in combined oxygen and glucose deprivation studies in cortical neurons[399].
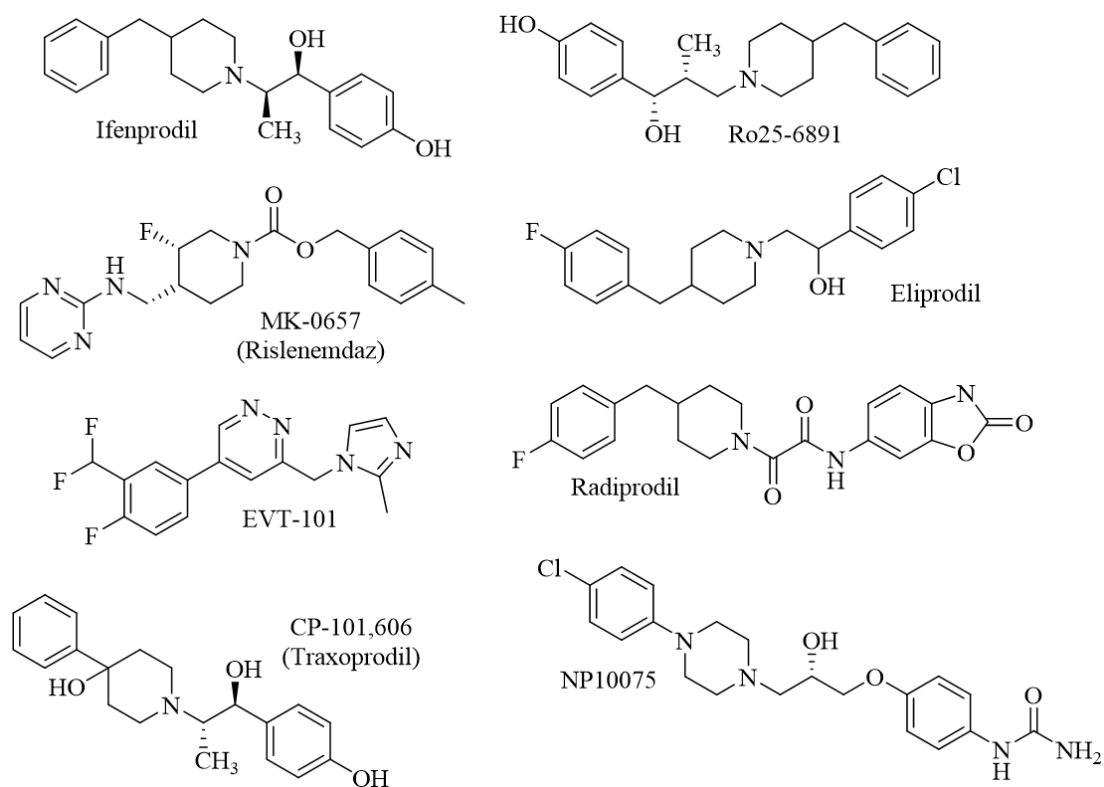
Figure 6. GluN2B-selective NMDAR negative allosteric modulators (NAMs).

Ifenprodil, along with Ro25-6981, Rislenemdaz (MK-0657), Eliprodil, EVT-101, Traxoprodil (CP-101,606), and Radiprodil **(Figure 6)**, were among the first GluN2B antagonists to be developed and clinically evaluated for treatment of traumatic brain injury, treatment-resistant depression, and neuropathic pain[233,400–403]. As expected, these compounds retained their efficacy while possessing an improved safety profile compared to the non-selective channel blockers[392,404]. However, once submitted for clinical trials, these compounds displayed minimal efficacy[401,405,406]. Traxoprodil (CP-101,606) was initially indicated for depression and Parkinson's disease and showed favorable results in phase I and II clinical trials[402,407]; however, failed to move forward due to cardiovascular toxicity, specifically QT prolongation[408]. Radiprodil is the first GluN2B-selective antagonist to be tested for treatment of infantile spasm syndrome, and has shown promising

results[409]. NP10679, developed by NeurOp, was recently granted orphan drug designation for the treatment of subarachnoid hemorrhage, a type of stroke characterized by bleeding in the areas surrounding the brain. NP10679 yielded encouraging Phase I trial results in 2019 and will be evaluated in Phase II trials in 2023[410].

1.7.3 The Role of NMDARs in Tolerance Development

The contributing role NMDARs have to tolerance development is well-documented. One major reason for this contribution is that central sensitization, a precursor to chronic pain pathogenesis[411,412], is NMDAR-mediated. As summarized by Fleming *et al*. in 2015, central sensitization is "a state in which the central nervous system amplifies sensory input across many organ systems"[413]. This amplified sensory input induces neuronal plasticity that ultimately primes the neurons for increased sensitivity to future stimulation. Central sensitization can manifest as either hyperexcitability or spontaneous activity and can be caused by either nerve or tissue injury[414,415]. Increased sensitivity in nociceptive neurons leads to development of many forms of chronic pain including allodynia (pain perception in response to an innocuous stimulus) and hyperalgesia (increased pain perception in response to a painful stimulus)[413]. The role NMDARs play in this process is the induction of wind up and LTP, which are characteristics of central sensitization[416].

Wind up is an electrophysiological response first described by Mendell and Wall in the 1960's, where repetitive stimulation of nerve fibers, particularly C fibers, causes progressively increasing neuronal activity[417,418]. Price *et al*. showed in 1971 that repeated stimulation of peripheral C fibers with constant intensity produced progressively increasing magnitude and duration of action potentials in dorsal horn neurons[419]. Wind up can be induced experimentally by stimulating at frequencies between 0.3 and 2 Hz, but this enhanced response only lasts for a few

minutes after the stimulus ends. In 1987, Davies and Lodge and Dickenson and Sullivan demonstrated that NMDAR antagonists, or channel blockers, such as ketamine, kynurenic acid, and aminophosphonovaleric acid (AP5), can inhibit wind up of dorsal horn neurons[420,421].

While they may be thought of as similar concepts, wind up is not the same as LTP. First described in hippocampal neurons in 1973 by Bliss and colleagues[422], LTP is defined as enhanced post-synaptic activity following tetanic stimulation of afferent pathways. It is the process by which synaptic connections become stronger following frequent stimulation. LTP is a mechanism by which the brain changes in response to experience, which also makes it a widely used model for studying the processes of learning and memory[306]. LTP can last for hours or days and can be induced experimentally by brief tetanic stimulation of 100 Hz which causes an increased response to subsequent stimulation. The NMDAR antagonist AP5 and the AMPAR antagonist 6-nitro-7-sulphomoylbenzoylquinoxaline-2,3-dione disodium (NBQX) have been shown to inhibit induction of LTP and ablate pre-established LTP[423,424].
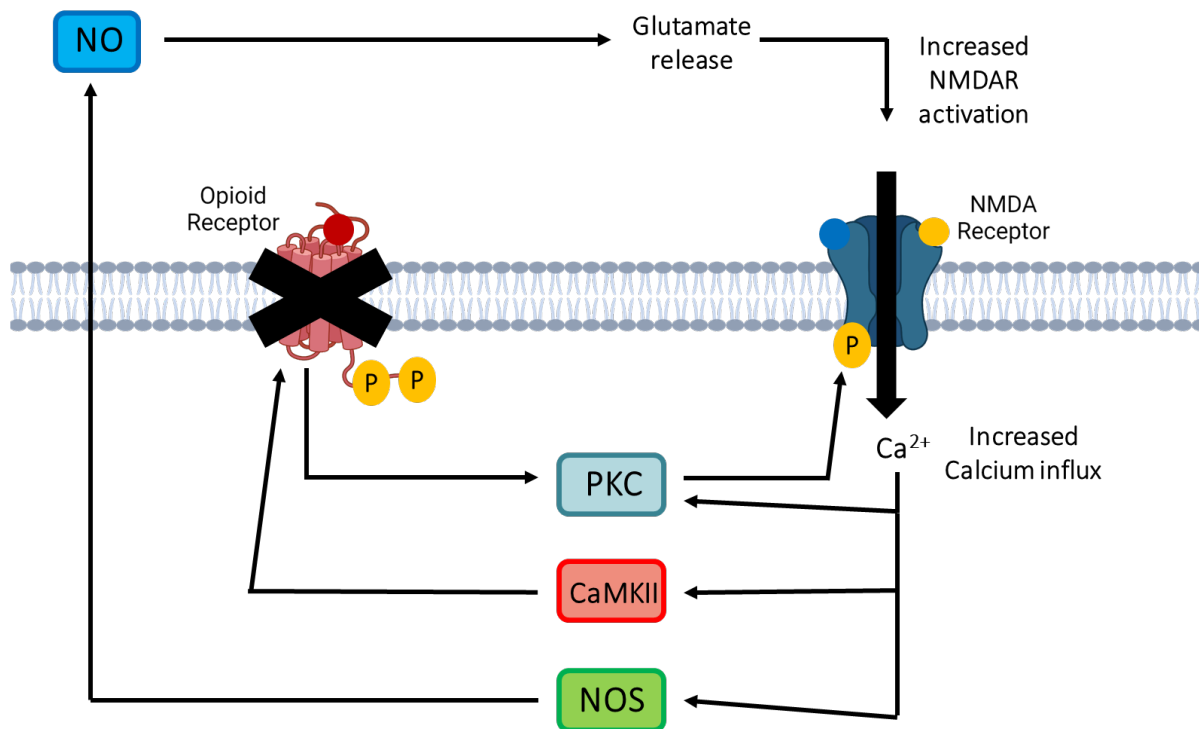
Figure 7. Analgesic tolerance development. Upon opioid binding and activation of the mu-opioid receptor (MOR), protein kinase C (PKC) is activated and phosphorylates the MOR. NMDAR activation permits the influx of calcium, a second messenger which can activate many signaling cascades including activation of PKC, calcium/calmodulin-dependent protein kinase II (CaMKII), and nitric oxide synthase (NOS). CaMKII can also phosphorylate MORs. Phosphorylation of the MOR desensitizes the receptor and targets it for internalization and recycling. NMDAR phosphorylation by PKC sensitizes the receptor, leading to an increased influx of calcium. NOS activation by calcium produces nitric oxide (NO), which stimulates glutamate release from the presynaptic neuron. Glutamate can further activate NMDARs.

As discussed in the **Analgesic Tolerance to Opioids**, increased glutamatergic input from NMDAR- and AMPAR-expressing PAG neurons is a key aspect of tolerance development[425]. NMDARs are highly expressed throughout the pain modulatory pathway and they colocalize with

MORs[426–428]. Activation of MORs leads to activation of kinases such as PKC and Src which phosphorylate NMDARs[429–431]. This phosphorylation sensitizes the receptor and increases open channel probability and open channel time, leading to excessive Ca^{2+} influx into the cell. Increased calcium means increased excitability of the cell and increased activation of Ca^{2+}-mediated signaling pathways. The NMDAR channel blockers MK-801 and dextromethorphan have been shown to inhibit tolerance development across a number of studies[92,432,433].

1.7.4 Connecting the GluN2B Subunit to Tolerance Development

Global antagonism of NMDARs produces adverse off-target effects including psychotomimetic effects (hallucinations and dysphoria), and cognitive and motor dysfunction[232,309]. Subunit-selective compounds have shown improved therapeutic efficacy and an improved off-target profile, making them attractive targets for treating NMDAR-mediated pathologies. The GluN2B subunit, in particular, has come into focus as a primary target for developing NMDAR antagonists that show efficacy in the context of pain and analgesic tolerance.

Many studies have demonstrated that while GluN2A and GluN2B have higher expression levels in the cortex compared to GluN2C and GluN2D[434], the GluN2B subunit has a more restricted localization pattern that suggests a contributing role to pain processing and tolerance. This restricted localization may also mean reduced off-target effects. GluN2B is localized primarily on nociceptive primary afferents, in the cortex, and in the spinal cord[324,403,435]. Within the spinal cord, GluN2B is localized to the superficial dorsal horn[232] which is composed of laminae I and II. Mutel *et al*. demonstrated this localization pattern using radiolabeled Ro25-6981[436]. Additionally, Wei *et al*. showed that overexpressed GluN2B in the cortex enhances pain-like behavior in rodents[437]. In addition to localization, mRNA and protein levels of GluN2B are upregulated following chronic administration of morphine[438,439].

As noted earlier, phosphorylation and subsequent sensitization of NMDARs is directly related to tolerance development (**Figure 7**). Although both GluN2A- and GluN2B-containing NMDARs get phosphorylated in pain-processing regions, only tyrosine phosphorylation at GluN2B shows an association with persistent pain after inflammation[440]. In tolerance development, NMDARs are stimulated which causes increased levels of calcium to enter the cell. This calcium influx activates many downstream effector proteins including CaMKII. Once CaMKII is activated, it binds to the GluN2B subunit and this binding locks CaMKII in its activated state. This locking cannot be reversed by phosphatases, so CaMKII is persistently activated[441].

GluN2B-selectve negative allosteric modulators have demonstrated efficacy in producing analgesic effects including reducing or inhibiting hyperalgesia in rodents. In mice, ifenprodil demonstrated increased paw lick latency in the hot plate test and decreased abdominal contractions in the phenylquinone writhing test[212]. Ro25-6981 demonstrated increased paw lick latency in both rats and mice in the hot plate test[442] as well as increased paw pressure threshold in the chronic nerve ligation allodynia model and carrageenan-induced mechanical hyperalgesia model[232]. CP101,606 was tested in rats using the carrageenan-induced mechanical hyperalgesia model and the capsaicin- and 4beta-phorbol-12-myristate-13-acetate (PMA)-induced antinociceptive tests and showed significant analgesic effects[233].

Finally, evidence has demonstrated that GluN2B-selective negative allosteric modulators have efficacy in reducing or inhibiting tolerance. Ko *et al*. demonstrated that chronic co-administration of morphine with Ro25-6981 attenuates analgesic tolerance in mice[442]. Ren *et al*. showed that Con-T[M8Q], a variant of the peptide conantokin-T, attenuated the development of analgesic tolerance to morphine in mice[443]. Allen and Dykstra showed that the competitive antagonist LY-235959 can also attenuate analgesic tolerance[444].

These previous results suggest that GluN2B-selective negative modulation could be an attractive strategy to mitigate tolerance development. Negative modulation of NMDARs decreases the amount of calcium entering the cell, which could decrease phosphorylation of MORs by calcium-activated kinases. Decreasing phosphorylation of MORs could maintain MOR expression at the membrane and therefore maintain opioid efficacy. Therefore, I chose to focus on GluN2B-selective NAMs and assess their efficacy in the context of pain and tolerance in rodents.

1.7.5 The 93 Series Compounds

Development of GluN2B-selective antagonists has resulted in a structurally diverse library of scaffolds. Ifenprodil, traxoprodil, radiprodil and eliprodil all are benzylpiperidine analogues. Since the development of these compounds, other classes of molecules have also been developed including oxamides[445], benzyl cinnamamidines[446], and 5-substituted benzimidazoles[447] among others.

The 93 series is a class of enantiomeric propanolamines that function as potent, noncompetitive GluN2B-selective negative allosteric modulators (NAMs). This class of compounds was identified in a high-throughput screening for GluN2B-selective NAMs. The initial hit and subsequent analogues were first synthesized by Yesim Tahirovic and other members of the Dennis Liotta research group and characterized by members of the Stephen Traynelis research group in the early 2000s[37]. These compounds, particularly 93-4, were shown to be neuroprotective in *in vitro* and *in vivo* models of cerebral ischemia. 93-4 and other compounds also have anticonvulsant properties *in vivo*.

NMDAR antagonists often are limited due to their influence on locomotor activity. Lower doses tend to increase locomotion while the highest doses have an anesthetic effect that can result in complete ataxia[448,449]. Unlike previous NMDAR channel blockers and GluN2B-selective

antagonists, compounds from the 93 series have no effect on locomotion in rodents. Additionally, compounds tested from this class did not show any major off target effects across a panel of glutamate receptors and ligand-gated ion channels such as nicotinic acetylcholine, GABA, and purinergic receptors. These compounds are brain-penetrant and many of them demonstrate an increase in potency as pH decreases, a phenomenon known as pH boost. This characteristic has implications in stroke, cerebral ischemia, traumatic brain injury, and other neuropathies characterized by changes in neuronal pH[398,450]. These compounds are structurally distinct from ifenprodil but bind in the same pocket, at the ATD interface of GluN1 and GluN2B[285,451]. The work in the following chapter highlights one member of the 93 series, 93-108, a novel GluN2B-selective NAM.

Chapter 2. Novel GluN2B-Selective NMDA Receptor Negative Allosteric Modulator Possesses Intrinsic Analgesic Properties and Enhances Analgesia of Morphine in Rodent Pain Models.

2.1 Abstract

Analgesic tolerance is characterized by a decreased response to the analgesic effects of opioids, requiring increasingly higher doses to maintain the desired level of pain relief. Overactivation of GluN2B-containing N-Methyl-D-Aspartate receptors is thought to play a key role in mechanisms underlying cellular adaptation that takes place in the development of analgesic tolerance. Herein, we describe a novel GluN2B-selective negative allosteric modulator, **EU93-108**, that shows high potency and brain penetrance. We describe the structural basis for binding at atomic resolution. This compound possesses analgesic properties in the spinal nerve ligation model of neuropathic pain, and in the tail flick test for thermal pain. EU93-108 has an acute and significant anodyne effect, whereby morphine when combined with EU93-108 produces a higher tail flick latency compared to that of morphine alone. These data suggest that engagement of GluN2B as a target has utility in treatment of pain, and EU93-108 could serve as an appropriate tool compound to interrogate this hypothesis. Future structure-activity relationship work around this scaffold could give rise to compounds that can be co-administered with opioids to diminish the onset of tolerance due to chronic opioid use, thereby modifying their utility.

2.2 Introduction

Drug overdose is the leading cause of accidental death in the United States[452,453]. From April 2021 to April 2022, there were over 100,000 new cases — an increase of nearly 30% compared to the previous year[454]. 75% of these drug overdose cases involved opioids, which remain the most effective treatment available for chronic pain conditions. However, problems such as addiction, physical dependence, analgesic tolerance, and risks of overdose when abused significantly complicate their utility[455]. Nevertheless, opioids remain important therapeutics given the crushing need for effective pain treatment. 1 in 5 people in the US[174,456,457] and globally[458], currently suffers from some form of chronic pain, which causes long-term disability which results in low quality of life, unemployment, anxiety, and depression[459]. Thus, a conundrum exists whereby there is a need for drugs like opioids due to their efficacy, but different aspects of opioid actions also create problems.

To recap, tolerance is a multi-faceted phenomenon that can develop to mitigate the on-target or off-target effects of any drug[246]. Analgesic tolerance to opioids is defined as a decreased response to the analgesic effects of opioids, such as morphine, fentanyl, oxycodone, and hydrocodone with continued use. Over time, the initial dose given becomes ineffective in relieving pain, therefore higher doses must be used to maintain the desired level of analgesia[244,245]. Tolerance to the analgesic effects of opioids can develop within weeks, and continually increasing doses can very quickly and unexpectedly result in fatal overdose[460,461], especially for patients who self-administer opioids[245,246].

In the case of morphine, there are multiple cellular adaptations that contribute to the development of analgesic tolerance following chronic exposure[82,264,462]. This work focuses on one specific adaptation – persistent activation of N-methyl-D-aspartate receptors (NMDARs) in the

brain[429,463,464]. NMDARs[284] **(Figure 4)** are excitatory ionotropic glutamate receptors, expressed in neurons throughout the brain, which mediate a slow Ca^{2+}-permeable component of excitatory synaptic transmission, synaptic plasticity[305,306], learning[307,308], and memory[309,465]. NMDARs are ligand-gated ion channels that are activated by the binding of the co-agonist neurotransmitters glutamate and glycine[317]. Upon ligand binding, if the membrane becomes depolarized sufficiently to relieve Mg^{+2} block, NMDARs can pass considerable currents[322,323,466]. Improper function of NMDARs have been suggested to participate in some fashion in multiple disease states such as Alzheimer's disease[358], Huntington's chorea[359], Parkinson's disease[360], schizophrenia[365,366], epilepsy[467], ischemic brain injury[353,468,469], depression[361,470], and neuropathic pain[356].

Activation of μ-opioid receptors (MORs) by opioids increases NMDAR activity via kinases PKC and Src[429,430,471]. PKC activates Src, which phosphorylates NMDARs at the C-termini of GluN2A and GluN2B subunits, increasing the permeation of calcium into the neuron[472,473]. This increased calcium allows for increased activation of CaMKII and NOS, among others[429,474]. CaMKII desensitizes MORs via phosphorylation[129,475,476], and NOS stimulates production of NO which increases glutamate release[474,477]. This creates a cycle of sustained NMDAR activation and MOR desensitization which ultimately contributes to analgesic tolerance development.

As discussed in the Introduction chapter, the GluN2B subunit is well-studied in the context of neuropathic pain and analgesic tolerance because it is highly expressed throughout the nociception pathway[403,478]. Primary afferents in the skin and tissue respond to noxious stimuli, and that information is transmitted to the spinal cord dorsal horn, specifically the substantia gelatinosa found in lamina II. The signal is then transmitted to the periaqueductal grey, thalamus, somatosensory cortex, and other regions of the brain that process painful stimuli[,51,264,479]. Analysis of mRNA and in situ hybridization in the CNS has shown that the dorsal horn of the spinal cord

has higher mRNA levels of GluN2B compared to the other GluN2 subunits, as well as higher protein expression, which suggests that GluN2B could play a contributing role in this region[232,324,480].

A large body of evidence shows that GluN2B-selective negative allosteric modulators (NAMs) including ifenprodil and Ro-256981, and non-selective channel blockers such as MK-801 and dextromethorphan **(Figure 8)** can inhibit morphine tolerance in rodents[212,432,433]. However, channel blockers, like MK-801 and dextromethorphan, are problematic for clinical use due to strong and complete block of all NMDARs and significant on-target effects. The prototypical GluN2B inhibitor, ifenprodil, has off-target actions on biogenic amine receptors, such as alpha-1-adrenergic receptors[403,481]. To further evaluate and advance the idea that GluN2B inhibitors have utility in pain and can blunt tolerance, it is important to develop and characterize new compounds that will maintain efficacy in reducing tolerance while possessing an improved safety profile.

In this study, we evaluated a novel piperazine-containing GluN2B-selective NMDAR NAM[410,482] for its effects on morphine-induced analgesic tolerance in rodents. We also assessed the actions of a class of enantiomeric propanolamines that function as potent GluN2B-selective NAMs[483]. Previously published compounds in this class display comparable efficacy to previous NAMs and show reduced off-target effects at concentrations up to 10x IC_{50}. Compound **29** in Tahirovic *et al.* (referred to here as EU93-4) is brain penetrant, neuroprotective in *in vitro* and *in vivo* models of cerebral ischemia[450], and did not elicit increased locomotion in rodents. We also evaluated compound **70** in Tahirovic *et al.* (2008), also referred to as EU93-31 (Yuan *et al*., 2015)[398]. These compounds are structurally distinct from ifenprodil, but bind in the same pocket in the ATD of the NMDAR at the interface between the GluN1 and GluN2B subunits[451].

Interestingly, EU93-31 also extends the *n*-butyl chain into the pocket occupied by an unconventional GluN2B-selective inhibitor, EVT-101 **(Figure 8)**[484].
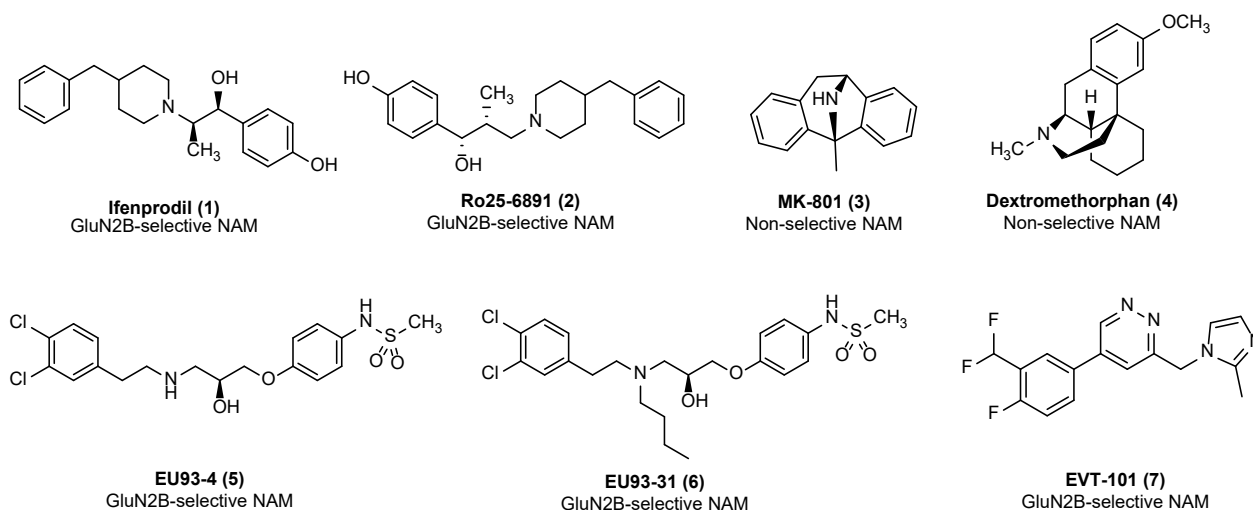
Figure 8. Previously published NAMs of the NMDAR.

2.3 Results

2.3.1 EU93-108 is a potent, GluN2B-selective NMDAR NAM

EU93-108 is a member of a class of piperazine-containing GluN2B inhibitors that show promising properties[410,482]. We assessed EU93-108 for its potency and subunit selectivity across NMDAR subtypes **(Table 1)**. Two-electrode voltage clamp recordings from *Xenopus laevis* oocytes expressing recombinant rat NMDAR subunits were used to determine IC_{50} and the extent of inhibition at 10 μM concentration of EU93-108 for all NMDAR GluN2 subunits. EU93-108 was tested at 10 μM which is 20 times higher than the IC_{50}. Inhibition of GluN2B by EU93-108 is approximately 18-fold higher than that of the other NMDAR subunits, confirming that it is selective for GluN2B **(Table 1)**.

Structure	MW (g/mol)	IC$_{50}$ pH 7.4 (µM)
93-108	441.5	0.557
Mean % Inhibition of EU93-108		
GluN1/GluN2A	**GluN1/GluN2B**	**GluN1/GluN2C**	**GluN1/GluN2D**
4.6 ± 1.5	86.8 ± 6.1	5.3 ± 2.2	4.6 ± 1.2
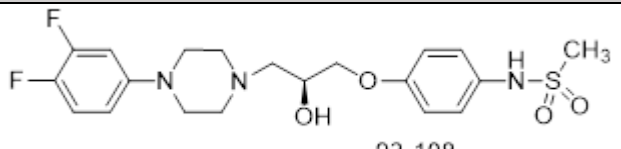
Table 1. EU93-108 is a potent, GluN2B-selective NMDAR NAM. The structure of EU93-108 is shown along with the molecular weight and experimentally determined IC$_{50}$. The percent inhibition of *Xenopus* oocytes expressing recombinant GluN1/GluN2A-D receptors is presented as mean ± SEM. Oocyte experiments were performed with 10 µM EU93-108 in the presence of 100 µM glutamate and 30 µM glycine. n=8 oocytes per NMDAR subtype.

2.3.2 EU93-108 concentration-response curves on diheteromeric and triheteromeric NMDARs

Diheteromeric NMDARs are assembled from GluN1 and only one type of GluN2 subunit (*e.g.,* GluN1/GluN2B), and thus possess two copies of GluN1 and two copies of the same GluN2 subunit. By contrast, triheteromeric NMDARs are assembled from the GluN1 subunit and two different types of GluN2 subunits (*e.g.,* GluN1/GluN2B/GluN2A)[284]. The majority of recombinant studies have utilized diheteromeric receptors, but biochemical and functional data have shown that a large proportion of NMDARs in the CNS are triheteromeric receptors[325,338,339]. Due to the prevalence of triheteromeric NMDARs *in vivo*, we constructed concentration-response curves for EU93-108 in both GluN2B diheteromeric and GluN2B/GluN2A triheteromeric receptors.

Concentration-inhibition curves for EU93-108 were constructed from current responses recorded from *Xenopus* oocytes expressing rat and human diheteromeric (GluN1/GluN2B/GluN2B) NMDARs, as well as from oocytes expressing rat triheteromeric (GluN1/GluN2A/GluN2B) NMDARs **(Figure 9)**. Triheteromeric receptors contained GluN2
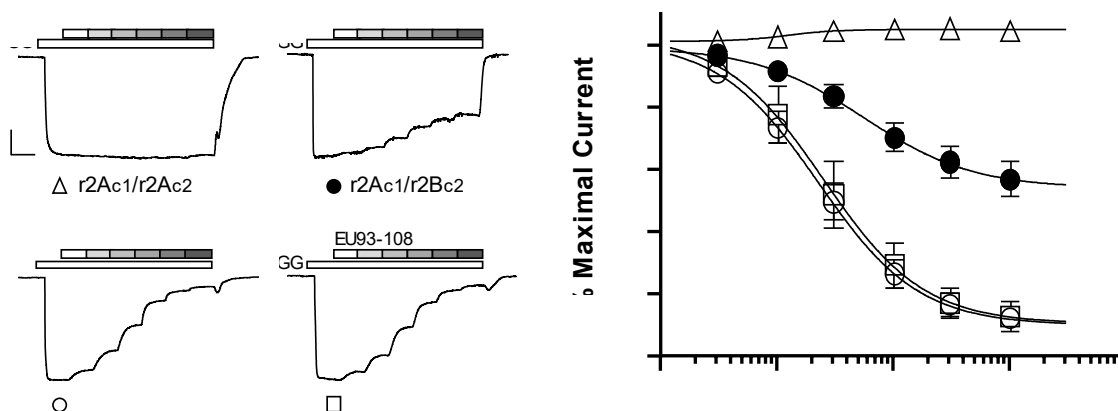
Figure 9. Inhibition of NMDA receptors by EU93-108. **A.** Current response course for maximal receptor activation by 100 µM L-glutamate and 100 µM glycine (GG) and then in the continuous presence of 100 µM L-glutamate and glycine plus increasing concentrations of EU93-108 at 0.03, 0.1, 0.3, 1, 3, and 10 µM are shown for each receptor subunit combination. The receptors tested are diheteromeric rat GluN1/GluN2Ac1/GluN2Ac2 (r2Ac1/r2Ac2), triheteromeric rat GluN1/GluN2Ac1/GluN2Bc2 (r2Ac1/r2Bc2), diheteromeric rat GluN1/GluN2Bc1/GluN2Bc2 (r2Bc1/r2Bc2), and diheteromeric human GluN1/GluN2B/GluN2B (h2B/h2B). All currents were normalized to the maximal response in 100 µM glutamate and glycine, set as 100%. The mean ± SEM for maximal current sizes for r2Ac1/r2Ac2 receptors was 295 ± 44 nA (n=6), for r2Ac1/r2Bc2 receptors 278 ± 39 nA (n=12), for r2Bc1/r2Bc2 receptors 353 ± 77 nA (n=8), and for h2B/h2B receptors 276 ± 63 nA (n=10). **B.** The concentration-effect curve for inhibition by EU93-108 for all four receptor subunit combinations, with same symbols as in (A). The mean ± SEM values are plotted for r2Ac1/r2Ac2 receptors (open triangles, n=6), r2Ac1/r2Bc2 receptors (closed circles, n=12), r2Bc1/r2Bc2 receptors (open circles, n=8), and h2B/h2B receptors (open squares, n=10) with increasing concentrations of EU93-108 applied in the presence of 100 µM glutamate and 100 µM glycine at -40 mV as described in the Methods section. Data collected by Scott Myers, PhD.

subunits with two coiled-coil domains (C1, C2) and an ER retention signal added to the intracellular C-terminal. The interaction of C1 and C2 can mask an exogenous ER retention signal,

thereby allowing only receptors that contain one C1 and one C2 domain to be trafficked to the plasma membrane[485]. The IC_{50} value for EU93-108 at r2Bc1/r2Bc2 receptors was 233 nM (196, 279 nM 95% CI; n=8) and at r2Ac1/r2Bc2 receptors was 543 nM (460, 640 nM 95% CI; n=12). The residual current remaining at 10 µM EU93-108 for r2Bc1/r2Bc2 receptors was 11% (8, 13% 95% CI; n=8) and for r2Ac1/r2Bc2 receptors was 54% (50, 58% 95% CI; n=12) **(Supplemental Table S1; Figure 9)**. As anticipated, EU93-108 was also an effective inhibitor of human diheteromeric GluN2B receptors (h2B/h2B) with an IC_{50} of 26 nM (197, 347 nM 95% CI; n=10) and with a residual current remaining at 10 µM EU93-108 of 12% (9, 15% 95%CI; n=10). Finally, EU93-108 shows no appreciable activity at r2Ac1/r2Ac2 diheteromers exhibiting a residual current at 10 µM of 105% (102, 108% 95% CI; n=6) **(Supplemental Table S1; Figure 9)**.

Taken together, these data demonstrate substantial selectivity for inhibition of GluN2B versus GluN2A NMDA receptors. In addition, EU93-108 is both more potent and can achieve a greater degree of maximal receptor inhibition and in 2B/2B diheteromeric assemblies compared to 2A/2B triheteromeric assemblies, thus potency and efficacy increase as the number of copies of the GluN2B subunit increases from one to two copies per receptor complex. Both IC_{50} potency and maximum % inhibition of r2Ac1/r2Bc2 receptors were significantly different from r2Bc1/r2Bc2 and h2B/h2B receptors by a one-way ANOVA and Tukey's multiple comparison test, $p<0.05$ or better. We also compared concentration-inhibition curves for rat and human 2B/2B assemblies, which show that EU93-108 inhibits rat and human 2B diheteromeric receptors in a similar manner.

An important control for triheteromeric experiments is to confirm that a minimal proportion of receptors contain two copies of GluN2A or two copies of GluN2B. To confirm negligible contribution from diheteromeric receptors, we introduced two mutations (R518K, T690I

for GluN2A and R519K, T691I for GluN2B, referred to as R-K, T-I) into the binding pockets of the GluN2 subunits. By injecting mRNA encoding one C-tagged subunit and the other C-tagged GluN2 subunit with the R-K,T-I mutations functional currents will only be expressed if diheteromeric receptors containing two copies of the subunit lacking the mutations escape the ER and reach the cell surface. By comparing the current amplitude in this situation to that observed for functional triheteromeric receptors, we can estimate the percentage of current that is from diheteromeric receptors **(Supplemental Figure S1)**.

2.3.3 Crystal structure of GluN1b-GluN2B ATD in complex with EU93-108

Once we established that EU93-108 is GluN2B-selective, we next wanted to confirm that this compound binds at the ATD interface of GluN1b and GluN2B, in the same pocket as ifenprodil, EU93-31, and other previously published GluN2B-selective NAMs[285,451].

To ascertain the binding site and pose for EU93-108, we utilized protein crystallography and X-ray diffraction to solve the structure of the isolated GluN1b-GluN2B ATD in complex with EU93-108 at 2.85 Å resolution **(Figure 10, Supplemental Table S2)**. It has been well established that the structure of the isolated ATDs is identical to the ATDs of the intact tetrameric receptors; thus, the EU93-108-bound structure presented here is physiologically relevant **(Figures 10A and 10B)**[285,286,290,392]. Specifically, the GluN1b-GluN2B ATD-EU93-108 structure is similar to the non-active1 conformation of the intact GluN1b-2B NMDARs (RMSD vs. 7SAA = 1.964 Å over 662 Cαs), where the bi-lobe structure (composed of R1 and R2) of GluN2B ATD is closed[486–488]. The quality of the electron density is sufficient for identifying and modeling EU93-108 with confidence **(Figure 10C)**, which permits us to visualize the binding mode precisely **(Figure 10D)**.

The crystal structure revealed the binding site of EU93-108 at the GluN1b-GluN2B ATD heterodimer interface, similar to that of EU93-31 and ifenprodil. Specifically, the binding site involves residues from GluN1b and GluN2B ATDs, especially around the α3 helix from GluN1b and α2' and α6' from GluN2B. The sulfonamide group of EU93-108 forms polar interactions with the backbone amides of GluN2B-Met207 and -Ser208. The phenyl group, the piperazine group, and the difluoro-phenyl group are in van der Walls contacts with residues such as GluN2B-Pro78, -Phe176, -Pro177, -Ile111, and -Phe114 and GluN1b-Phe113, -Ile133, and -Leu135. EU93-108 has similar sets of polar interactions as EU93-31[451] but not ifenprodil[392] **(Figure 10E)**. The van der Walls contacts are similar between EU93-108, ifenprodil, and the backbone of EU93-31 **(Figure 10E)**.

A ATD / LBD / TMD

B GluN1b / GluN2B
NT α2 α3 α1' α2' α6' NT
R1 R2 CT CT R1 R2

C GluN1b GluN2B
α3 α2' α6'

D GluN1b GluN2B
GluN2B-P78, GluN2B-F114, α2', GluN2B-I111, GluN1b-F113, GluN1b-Y109, α3, GluN2B-Q110, GluN1b-I133, GluN2B-M134, GluN1b-L135, GluN2B-P177, GluN2B-S208, GluN2B-F176, α6', GluN2B-M207, GluN2B-E236

E ~90°
EU93-108
EU93-31
Ifenprodil
GluN2B-F114, GluN2B-P78, GluN1b-Y109, GluN1b-F113, GluN2B-P177, GluN2B-E236

Figure 10. Structure of GluN1b-GluN2B ATD in complex with EU93-108. (A) The GluN1b-GluN2B ATD bound to EU93-108 is superposed to the structure of the intact GluN1b-2B NMDAR in complex with glycine and glutamate in non-active1 (PDB code: 7SAA; in gray). GluN1b-R1, GluN1b-R2, GluN2B-R1, and GluN2B-R2 are colored dark orange, light orange, dark cyan, and light cyan, respectively. (B) GluN1b-GluN2B ATD viewed from the eye in panel A. EU93-108 is shown as spheres. (C) FoFc omit map contoured at σ =3.8. (D) The binding site of EU93-108 (purple stick). The interacting residues are shown as sticks. Dash represents polar interaction. (E) Superposition of EU93-108 with ifenprodil (yellow; PDB: 3QEL), EU93-31 (cyan; PDB: 6E7U). Data collected by Hiro Furukawa, PhD and Michael Regan, PhD at Cold Spring Harbor Laboratory.

2.3.4 Determination of intrinsic antinociceptive properties of GluN2B-selective NAMs

After evaluating EU93-108 *in vitro*, we next evaluated a panel of GluN2B inhibitors for their ability to produce an antinociceptive effect using a classical model of pain perception, determination of tail flick latency for mice when their tails are placed in hot water **(Figures 11 and 12)**. The hot water tail immersion test is a well-validated method of assessing reflexive (*i.e.* spinal) pain-like response in rodents[214,215,489,490]. We interpret a drug-induced increase in tail flick latency as analgesia.

The inhibitors were injected i.p. 30 mins prior to a hot water tail immersion test. Four treatment groups and one control group were used (n=8 per group) where the control group received vehicle (10% DMSO, 20% PEG, 2% DMA in water) and groups 1 through 4 were randomly assigned one dose of the appropriate compound.
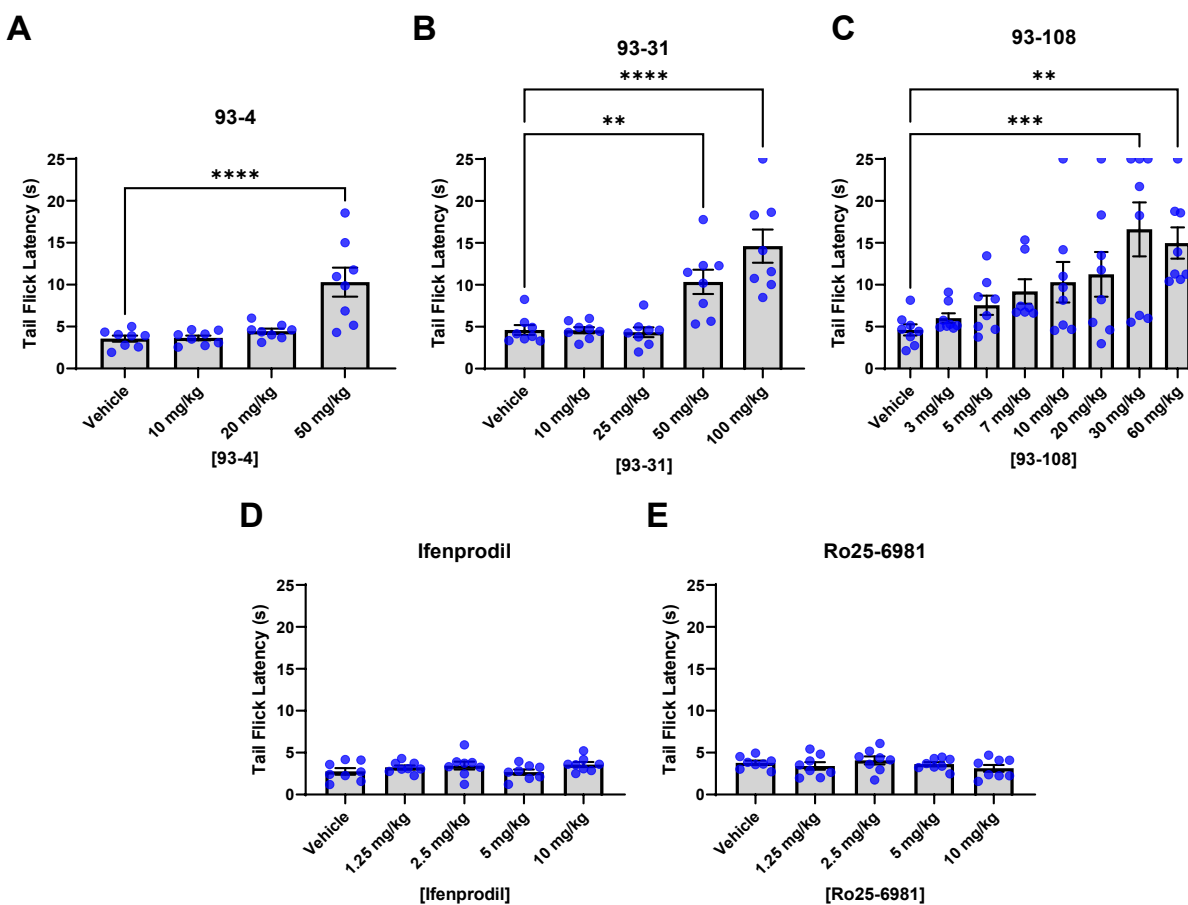
Figure 11. Intrinsic antinociceptive properties of EU93-4 (A), EU93-31 (B), EU93-108 (C), ifenprodil (D), and Ro25-6981 (E) in male C57BL/6J mice. Each dot represents one mouse (n=8 per group) and data are presented as mean ± SEM. Data were analyzed using one-way ANOVA and Dunnet's *post hoc* test for multiple comparisons, where each group was compared to vehicle.

Male mice that received compound EU93-4 displayed significant increases in tail flick latency at 50 mg/kg, the highest dose tested **(Figure 11)**. Mice that received EU93-31 displayed significant increases in latency at the two highest doses tested (50 and 100 mg/kg). Mice that received EU93-108 also displayed significant increases in latency at the two highest doses tested (30 and 60 mg/kg). The mean latency increase in the EU93-108 group was significantly higher than that of the EU93-4 or EU93-31 groups – 16 seconds compared to 10 seconds. Male mice that received ifenprodil, or Ro25-6981 did not display significant increases in latency at the doses

tested. These data suggest that EU93-108 has more potent intrinsic analgesic effects than the other inhibitors tested. Significant latency increases were achieved at a lower dose of EU93-108 compared to EU93-4 or EU93-31 (30 mg/kg compared to 50 mg/kg).
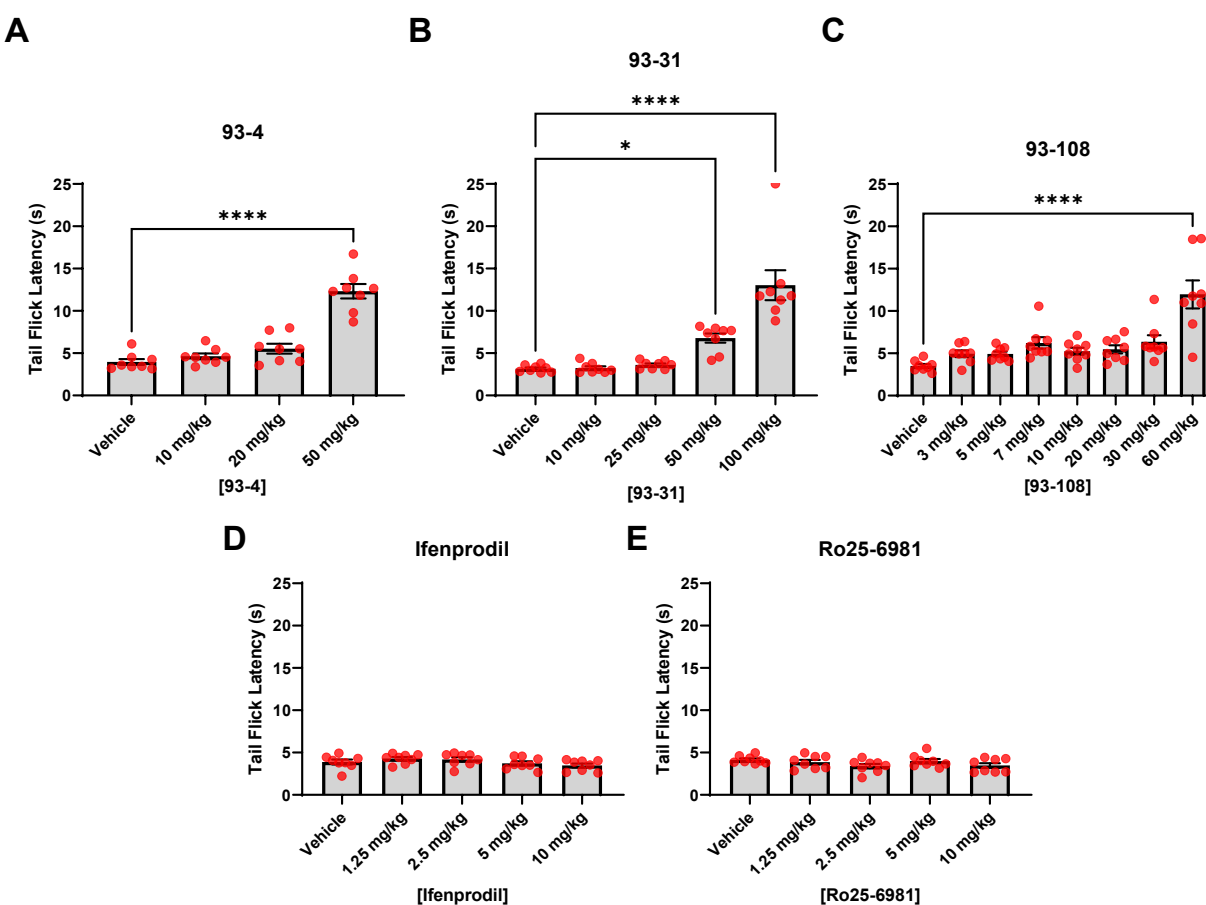
Figure 12. Intrinsic antinociceptive properties of EU93-4 (A), EU93-31 (B), EU93-108 (C), ifenprodil (D), and Ro25-6981 (E) in female C57/Bl6J mice. Each dot represents one mouse (n=8 per group), and data is presented as mean ± SEM. Data was analyzed using one-way ANOVA and Dunnet's *post hoc* test for multiple comparisons, where each group was compared to vehicle.

Female mice that received EU93-4 or EU93-31 displayed significant increases in latency at the highest doses tested for each compound, 50 and 100 mg/kg respectively **(Figure 12)**. Female mice that received EU93-108 also displayed increased latency, but only at 60 mg/kg, the highest dose tested. The mean increase of this group was comparable to the EU93-4 and EU93-31 groups.

As seen in the male mice, ifenprodil and Ro25-6981 did not produce any significant increases in latency at the doses tested. EU93-4 and EU93-31 have similar intrinsic analgesia in male and female mice. However, EU93-108 appears to be more potent in male mice because significant increase in latency was achieved at half the dose in males compared to females (30 mg/kg compared to 60 mg/kg).

2.3.5 EU93-108 decreases mechanical allodynia and has sustained brain and plasma concentrations

Given the direct effect of EU93-108 in the tail immersion test, we explored its actions in male rats in a model of chronic pain that involves an inflammatory component. The Chung Spinal Nerve Ligation (SNL) method[241], first published in 1992, is a well-validated and widely used model of nerve injury and neuropathic pain. Briefly, the method involves tightly ligating either the L5 and L6 spinal nerves, or just the L5 nerve, of an anesthetized rodent. The spinal ligation elicits a strong local inflammatory response causing hypersensitivity in the affected hind paw. This model has been used to investigate a number of analgesic drugs[491–493] and to further elucidate how NMDARs are involved in the development of persistent pain following peripheral nerve injury[494–497].
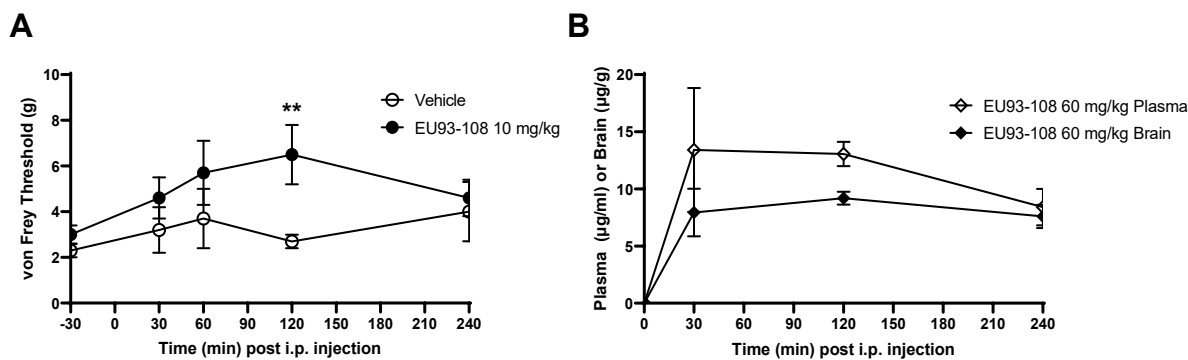
Figure 13. EU93-108 is efficacious in the Chung SNL model of allodynia and has sustained plasma and brain concentrations over 4 hours. The allodynia data (A) compares vehicle (5% DMSO, 50% PEG, 5% DMA in water, open circles) with 10 mg/kg EU93-108 (closed circles). Von Frey testing took place 30 minutes prior to injection and 30-, 60-, 120-, and 240-minutes post injection. Each symbol indicates n=10 rats. (B) EU93-108 concentrations are shown for plasma (open diamonds) and brain (closed diamonds). Brain and plasma concentrations were measured at 0-, 30-, 120-, and 240-minutes post injection. Each symbol indicates n=3 rats. For panels A and B, all injections were given i.p. and results are shown as mean ± SEM. Panel A data collected by Algos Therapeutics in collaboration with Raymond Dingledine, PhD. Panel B data collected by Scott Myers, PhD.

Male Sprague-Dawley rats were used for the experiments shown in Figure 6. For the mechanical allodynia data, 10 mg/kg of EU93-108 was given i.p. and von Frey thresholds were measured 30 minutes prior to injection and at 30-, 60-, 120-, and 240-mins post injection. EU93-108 significantly increased von Frey threshold at 2 hours post injection, suggesting that EU93-108 can decrease mechanical allodynia in male rats. **(Figure 13A)** We tested 10 mg/kg and 60 mg/kg doses of EU93-108 to establish an ED_{50} of approximately 11 mg/kg (data not shown). Because we intended to co-administer this compound with morphine, an intermediate dose of EU93-108 was needed. Therefore, we chose 10 mg/kg for our subsequent studies on analgesia to observe potential enhancement effects.

In a separate experiment, brain and plasma concentrations of EU93-108 were measured 30, 120, and 240 mins following an i.p. injection of 60 mg/kg. Brain concentrations were measured from whole forebrain homogenate at each time point. EU93-108 reached peak concentration 30

mins post injection sustained for the duration of the experiment. EU93-108 reached a C_{max} of 18 µM in brain and 30 µM in plasma after 60 minutes, yielding a brain-to-plasma ratio of 0.6. Due to the minimal decrease in concentration over the course of the 240-minute experiment, the half-life of EU93-108 must be greater than 4 hours **(Figure 13B)**.

2.3.6 Acute morphine and EU93-108 co-administration produce enhanced tail flick latency

After observing that EU93-108 possessed intrinsic antinociceptive properties in both the hot water tail immersion test and in the von Frey apparatus, we chose to focus on this compound for the remaining experiments. We were next interested in evaluating the effects of EU93-108 when given acutely in combination with morphine. 5 mg/kg morphine was chosen because this dose elicited an approximately half-maximal response in our initial morphine dose-response curve **(Supplemental Figure S2)**. This half-maximal response would allow us to see any changes in tail flick latency that EU93-108 might elicit.

Four treatment groups and one control group were used (n=8 per group). The control group received vehicle i.p. (10% DMSO, 20% PEG, 2% DMA in water) plus 5 mg/kg morphine s.c. formulated in normal saline, and groups 1-4 were randomly assigned one dose of EU93-108 i.p. plus 5 mg/kg morphine s.c. The doses used were the same as in the intrinsic analgesia experiments.
`
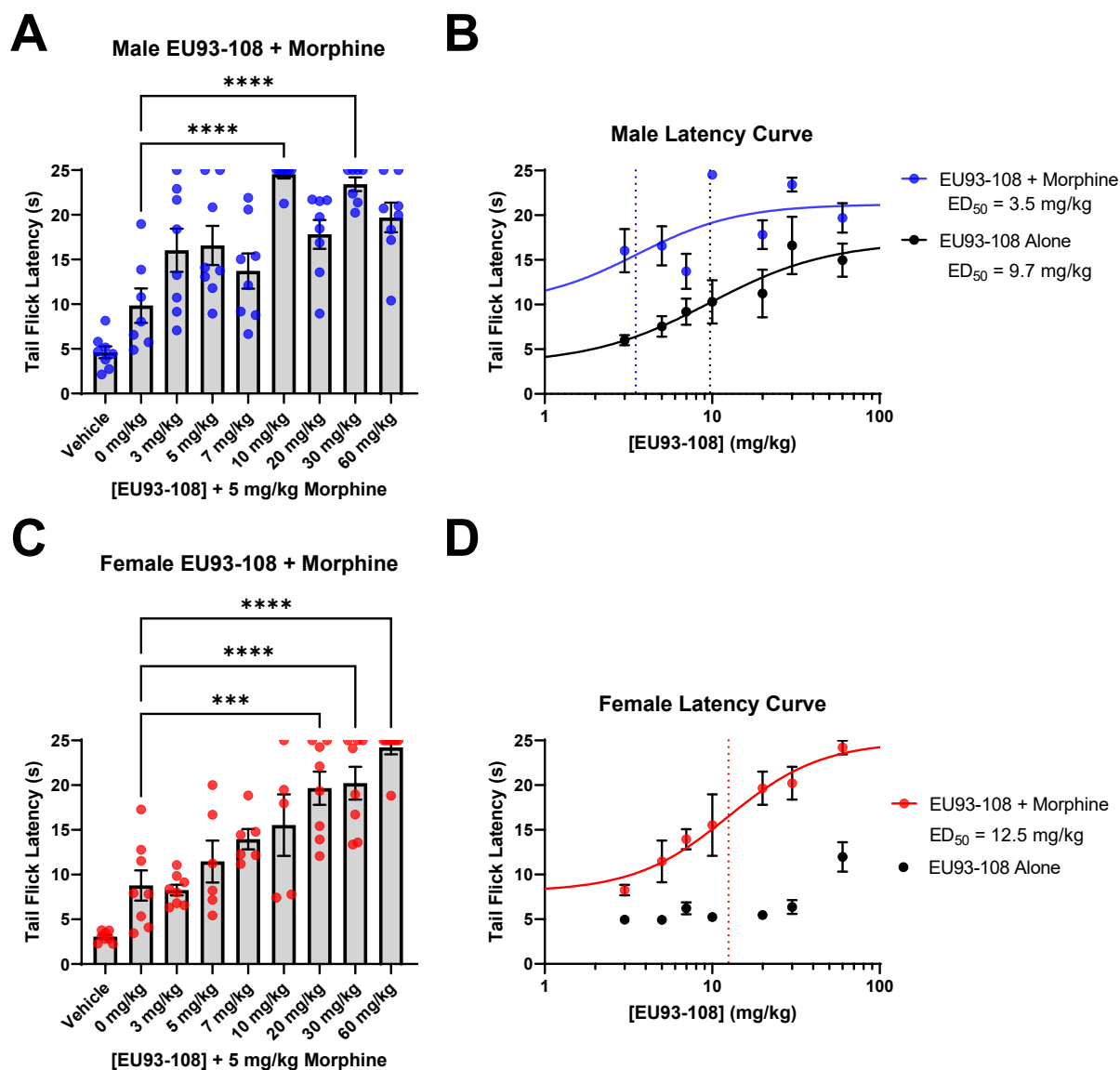
Figure 14. (A and C) Acute co-administration of EU93-108 and 5 mg/kg of morphine in male (A, blue circles) and female (C, red circles) mice. Each dot in panels A and C represents one mouse (N=8 per group). Data were analyzed using one-way ANOVA and Tukey's *post hoc* test for multiple comparisons, where all groups were compared to each other. (B and D) Fitted dose-response curves for EU93-108 in male (B) and female (D) mice. The dotted lines depict estimated ED_{50} values. All data are presented as mean ± SEM.

A dose-dependent increase in tail flick latency was observed in both male and female mice. In male mice, the highest tail flick latency was observed when 10 mg/kg of EU93-108 was combined with 5 mg/kg of morphine **(Figure 14A)**. The majority of mice in this group did not

have a tail flick response within 25 seconds in three consecutive tests (*i.e.,* maximal analgesia). 10 mg/kg was the lowest dose that significantly increased latency in male mice. **Figure 8B** depicts the fitted ED_{50} curves for EU93-108 with and without morphine in male mice. In male mice, EU93-108 is approximately 3-fold more potent when combined with morphine versus EU93-108 alone **(Figure 14B)**. In female mice, the lowest dose of EU93-108 that significantly increased latency was 20 mg/kg **(Figure 14C)**. The effect of EU93-108 in female mice was less variable than male mice, and apparently more robust. However, the estimated ED_{50} for EU93-108 plus morphine in female mice was higher than in male mice, suggesting that lower doses of EU93-108 may be more efficacious in male mice compared to female mice. The data for EU93-108 alone in female mice did not yield a sufficient curve and was therefore not fitted **(Figure 14D)**.

2.3.7 EU93-108 has sedative effects at high doses

Some NMDAR antagonists can impact locomotor behavior in animals[448,498,499]. Lower doses have minimal impact while high doses can have anesthetic action that can produce complete immobility. We evaluated this potential side effect in a locomotor assay using a range of doses of EU93-108. We used these data along with the previously described data in Figures 10, 11, and 13 to choose a target dose to use for the chronic morphine administration/tolerance experiments shown in **Figures 17 and 19**. We defined a target dose as that exhibits enhancement in tail flick latency when combined with morphine, while showing little to no effect on locomotor activity.
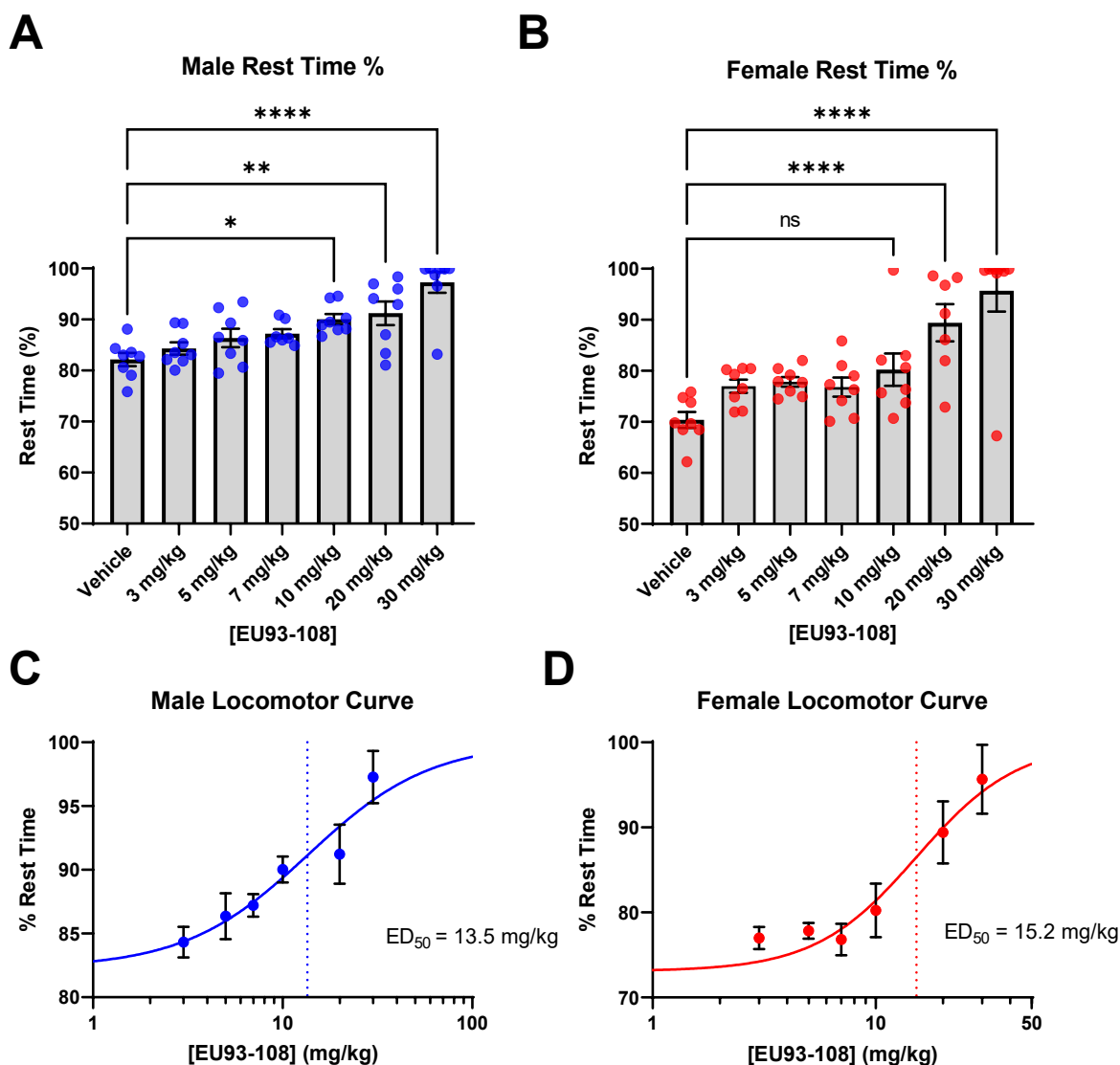
Figure 15. Rest time data for EU93-108 in male (A, blue circles) and female (B, red circles) mice. Rest time percentage was used to calculate dose-response curves for males and females (C and D respectively). Each circle in A and B represents one mouse (n=8 per group), while each circle in C and D represent the mean ± SEM of all 8 mice for each group. The dotted lines depict estimated ED_{50} values. Data were analyzed using one-way ANOVA and Dunnet's *post hoc* test for multiple comparisons, where each group was compared to vehicle.

In both males and females, we observed dose-dependent decreases in total distance traveled, number of movements made, and percentage of time spent moving **(Supplemental**

Figure 3). Conversely, we observed a dose-dependent increase in percentage rest time **(Figures 15A and 15B)**. Groups that received 30 mg/kg of EU93-108 showed sedation, with rest time increasing from 72% to on average 99% of the experiment time. We used rest time percentage to calculate the sedation ED_{50} curves shown in Figure 8C and 8D. ED_{50} values were similar for males and females **(Figures 15C and 15D)**.

2.3.8 Chronic co-administration of morphine with EU93-108 did not inhibit development of tolerance

Given that acute doses of EU93-108 increase tail flick latency in the presence and absence of morphine, we subsequently assessed changes in tail flick latency when given chronically (*i.e.,* multiple injections over multiple days). Specifically, we were interested in whether the presence of EU93-108 would inhibit the development of analgesic tolerance to morphine.

To decide on a target dose for the chronic administration studies, we used the difference between our tail flick latency ED_{50} and locomotor activity ED_{50} as the therapeutic window between increase in tail flick latency (*i.e.,* analgesia) and sedation. For males, the ED_{50} of analgesia with morphine was 3.5 mg/kg **(Figure 14)** and the ED_{50} of sedation was 13.5 mg/kg **(Figure 15)**. We chose 10 mg/kg EU93-108 because that dose falls within the therapeutic window, it yielded maximal analgesia with morphine, and it is below the ED_{50} of the sedation curve. We know from our previous data that females require higher doses to achieve the same effects seen in males. In our tail flick data, we saw that females required twice the dose needed for males, so we selected 20 mg/kg EU93-108 for testing in female mice.
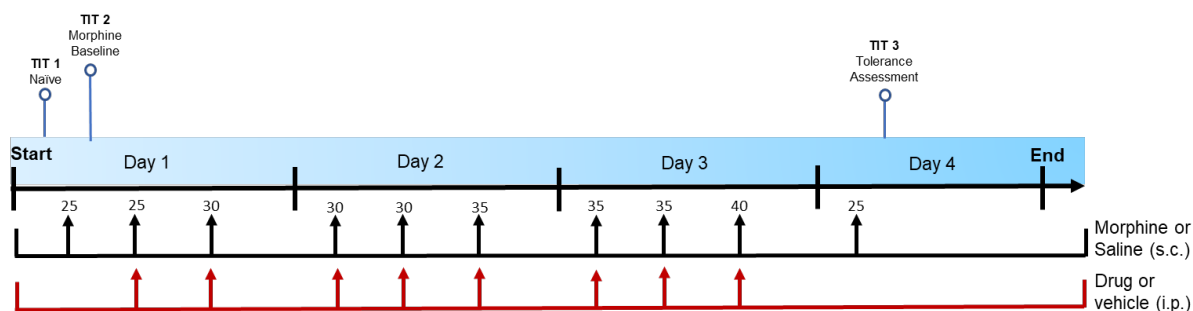
Figure 16. Morphine analgesic tolerance "stair stepping" dosing regimen. TIT = tail immersion test. On day 1, TIT was conducted to determine baseline latencies for all mice. On days 1 through 3, each mouse was administered morphine s.c. three times per day at doses increasing from 25 mg/kg to 40 mg/kg at 8:00am, 12:00pm, and 4:00pm. Doses of morphine are shown above the arrows, in mg/kg. Mice were also randomly assigned to receive either vehicle, one dose of EU93-108 (10 mg/kg for males and 20 mg/kg for females), or one dose of ifenprodil (10 mg/kg for males and 20 mg/kg for females), i.p. at the same time points. Each mouse received an i.p. injection of drug or vehicle followed by a sc. injection of morphine or saline. On day 4, each mouse was challenged with the minimum dose of morphine (25 mg/kg) 30 mins prior to a tail immersion test.

To assess whether EU93-108 had an inhibitory effect on the development of morphine tolerance, four groups were used (n=8 per group): vehicle/saline, vehicle/morphine, ifenprodil/morphine, and EU93-108/morphine. Morphine tolerance was induced using repeated administration of increasing doses of morphine from 25 mg/kg to 40 mg/kg three times a day at 3 to 4-hour intervals over three consecutive days **(Figure 16)**. This procedure was adapted from previous publications[500–502].

A

B
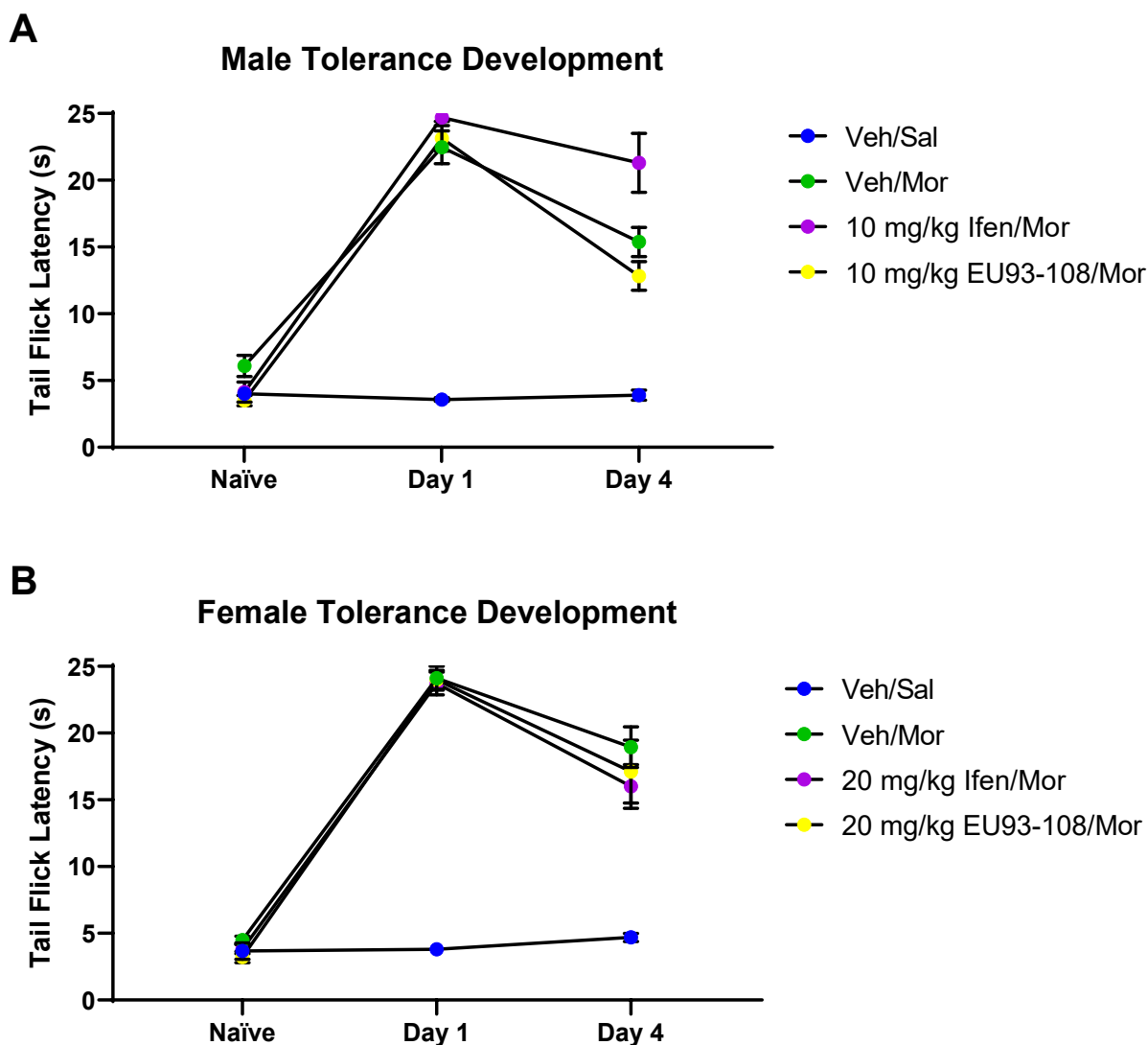
Figure 17. Effects of co-administration of EU93-108 and morphine on tolerance development in male (A) and female (B) mice. Mice received either vehicle and saline (blue circles), vehicle and morphine (green circles), ifenprodil and morphine (purple circles) or EU93-108 and morphine (yellow circles). Naïve indicates latencies prior to the first morphine dose. Day 1 indicates latencies after first morphine dose and day 4 indicates latencies after final morphine dose once tolerance has developed. Each circle represents n=8 mice and data are presented as mean ± SEM.

The vehicle/morphine groups, which were the tolerance controls, successfully developed a tolerance phenotype, as shown by the decrease in latency on day 4 compared to day 1 **(Table 2)**.

In both male and female experiments, EU93-108 failed to inhibit the development of tolerance when co-administered with morphine three times a day for three consecutive days **(Figure 17)**.

Male Mice				
Comparison	Paired or unpaired?	Unadjusted p value	Bonferroni corrected p value	Significant after adjustment?
Day 4 108/mor - Day 1 108/mor	Paired	0.0004	0.0016	Yes
Day 4 veh/mor - Day 1 veh/mor	Paired	0.0043	0.0172	Yes
Day 4 ifen/mor - Day 1 ifen/mor	Paired	0.139	0.558	No
Day 4: 108/mor - veh/mor	Unpaired	0.118	0.47	No
Female Mice				
Comparison	Paired or unpaired?	Unadjusted p value	Bonferroni corrected p value	Significant after adjustment?
Day 4 108/mor - Day 1 108/mor	Paired	0.0317	0.127	No
Day 4 veh/mor - Day 1 veh/mor	Paired	0.0156	0.0624	No
Day 4 ifen/mor - Day 1 ifen/mor	Paired	0.0003	0.0012	Yes
Day 4: 108/mor - veh/mor	Unpaired	0.553	2.21	No

Table 2. P values for tolerance development experiments (Figure 9). For male and female mice, all relevant comparisons were analyzed using paired or unpaired Student's t-tests as appropriate. T-tests were followed by Bonferroni correction where each p-value was multiplied by the total number of comparisons made, yielding an adjusted p-value. We also indicated whether the adjusted p-values were significant (<0.05).

2.3.9 Co-administration of EU93-108 and morphine slows worsening of pre-established tolerance

We next wanted to assess EU93-108 for effects on other facets of tolerance. Specifically, we were interested in whether EU93-108 could increase tail flick latency in mice that are already tolerant to morphine (*i.e.,* pre-established tolerance). To assess the effect of EU93-108 on pre-established tolerance, five groups were used (n=8 per group): vehicle/saline, vehicle/morphine, ifenprodil/morphine, EU93-108/saline and EU93-108/morphine. All groups except for the vehicle/saline control group were administered morphine three times per day (according to the stair stepping protocol outlined in **Figure 18**) at gradually increasing doses from 25 mg/kg to 40

mg/kg three times a day at 3 to 4-hour intervals for three consecutive days until tolerance was

observed on day 4 **(Figure 19, black circles)**.
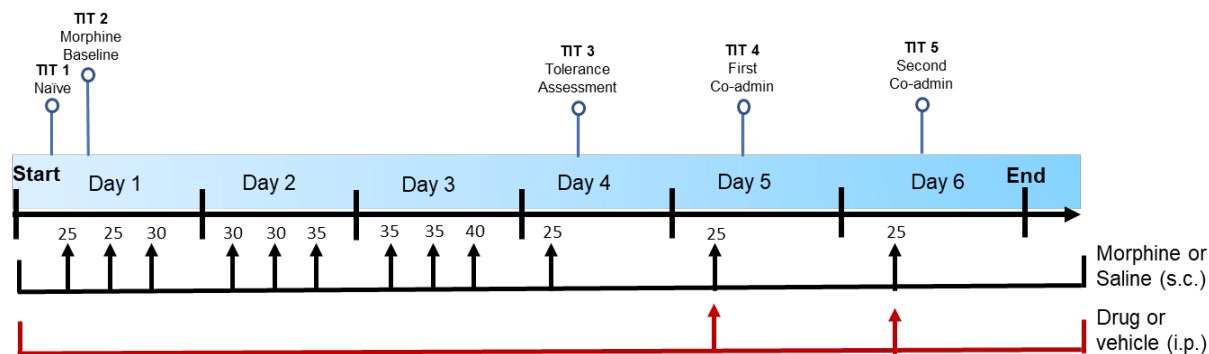
Figure 18. Dosing regimen to assess effects of EU93-108 on tolerant mice. TIT = tail immersion test. All mice received morphine or saline three times a day according to the protocol in Figure 9. Doses of morphine are shown above the arrows, in mg/kg. Once tolerance was established on day 4, mice were randomly assigned to receive either vehicle, EU93-108, or ifenprodil once a day for two consecutive days. TIT was conducted at the same time points as in Figure 9 and 30 minutes after injection on days 5 and 6.

Once tolerance was established, mice were randomly assigned to receive either vehicle, EU93-

108, or ifenprodil once a day for two consecutive days **(Figure 19)**. The doses differed between

males and females: males received 10 mg/kg EU93-108 and 10 mg/kg ifenprodil, while females

received 20 mg/kg EU93-108 and 20 mg/kg ifenprodil. Tail immersion tests were conducted 30

minutes post injection of EU93-108 or ifenprodil on days 5 and 6.
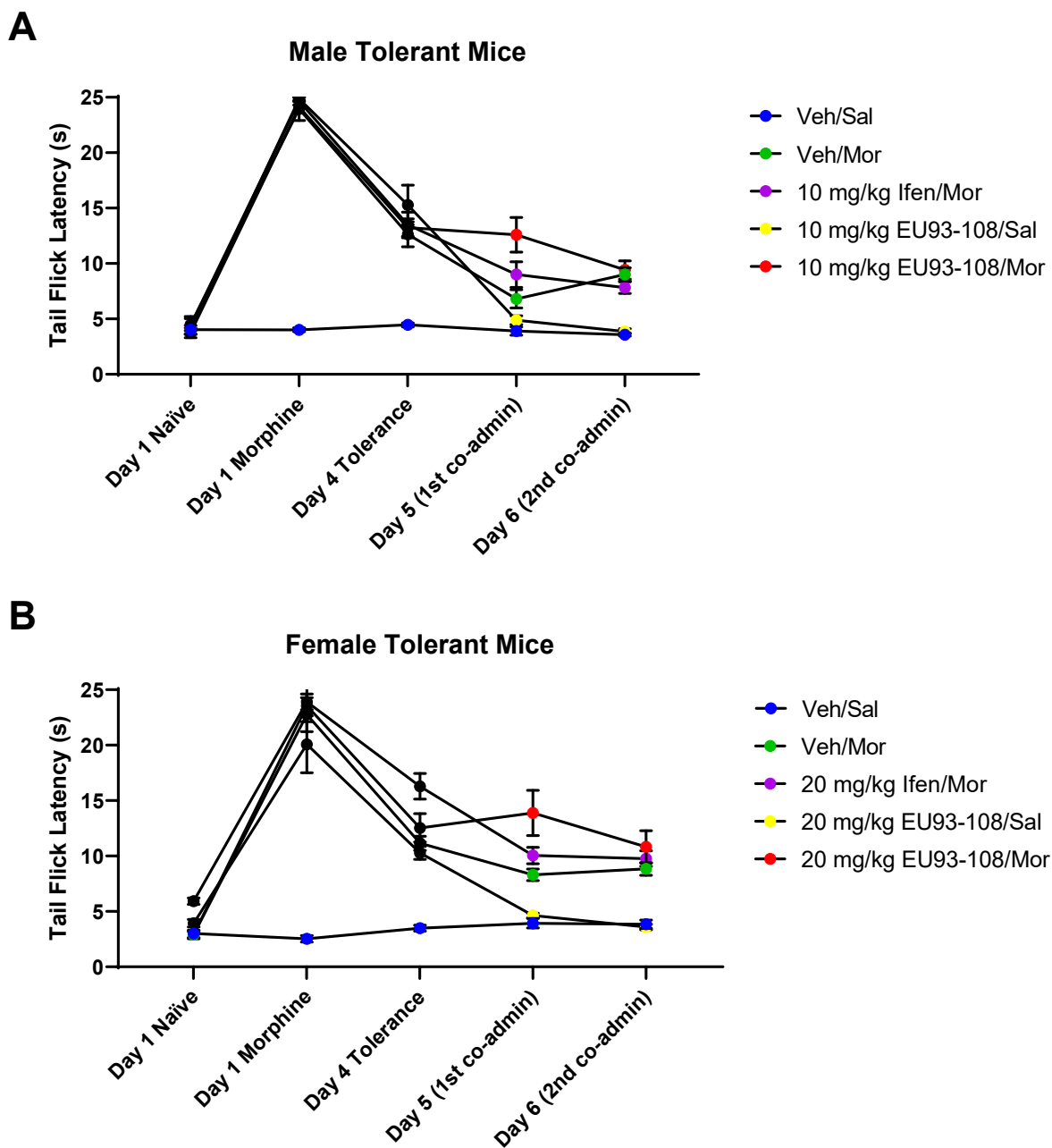
Figure 19. Effects of EU93-108 on tolerant male (A) and female (B) mice. Black circles show that all mice were treated the same and given only morphine to establish tolerance on days 1 through 4. Once tolerance was established (Day 4 Tolerance), mice were randomly assigned to receive either vehicle and morphine (green circles), ifenprodil and morphine (purple circles), EU93-108 and saline (yellow circles) or EU93-108 and morphine (red circles). Blue circles depict mice that did not receive any drug for the duration of the experiment. For the male mice, the dose of ifenprodil and EU93-108 was 10 mg/kg, and for female mice the dose was 20 mg/kg. Days 1

through 4 depict tolerance development. Days 5 and 6 represent latencies 30 minutes after the first and second co-administrations, respectively.

Male and female mice in all groups successfully developed tolerance over days 1 through 4 **(Figure 19, black circles)**. The vehicle/morphine, ifenprodil/morphine and EU93-108/saline latencies all continued to decrease on day 5 **(Table 3)**, followed by a plateau on day 6. The EU93-108/saline group showed the most significant decrease in latency and plateaued at values equivalent to the vehicle/saline baseline. In contrast, the EU93-108/morphine group did not show a further decrease in latency on day 5, meaning the latencies on days 4 and 5 were equivalent. The EU93-108/morphine group also had the highest latency on day 5 compared to the other groups. In the male mice, this increase in latency was only seen on day 5, whereas in females the effect remained constant through day 6. Morphine alone and EU93-108 alone did not increase tail flick latency in tolerant mice, but EU93-108 plus morphine did increase latency. This suggests that EU93-108 requires co-administration with morphine to slow the worsening of the tolerance phenotype in tolerant mice.

| Male Mice				
Comparison	Paired or unpaired?	Unadjusted p value	Bonferroni corrected p value	Significant after adjustment?
Day 4 108/Sal - Day 5 108/Sal	paired	0.0024	0.012	Yes
Day 4 108/Mor - Day 5 108/Mor	paired	0.711	3.55	No
Day 4 Veh/Mor - Day 5 Veh/Mor	paired	0.0252	0.126	No
Day 5: 108/Mor - 108/Sal	unpaired	0.0004	0.002	Yes
Day 5: 108/Mor - Veh/Mor	unpaired	0.0268	0.134	No
Female Mice				
Comparison	Paired or unpaired?	Unadjusted p value	Bonferroni corrected p value	Significant after adjustment?
Day 4 108/Sal - Day 5 108/Sal	paired	0.0002	0.001	Yes
Day 4 108/Mor - Day 5 108/Mor	paired	0.543	2.72	No
Day 4 Veh/Mor - Day 5 Veh/Mor	paired	0.0035	0.0175	Yes
Day 5: 108/Mor - 108/Sal	unpaired	0.0003	0.0015	Yes
Day 5: 108/Mor - Veh/Mor	unpaired	0.0146	0.073	No

Table 3. P values for tolerant mice experiments (Figure 18). All relevant comparisons were analyzed using paired or unpaired Student's t-tests as appropriate. T-tests were followed by Bonferroni correction where each p-value was multiplied by the total number of comparisons made, yielding an adjusted p-value. We also indicated whether the adjusted p-values were significant (<0.05).

2.3.10 Off-Target Effects of EU93-108

EU93-108 was further examined for its behavior against common off-target receptors. First, selectivity for GluN2B over other ion channels in the brain was examined via two-electrode voltage clamp recordings of *Xenopus* oocytes expressing AMPA, kainate, nicotinic acetylcholine, serotonin, GABA, glycine, and ATP receptors. Current responses were tested with saturating concentrations of agonist in both the absence and presence of 10 μM EU93-108, and confirmed selectivity for GluN2B-containing NMDA receptors over AMPA, kainate, GABA, glycine, ATP, and 5-HT3A receptors **(Supplemental Table S3).**

Compound EU93-108 was also tested for inhibition of binding of probes to a range of GPCRs and other targets **(Table 4 and Supplemental Table S4)**. We found that EU93-108 has multiple off-target receptor interactions, some of which are consistent with liabilities of previously described GluN2B-selective NAMs including ifenprodil[396,398,407,447,503,504]. EU93-108 produced significant displacement of binding probes for the 5-HT$_2$ receptors and alpha-1-adrenergic receptors, as well as D$_3$, H$_1$, and σ$_1$ receptors.

Concentration-response binding competition curves for these targets were used to determine K$_i$ values **(Table 4)**. Given that the brain concentration of EU93-108 achieved 30 minutes post i.p. injection is 18 μM **(Figure 13)**, the doses that yield our desired antinociceptive effects may engage some of the receptors listed in Table 4.

Receptor	Log(K$_i$)	K$_i$ (nM)	K$_i$/IC$_{50}$ of 93-108 (nM)	Receptor	Log(K$_i$)	K$_i$ (nM)	K$_i$/IC$_{50}$ of 93-108 (nM)
5-HT$_{2A}$	-6.31	490	0.88	Alpha$_{2B}$	-6.14	728	1.31
5-HT$_{2B}$	-6.01	976	1.75	Alpha$_{2C}$	-6.06	862	1.55
5-HT$_{2C}$	-5.74	1825	3.28	D$_3$	-6.72	190	0.34
Alpha$_{1A}$	-6.77	170	0.31	H$_1$	-6.59	254	0.46
Alpha$_{1D}$	-6.44	359	0.65	Sigma$_1$	-6.3	505	0.91
Alpha$_{2A}$	-5.94	1151	2.07				

Table 4. Secondary Off-Target Screen. Dose-response curves were constructed for any receptors that showed 50% or greater mean inhibition in a primary high-throughput screen (Supplemental Table S4). The associated K$_i$ values are shown along with the ratio of K$_i$ to the IC$_{50}$ for EU93-108 (555 nM). Ratios less than 1 correspond to receptors that EU93-108 has a higher affinity for compared to GluN2B-containing NMDARs. These constitute the strongest off-target effects.

2.4 Discussion

The 93 series is a class of potent, brain penetrant, GluN2B-selective NAMs. These compounds have shown utility as *in vitro* and *in vivo* tool compounds but have never been evaluated in the context of pain and opioid tolerance. We report a novel and potent GluN2B-

selective NMDAR inhibitor, EU93-108, and explore the structural basis for its binding to the GluN1/GluN2B NMDAR ATD using X-ray crystallography. This compound is highly brain penetrant and maintains high brain and plasma concentrations for at least 4 hours post i.p. injection. EU93-108 possesses intrinsic analgesic properties in the Chung spinal nerve ligation model of allodynia and the rodent tail immersion test. We also observed a significant, acute enhancement in tail flick latency where the combination of EU93-108 and morphine yielded higher latencies compared to either compound alone. This combination also transiently slowed worsening of tolerance in tolerant mice.

Limitations of EU93-108 include several off-target interactions, some of which have previously been described as liabilities for other GluN2B-selective NAMs. The strongest interactions were at alpha-1-adrenergic, D_3, H_1, and 5-HT_2 receptors. Among the interactions observed, the sedative effect seen in the locomotor data may reflect inhibition of the H_1 histamine receptor and could complicate use of this compound as a tool for *in vivo* experiments.

The favorable effects of EU93-108 appear to be acute as opposed to chronic or cumulative. The most promising data shown in this study corresponds to the immediate effects of EU93-108, either at T_{max} (30 mins), or in the allodynia data, up to 4 hours post-injection. In the tolerance development experiments shown in **Figure 11**, we did not observe any cumulative effect of multiple doses of EU93-108 when the mice were assessed for tolerance.

Another interesting aspect of EU93-108 is that it has opposite effects in tolerant versus non-tolerant mice when given alone, whereas with morphine it has similar acute effects in either case. In **Figures 4-6**, we showed that EU93-108 alone can increase analgesia in non-tolerant mice. However, once mice have developed tolerance to morphine, administering EU93-108 without morphine appears to further exacerbate tolerance **(Figure 19, yellow circles)**. When EU93-108 is

co-administered with morphine, we observed enhancement of morphine-induced analgesia in non-tolerant mice, as well as an acute plateau of tolerance in tolerant mice. In both cases, the combination of EU93-108 and morphine yielded favorable effects.

The potency of EU93-108 is sex-dependent, with males requiring lower doses than females for the same effect. Two potential explanations for this sexual dimorphism that have been quantified in the literature are differences in cytochrome P450 (CYP) expression and differences in analgesia. It is well documented that male and female mice have differential expression of several CYP enzymes[505–507]. For example, CYP2D9 is almost exclusively expressed in male mice[505], whereas CYPs 2B9 and 2B13 are almost exclusively expressed in female mice[505]. CYP3A4, the isoform responsible for approximately 50% of phase-I metabolism of drugs, shows higher expression and activity in female mice[508]. This could suggest that EU93-108 is cleared faster in female mice and therefore more frequent dosing might be needed to see increased analgesic effects. CYP reaction phenotyping of EU93-108 would be needed to explore this idea further.

Pain tolerance and analgesia differ between strains of mice[509] and between sexes[509–512]. Female mice tend to have lower pain tolerance than males[509,510,513]. Opioids such as morphine also have higher potency in male mice compared to female mice[510,511,514]. This suggests that female mice might require higher doses of opioids compared to male mice. Additionally, morphine is metabolized faster in female mice[515]. This is primarily due to increased activity of UGT2B7, the primary UDP-glucuronosyltransferase that metabolizes morphine into its two main metabolites, M3G and M6G[516–518]. This suggests that elimination of drugs is accelerated in female mice, therefore more frequent dosing of opioids or other analgesics might be required to achieve the same level of pain relief observed in males.

This work introduces a promising tool compound on which to base future structure-activity relationship (SAR) studies. The insights gained from EU93-108 help to create a blueprint for the next generation of GluN2B-selective inhibitors, highlighting aspects of GluN2B negative modulation that are beneficial and some that are detrimental in the context of pain relief. We have demonstrated that negative modulation of GluN2B can both increase analgesia in the absence of an opioid and enhance the analgesic properties of an opioid with co-administration. These are aspects that need to be maintained in the next generation of compounds based on this scaffold. Conversely, EU93-108 has several off-target liabilities, therefore the next iteration of inhibitors must possess an improved off-target profile. Ultimately, this new generation of GluN2B-selective NAMs may be evaluated for clinical use alongside opioids. These candidates would be co-administered with opioids to enhance their effect, which would decrease the dose of opioid needed for suitable analgesia. Decreasing opioid dose could decrease the rate of development of tolerance and decrease risk of physical dependence and addiction with chronic use.

2.5 Materials and Methods

Chemicals

Buffers, salts, agonists, and ifenprodil-(+)-tartrate salt were purchased from Millipore Sigma. Morphine sulfate was purchased from McKesson Medical Surgical. All other compounds were synthesized at Emory according to published methods or as described below. Ifenprodil was formulated in 10% DMSO, 20% PEG, 2% DMA in water. Morphine sulfate was formulated in a 0.9% saline solution. All 93 series compounds were formulated in 10% DMSO, 20% PEG, 2% DMA in water.

General 93 Series Synthesis[483]
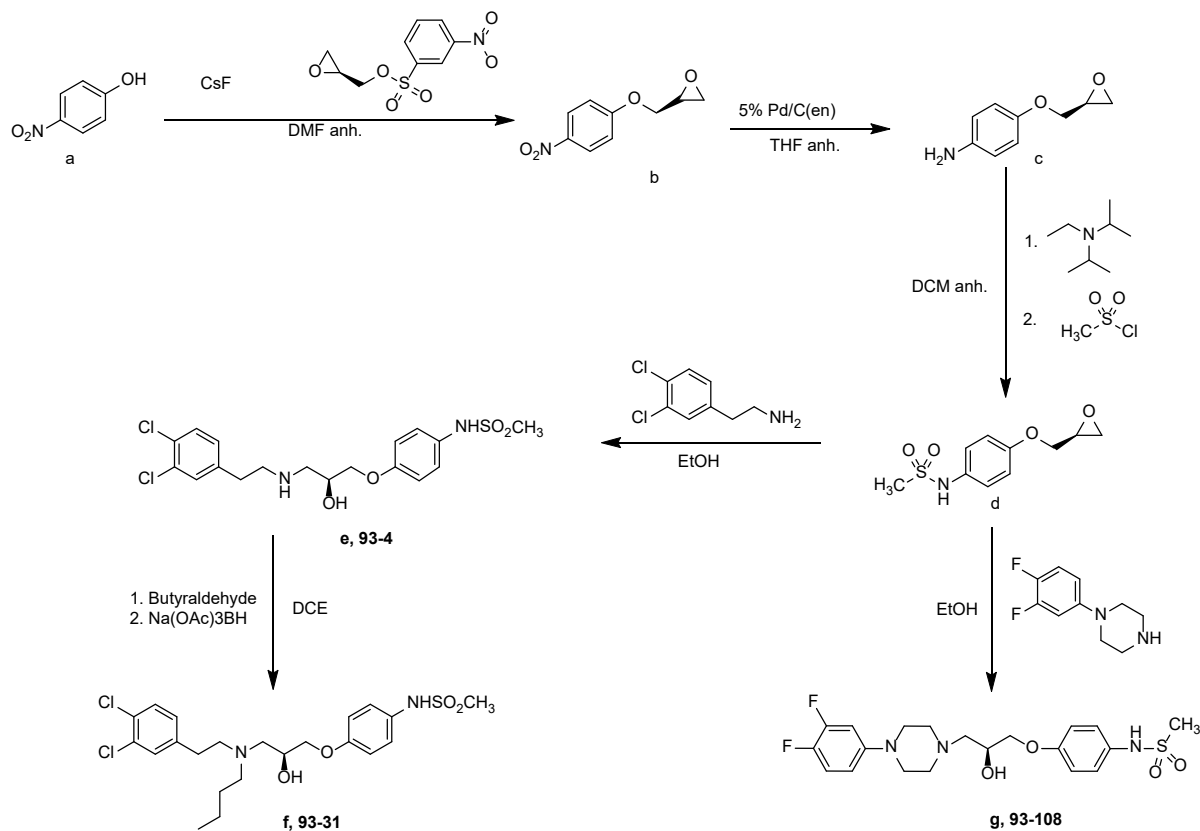
Scheme 1. 93 series synthesis. Para-nitrophenol was combined with (S)-(+)-glycidyl nosylate and cesium fluoride to afford the nitro intermediate, b. The nitro group was reduced to an amine using poisoned palladium on carbon. The unstable amine was immediately combined with N,N-diisopropyl-N-ethyl amine and methane sulfonylchloride to afford the sulfonamide intermediate, d. The sulfonamide was combined with 3,4-dichlorophenethylamine under reflux conditions to afford EU93-4. EU93-31 was afforded by combining EU93-4 with the appropriate aldehyde and sodium triacetoxyborohydride. EU93-108 was synthesized by combining the previous sulfonamide intermediate, d, and 1-(3,4-difluorophenyl)piperazine in ethanol under reflux conditions.

The compounds EU93-4 and EU93-31 (Scheme 1) were synthesized according to previously published methods[450,519,520].

Synthesis of EU-93-108 ((S)-N-(4-(3-(4-(3,4-difluorophenyl)piperazin-1-yl)-2-hydroxypropoxy)phenyl)methanesulfonamide):

93-108
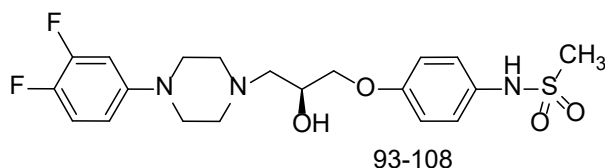
N-[4-[[(2S)-Oxiran-2-yl]methoxy]phenyl]methanesulfonamide (75 mg, 0.31 mmol) and 1-(3,4-difluorophenyl)piperazine (61 mg, 0.31 mmol) were dissolved in ethanol (5 mL) and heated at reflux for 3-4 hours. The reaction mixture was then cooled to rt, and the solvent was evaporated in vacuo. The remaining residue was then purified via column chromatography on silica gel using

0-30% 90:10:0.5% DCM:methanol:NH$_3$ in DCM to yield N-[4-[(2S)-3-[4-(3,4-difluorophenyl)piperazin-1-yl]-2-hydroxy-propoxy]phenyl]methanesulfonamide (82 mg, 0.19 mmol in 60 % yield).

^{1}H NMR (500 MHz, CDCl$_3$): δ 7.20 – 7.12 (m, 2H), 7.02 (dt, J = 10.3, 9.2 Hz, 1H), 6.91 – 6.85 (m, 2H), 6.69 (ddd, J = 13.3, 6.8, 2.9 Hz, 1H), 6.60 – 6.53 (m, 1H), 4.15 – 4.09 (m, 1H), 4.00 – 3.92 (m, 2H), 3.15 – 3.10 (m, 4H), 2.92 – 2.89 (m, 3H), 2.84 – 2.77 (m, 2H), 2.68 – 2.59 (m, 3H), 2.56 (dd, J = 12.5, 3.8 Hz, 1H). ^{13}C NMR (126 MHz, CDCl$_3$): δ 156.96, 150.24, 148.20, 144.35, 129.74, 124.34, 115.45, 111.53, 109.98, 105.44, 70.49, 65.67, 60.40, 53.13, 49.54, 38.76. HRMS calc'd for C26H26O4N3F2S 442.16066; found 442.16148 [M+H].

Two-Electrode Voltage Clamp Recordings from Xenopus laevis Oocytes

Rat cDNA encoding GluN1-1a, (GluN1, RefSeq NP_058706), GluN2A (NP_036705), GluN2B (NP_036706), GluN2C (NP_036707), and GluN2D (NP_073634) were obtained from Drs. S. Heinemann (Salk Institute), S. Nakanishi (Kyoto University), and P. Seeburg (University of Heidelberg). cRNA was transcribed in vitro from linearized plasmids containing NMDAR cDNAs according to manufacturer's instructions (mMessage mMachine, Ambion; ThermoFisher Scientific, Waltham, MA). NMDARs were expressed in *Xenopus laevis* oocytes following microinjection of 3-5 ng of the GluN1 subunit cRNA and 7-10 ng of GluN2B subunit cRNA in 50 nL of RNAse free water as previously described[521]. Oocytes were incubated in Barth's solution at 18°C, and recordings were made 2-7 days after the injections at room temperature using two two-electrode voltage clamp amplifiers at a holding potential of -40 mV.

Oocytes were perfused with a solution of 90 mM NaCl, 1 mM KCl, 10 mM HEPES and 0.5 mM $BaCl_2$ and the pH was adjusted to 7.4 using 1 M NaOH. 10 µM of EDTA was added to chelate contaminant divalent ions such as Zn^{2+}. Oocytes were placed in a dual-track plexiglass recording chamber that was assumed to be at a reference potential of 0mV. The glass microelectrodes were filled with KCl—300mM for the voltage electrode, and 3M for the current electrode. Bath clamps communicating across silver chloride wires were placed into each side of the recording chamber. The IC_{50} data was obtained by applying 100 µM glutamate and 30 µM glycine, followed by application of glutamate and glycine plus increasing concentrations of the test compound up to 30 µM. Current responses of less than 50 nA were not included. The level of inhibition was calculated as a percent of the initial glutamate response, averaged across all oocytes from a single frog. Each experiment used 6-7 oocytes from the same frog. The results from these experiments were pooled and fitted to the equation,

$$\text{Percent Response} = (100 - \text{minimum}) / (1 + ([\text{conc}]/IC_{50})^{nH}) + \text{minimum}$$

where minimum is the residual percent response at saturating concentration of the test compound and nH is a slope factor for the steepness of the inhibition curve.

Triheteromeric NMDAR Constructs

Triheteromeric receptor constructs were generated using rat GluN1 and GluN2A with modified C-terminal peptide tags as previously described[485]. Briefly, C-terminal peptide tags were generated from leucine zipper motifs found in $GABA_{B1}$ (referred to as C1) and $GABA_{B2}$ (referred to as C2). These tags were placed downstream of a synthetic helical linker and upstream of a

KKTN endoplasmic reticulum retention signal[522–524]. The tag was introduced in frame and in place of the stop codon at the GluN2A C-terminal tail to make $2A_{C1}$ and $2A_{C2}$. A chimeric GluN2B subunit was constructed in which the 2B carboxyl tail after residue 838 was replaced by the GluN2A carboxyl tail and C-terminal-linker-C1 or -C2-ER retention motifs to make $2B_{AC1}$ and $2B_{AC2}$[485]. The C1 and C2 leucine zipper motifs can form a coiled-coil structure that masks the KKTN retention motif and allows for expression of only triheteromeric receptors on the cell surface. Recordings were taken at pH 7.4.

Measurement of "escape" currents was used to assess the efficiency of the peptide tags which control surface expression. Our average escape currents were typically less than 10% and this was an acceptable threshold. Currents were estimated using pairs of mutations (GluN2A-R518K,T690I and GluN2B-R519K,T691I) that render the agonist binding domain incapable of binding glutamate, and therefore unable to pass current.

Expression and purification of intact NMDARs

Expression and purification methods of intact NMDAR receptors were based on previously established methods[488]. The membrane fractions (100 mg/ml) of the infected insect cells were solubilized in the buffer containing 20 mM HEPES-Na pH7.5, 150 mM NaCl, 1 mM Glycine, 1 mM Na-glutamate, and 0.5% lauryl maltose neopentyl glycol (LMNG) for 2 hours at 4°C and centrifuged at 125,000g for 40 minutes. The supernatant was purified using Strep-tactin resin followed by Superose 6 Increase column (GE Healthcare) size exclusion chromatography (SEC) which was pre-equilibrated with 20 mM HEPES-Na pH 7.5 and 150 mM NaCl. All of the purification steps above were conducted in the absence of glycine and glutamate.

Structural biology of GluN1b-GluN2B ATD

Coexpression and purification of the *Xenopus laevis* GluN1b and rat GluN2B ATD heterodimer were performed as described previously[290,392]. Briefly, Trichoplusia ni (High Five, Thermo Fisher) insect cells were infected with a baculovirus harboring *Xenopus* GluN1b ATD and rat GluN2B ATD cDNAs for 48 h. The concentrated medium was subjected to purification by Chelating-Sepharose charged with $CoCl_2$. Poly-Histidine tags at the C-terminus of GluN1b ATD and the N-terminus of the GluN2B ATD were removed by thrombin digestion and the digested samples were further purified by Superdex200 (GE Lifescience). Purified protein was concentrated to 10 mg/mL and dialyzed against 50 mM NaCl, 10 mM Tris (pH 8.0), and 1 μM ifenprodil hemi-tartrate (Tocris). The dialyzed protein was filtered through a 0.1μm spin filter (Millipore) prior to the crystal screens. Crystals grew in sodium formate/HEPES as previously described[290], taking 3–4 days to appear, then continuing to grow for up to 2–3 weeks at 18 °C. Crystals were transferred to 2 μL drops containing 4 M sodium formate, 0.1M HEPES (pH 7.5), 35 mM NaCl, 7 mM Tris (pH 8.0), and 50 μM of EU93-108, and allowed to soak overnight. Crystals were then transferred to a new drop of the same condition and soaked overnight again. Crystals were flash-frozen in liquid nitrogen for X-ray diffraction data collection by sequentially transferring them to 4.5 M and 5 M sodium formate and left overnight.

Chung Spinal Nerve Ligation

The Chung spinal nerve ligation model was implemented by Algos Therapeutics. Male Sprague-Dawley rats (Hsd:Sprague-Dawley®™SD®™, Harlan, Indianapolis, Indiana, U.S.A.) weighing 222 ± 1 g were housed three per cage and given *ad libitum* access to food and water. Animal holding rooms operated on a 12:12h light/dark schedule for the entire duration of the study.

The animal colony was maintained at 21ºC and 60% humidity. All experiments were conducted in accordance with the International Association for the Study of Pain guidelines and were approved by the University of Minnesota Animal Care and Use Committee.

Allodynia was induced via the Chung spinal nerve ligation (SNL) method[241] in which the animals were anesthetized with isoflurane, the left L5 transverse process was removed, then the L5 and L6 spinal nerves were tightly ligated with 6-0 silk suture. Finally, the wound was closed with internal sutures and external staples. Allodynia was assessed using 8 Semmes-Weinstein filaments (Stoelting, Wood Dale, IL, USA) with varying stiffness (0.4, 0.7, 1.2, 2.0, 3.6, 5.5, 8.5, and 15 g) following the up-down method[219] first published by Chaplan et al. in 1994. Baseline measurements were taken two weeks following SNL and prior to compound administration. Measurements were also taken 30, 60, 120 and 240 minutes post intraperitoneal compound injection. Any animals displaying lethargy were excluded from the study.

Determination of Plasma and Brain Concentrations of EU93-108

EU93-108 was formulated in 2% DMA, 10% DMSO, and 20% PEG in sterile water and administered intraperitoneally (i.p.) with a 10 mL/kg dose volume to adult male Spraque-Dawley rats (7-8 wks, approx. 200 g; Charles River, USA). At 30-, 120-, and 240-min post administration the rats were briefly anesthetized with isoflurane and then decapitated. Trunk blood was collected in K-EDTA tubes and then spun in a microcentrifuge at 3500 rpm for 10 min to separate plasma, which was then transferred to a clean tube and frozen on dry ice. To prepare forebrain tissue samples, the whole brain was removed from the skull, the cerebellum and brainstem cut away, the meninges were removed, and the forebrain then rinsed with ice-cold normal saline, after which it was blotted dry with filter paper and weighed on a microbalance. To each forebrain 2.5 mL of ice-

cold 50 mM K-phosphate buffer (pH 7.4) was then added and the samples homogenized with a hand-held homogenizer. The brain homogenates were then transferred to clean tubes (2 per brain) and frozen on dry ice.

Plasma and brain homogenate samples were analyzed by LC-MS/MS operating in multiple reaction monitor mode (MRM) by Ricerca Biosciences (Dublin, OH). Briefly, plasma and brain were centrifuged at 4000 rpm for 15 minutes to clarify a supernatant from which fractions were collected and injected onto the LC-MS/MS. The amount of parent compound in each plasma or brain sample was calculated by comparing the response of the analyte in the sample to that of a standard curve (Ricerca, OH).

Hot Water Tail Immersion Paradigm[525–528]

All animal studies performed at Emory have been approved by the Institutional Animal Care and Use Committee at Emory University. Male and female C57BL/6J mice weighing between 20-30 g were housed five per cage and given *ad libitum* access to food and water. Mice were 8-10 weeks of age at the time of experimentation. Animal holding rooms operated on a 12-hour dark/light cycle with the dark cycle from 7:00pm to 7:00am. Mice were allowed to acclimate in cages for one week after arrival. Mice were handled regularly and habituated to scruffing and cloth restraint for 3-5 days prior to experimentation.

Mouse weights were recorded on the day of each experiment. Mice were given the appropriate treatment(s) 30 mins prior to testing. All injection volumes were 10 mL/kg (*e.g.* 350 µL for a 35 g mouse). For the tail immersion experiments, each mouse was restrained with a Wypall cloth, leaving the tail exposed. The distal two-thirds of the tail was lowered into a sous vide water bath set to 48°C, and a stopwatch with a resolution of 0.01 s was used to record the

time elapsed between immersion and tail flick. Three recordings were taken for each mouse, and each data point is expressed as the mean of the three recordings. A cut-off time of 25 s was implemented to prevent tissue damage or scarring. For each experiment, the identities of the doses were coded by an independent researcher to ensure blinding. The identities were not decoded until the data were analyzed.

Prism™ 9.3.1 software (GraphPad, San Diego, CA, USA) was used for all data analysis and visualization. Data for intrinsic antinociception was analyzed using one-way ANOVA and Dunnett's *post hoc* test for multiple comparisons where each group was compared to vehicle. Data for acute morphine potentiation experiments was analyzed using one-way ANOVA and Tukey's *post hoc* test for multiple comparisons was also used, where each group mean was compared to the mean of every other group. Data for tolerance experiments was analyzed using repeated measures two-way ANOVA and Bonferroni *post hoc* analysis. Data is presented as mean ± SEM and $p < 0.05$ constitutes significance.

An *a priori* power analysis was conducted using G*Power3[529] to test the difference between two independent group means using a two-tailed test, a large effect size (d= 0.80), and an alpha of 0.05. The results showed that a total sample of n = 7 animals per group was required to achieve a power of 0.80.

Locomotor Assessment

For both male and female mice, n = 8 mice per group were used. Locomotor activity was assessed at 3, 5, 7, 10, 20, and 30 mg/kg of EU93-108. Mice were brought to the experiment room the night before and given *ad libitum* access to food and water. Each mouse was given an i.p. injection of the appropriate dose or vehicle 30 mins prior to starting the locomotor boxes

(Versamax420 Animal Activity Monitoring System, AccuScan Instruments Inc., Columbus, OH, USA). Movements of the mice were tracked for 1 hour then the mice were placed back in their cages. Data were analyzed using one-way ANOVA and Dunnett's *post hoc* test for multiple comparisons where each group was compared to vehicle. Data are presented as mean ± SEM.

Radioligand Binding Assay

Conventional competition and saturation radioligand binding assays were used to determine the affinities of reference standards and EU93-108. Experiments were carried out by the NIMH Psychoactive Drug Screening Program (PDSP) were performed as previously described[530]. The detailed experimental protocols for the radioligand assays are available on the NIMH PDSP website at https://pdsp.unc.edu/pdspweb/content/UNC-CH Protocol Book.pdf

Author Contributions

Synthesis of the 93 series compounds was completed by Y.A.T., N.S.A., and L.D.H. Oocyte recordings were performed by K.A.N. and L.D.H. S.J.M. performed the triheteromeric recordings. Crystal structure data were provided by H.F. and M.C.R. Spinal nerve ligation and plasma and brain concentration data were collected and analyzed by R.D., S.J.M., and L.J.W. L.D.H performed all tail immersion and locomotor experiments. L.D.H., M.C.R., S.J.M., H.F., L.J.W., R.D., S.F.T., and D.C.L. were involved in experimental design. Data were analyzed by L.D.H., M.C.R., S.J.M., and H.F. All authors were involved in writing the manuscript.

2.6 Supplemental Data

Receptor	IC$_{50}$ μM	IC$_{50}$ μM 95% CI	nH	nH 95% CI	Ymin	95% CI	N
r2Ac1/r2Ac2	ND	ND	ND	ND	104.8	(102, 107.5)	6
r2Ac1/r2Bc2	0.543*	(0.460, 0.640)	-0.92*	(-1.0, -0.85)	54.0*	(50.3, 57.7)	12
r2Bc1/r2Bc2	0.233	(0.196, 0.279)	-1.06	(-1.09, -1.02)	10.6	(7.9, 13.3)	8
h2B/h2B	0.261	(0.197, 0.347)	-1.16	(-1.25, -1.07)	12.0	(8.5, 15.5)	10

Supplemental Table S1. Table of EU93-108 concentration-inhibition results at NMDA receptors expressed in *Xenopus* oocytes. Receptor subtypes shown correspond to receptor subtypes and data presented in Figure 2. * indicates a significant difference from r2Bc1/r2Bc2 and h2B/h2B receptors by one-way ANOVA and Tukey's multiple comparison test, p<0.05 or better. Statistical tests were conducted on the LogIC$_{50}$ values. N represents the number of oocytes evaluated.
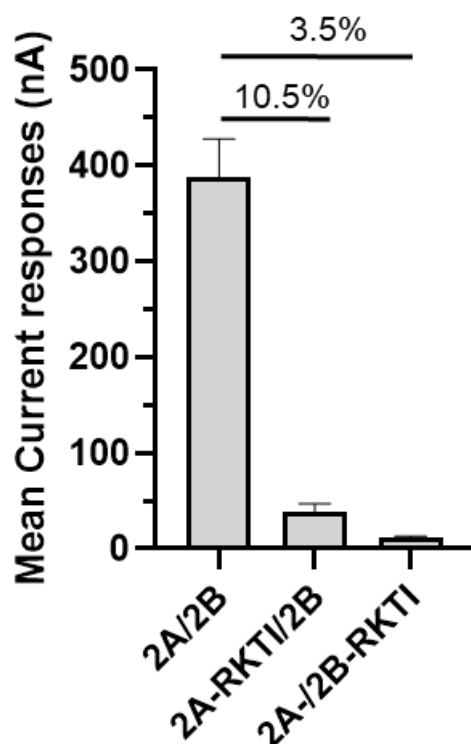
Supplemental Figure S1: The mean raw current ± SEM in nanoamperes (nA) in response to exposure of Xenopus oocytes recorded under two electrode voltage clamp to 100 µM glutamate and 100 µM glycine. Values for wild type (2A/2B) or variant $GluN1/GluN2A_{C1}/GluN2B_{C2}$ triheteromeric NMDARs are shown that have a wild type agonist binding domain or harbor the RKTI mutations in the agonist binding domain that renders the indicated GluN2 subunit incapable of binding glutamate (see Methods). The average nA current response for RKTI mutations is shown as the percentage of that observed for NMDARs with functional glutamate binding sites indicated at the top. This percentage is an estimate of the amount of current that could potentially reflect diheteromeric receptors that escape the ER retention strategy and reach the surface with two copies of either the $GluN2_{C1}$ or two copies of $GluN2_{C2}$ subunit (see Hansen et al., 2014).

Data Collection	ATD + EU93-108
Beamline	NSLS-II (17-ID-1)
Space group	C2
Wavelength (Å)	0.9198
Unit cell dimensions	
a, b, c (Å)	269.172
	60.076
	145.572
β (º)	117.020
Resolution (Å)	50.00-2.85 (2.90)
R_{merge}	0.073 (0.776)
I/σs	14.7 (1.0)
Completeness (%)	99.1 (91.2)
Redundancy	3.3 (2.3)
Refinement	
Resolution (Å)	35 – 2.85
No. reflection	48,988
R_{work}/R_{free}	0.174/0.246
No. atoms	
Protein	11,244
Ligand	60
Na	2
Water	94
B factors (Å^2)	
Protein	57.01
Ligand	54.40
Na	44.79
Water	39.00
R.M.S. deviations	
Bond length (Å)	0.007
Bond angles (º)	1.527

Supplemental Table S2. X-ray crystallographic data collection and model refinement statistics. All datasets were collected from a single crystal. Values in parentheses are for the highest-resolution shell.

Morphine Dose-Response Curve
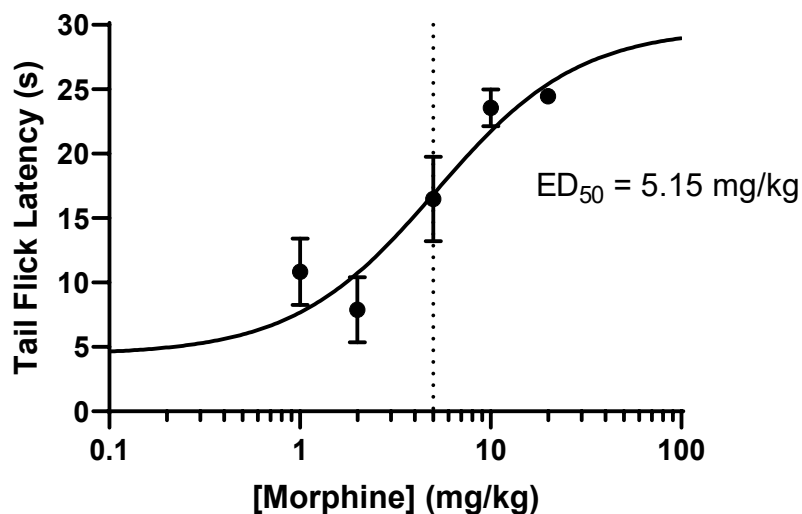
Supplemental Figure S2. Morphine dose-response curve in male C57BL/6J mice. Morphine was given s.c. at 1, 2, 5, 10 and 20 mg/kg (n=8 mice per dose). Tail immersion tests were conducted 30 minutes post injection. A 25-second cut-off time was implemented for each experiment. Each circle represents the mean ± SEM for each dose. The dotted line depicts the estimated ED_{50} value.
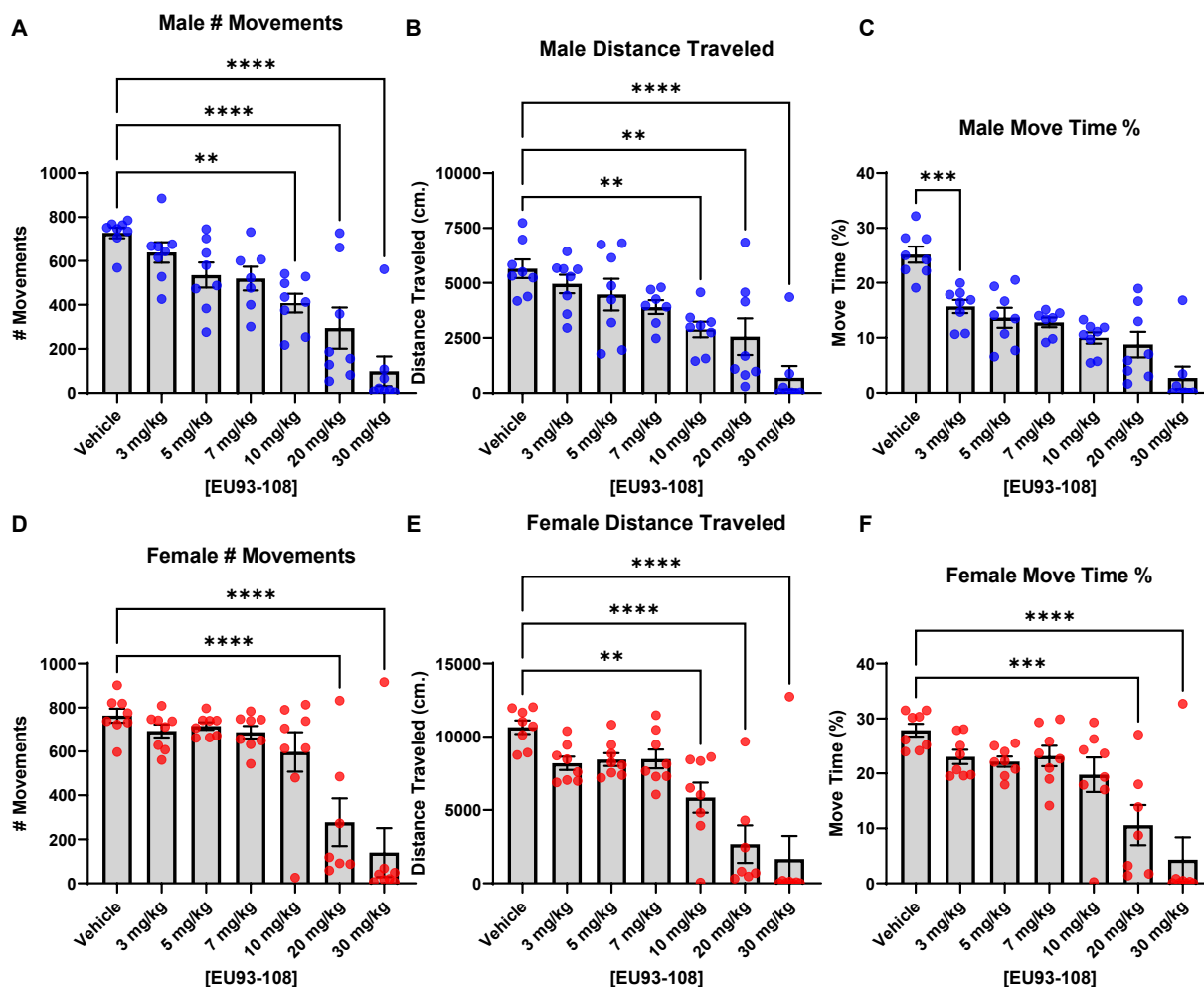
Supplemental Figure S3. Locomotor activity of EU93-108. Data for male mice are shown in panels A-C, and data for female mice shown in panels D-F. (A) and (D) depict the number of movements made in the locomotor box during the one-hour experiment. (B) and (E) depict the average distance traveled in centimeters. (C) and (F) depict the average percentage of time the mice spent moving. All data are presented as mean $\pm$ SEM. Each dot represents one mouse, N=8 mice per group. Data were analyzed using a one-way ANOVA and Dunnett's *post hoc* test for multiple comparisons, where each group was compared to vehicle. $P < 0.5$ constitutes significance.

Receptor	Agonist	% Control 10 μM EU93-108
GluN1/GluN2A	100 μM glutamate, 30 μM glycine	95.6 ± 1.6 (7)
GluN1/GluN2B	100 μM glutamate, 30 μM glycine	13.2 ± 6.1 (8)
GluN1/GluN2C	100 μM glutamate, 30 μM glycine	97 ± 2.8 (7)
GluN1/GluN2D	100 μM glutamate, 30 μM glycine	97 ± 1.9 (6)
GluA1	100 μM glutamate	101.3 ± 1.9 (8)
GluA2-R607Q	100 μM glutamate	98.4 ± 0.57 (8)
hGluA3-L531Y	100 μM glutamate	94.7 ± 5.1 (8)
GluK2	100 μM glutamate	88.1 ± 4.4 (8)
hGluN1/GluN3A	100 μM glycine	103.6 ± 1.7 (9)
rGluN1/GluN3B	100 μM glycine	108.8 ± 4.0 (8)
$\alpha4\beta2$-nACh	10 μM acetylcholine	3.2 ± 0.7 (8)
$\alpha7$-nACh	300 μM acetylcholine	70.9 ± 6.5 (7)
5-HT$_{3A}$	100 μM serotonin	92.8 ± 2.7 (8)
$\alpha1\beta2\gamma2S$-GABA$_A$	100 μM GABA	92.8 ± 1.5 (9)
ρ-GABA$_C$	100 μM GABA	97 ± 1.5 (5)
$\alpha1$-Glycine	100 μM glycine	105 ± 6.6 (8)
hP2x	9 μM ATP	96.6 ± 4.3 (11)

Supplemental Table S3. Off-target actions of EU93-108 at ligand-gated ion channels expressed in *Xenopus* oocytes. The mean ± standard error of the mean for agonist plus 10 μM EU93-108 as a percentage of agonist in vehicle are given for each compound and receptor tested. Number of oocytes tested is given in parentheses.

Receptor	Mean % Inhibition	Receptor	Mean % Inhibition	Receptor	Mean % Inhibition
5-HT$_{1A}$	22.81	Alpha$_{2B}$	67.97	H$_2$	13.66
5-HT$_{1B}$	-7.29	Alpha$_{2C}$	62.97	H$_3$	22.66
5-HT$_{1D}$	39.2	Beta$_1$	29.14	H$_4$	2.12
5-HT$_{1E}$	1.68	Beta$_2$	13.7	KOR	-3.1
5-HT$_{2A}$	83.75	Beta$_3$	-10.49	M$_1$	-18.06
5-HT$_{2B}$	67.36	BZP Rat Brain Site	14.68	M$_2$	-23.09
5-HT$_{2C}$	71.28	D$_1$	24.67	M$_3$	9.26
5-HT$_3$	0.87	D$_2$	23.12	M$_4$	51.36
5-HT$_{5A}$	12.99	D$_3$	67.14	M$_5$	-0.11
5-HT$_6$	25.27	D$_4$	11.37	MOR	4.04
5-HT$_{7A}$	55.89	D$_5$	8.94	NET	12.52
Alpha$_{1A}$	86.3	DAT	-7.01	PBR	-0.34
Alpha$_{1B}$	5.09	DOR	-8.82	SERT	15.1
Alpha$_{1D}$	76.65	GABA$_A$	1.91	Sigma$_1$	69.21
Alpha$_{2A}$	77.72	H$_1$	76.87	Sigma$_2$	47.16

Supplemental Table S4. Off-Target Actions of EU93-108: Primary GPCR Screen. Cloned human molecular targets were individually expressed and submitted to molecular target-based screening with initial screens performed at a final concentration of 10 µM in quadruplicate. Complete protocols for the assays have been previously published (Besnard J *et al*. 2012). Where inhibition greater than 50% was measured, secondary screens were performed wherein K$_i$ values were calculated (see Table 4).

Chapter 3: Considerations, Future Directions, and Broader Implications

3.1 Summary

In Chapter 1 of this dissertation, I first discussed the neurocircuitry of beneficial and pathological pain, including types of pain and interventions for pain management. Next, I introduced opioid receptors and discussed activation and deactivation and opioid mechanisms of action. I then discussed the opioid receptor's role in the dopamine reward system, exploring the addictive nature of opioids. Next, I discussed the US opioid epidemic including contributing factors and societal impact. I then introduced the concept of analgesic tolerance and explained several proposed mechanisms for its development and also discussed the role of NMDARs and GluN2B-containing NMDARs in tolerance development. Finally, I introduced the 93 series of Glun2B-selective NAMs developed by the Liotta lab, and the novel compound from this class that was the focus of Chapter 2, EU93-108.

In Chapter 2, I set out to answer four research questions:

1. What is the effect of EU93-108 on tail flick latency when used alone?

2. What is the effect of the combination of EU93-108 and morphine on tail flick latency?

3. Does EU93-108 have an effect on the development of analgesic tolerance due to chronic morphine administration?

4. Does EU93-108 have an effect on tail flick latency in tolerant mice?

Previously published compounds from the 93 series have shown utility as *in vitro* and *in vivo* tool compounds, but have never been evaluated in the context of chronic pain and opioid tolerance. In Chapter 2, I reported a novel and highly potent GluN2B-selective NMDAR inhibitor, EU93-108. We have reported the structural basis for binding of EU93-108 via single particle cryo-EM, and

found that this compound is highly brain penetrant and maintains high brain and plasma concentrations for at least 4 hours post i.p. injection. EU93-108 possesses intrinsic analgesic properties in the spinal nerve ligation model of neuropathic pain and the rodent tail flick test for thermal pain. We also observed a significant, acute enhancement in tail flick latency where the combination of EU93-108 and morphine yielded higher latencies compared to either compound alone. This combination also briefly slowed worsening of tolerance in tolerant mice, but had no effect on the development of tolerance in naïve mice.

3.2 Experimental Considerations

3.2.1 Analgesia vs Sedation

One critique of this work is the nature of reflexive behavioral studies in rodents. The output for both tail immersion and mechanical allodynia tests is a reflexive behavior (i.e. tail or hind paw movement), and in both paradigms the absence of these reflexes is interpreted as analgesia. The problem with this method of evaluation is that EU93-108 has sedative properties, which means we cannot separate whether this absence of reflex is due to actual analgesia or sedation, as both produce the same outcome.

In my work with EU93-108, I calculated that the ED_{50} for analgesia (tail flick latency) in male mice in the absence of morphine was 9.7 mg/kg. In male mice, the ED_{50} for sedation (rest time) was 13.5 mg/kg. The data show that there is a dose dependent increase in both analgesia and sedation outputs, whereby the same doses that produce the highest increases in tail flick latency also produce the highest rest time percentages in the locomotor experiment. This suggests that these two effects are not easily distinguishable. The sedative property of EU93-108 significantly impacts interpretation of the tail flick latency results.

There are two potential solutions for this issue: either ensure the compound of interest does not possess any sedative or other confounding properties prior to evaluating it in a reflexive behavioral paradigm or choose a non-reflexive paradigm. The first solution might require administering a range of compound doses then subjecting the rodents to a locomotor box or rotarod test. If the compound-treated animals have similar move and rest times in the locomotor box or similar latencies to fall off the rotarod compared to vehicle-treated animals, this would suggest that the chosen dose range does not elicit significant locomotor dysfunction. For the second solution, there are several non-reflexive paradigms that can be used to evaluate pain-like behaviors in rodents. However, it is important to note that sedative properties of the test compound might also impact interpretation of non-reflexive behavioral tests as the output is still movement.

Conditioned place preference/aversion[531]

Place conditioning is a type of Pavlovian or classical conditioning where the test subject makes decisions about its location based on the presence of a rewarding or aversive stimulus. This behavioral paradigm has commonly been used to evaluate the rewarding effects of drugs and has been validated in many animal models. The paradigm has also been adapted to evaluate locomotor dysfunction and tolerance to drugs with repeated use.

For a tolerance experiment, the set up could include one bright chamber and one dark chamber equipped with a slit to insert a brush or another item to elicit a pain-like response in the test subjects. The animal must decide whether to remain in the aversive bright light or withstand the pain caused by the brush in the dark chamber. For tolerant mice, the morphine given would not be as effective, therefore one might expect that those mice would spend more time in the bright light due to their higher sensitivity to the painful stimulus in the dark chamber compared to non-tolerant mice.

Mechanical conflict avoidance apparatus (MCAA)[532,533]

The MCAA is a more sophisticated version of the conditioned place preference/aversion paradigm. It contains three chambers: one dark (preferred), one with bright light (aversive but not painful), and a middle chamber with either sandpaper or nociceptive probes (aversive and painful). The mice are placed in the bright light chamber, then time spent in the bright chamber and the number of successful crosses to the dark chamber are recorded. Mice who are in no pain are more likely to subject themselves to a small amount of pain in the middle chamber to escape the aversive light. However, mice who are in pain are less likely to traverse the whole apparatus to get to the dark chamber because their sensitivity to the painful middle chamber is higher.

This paradigm could be used to evaluate tolerance development in mice. Mice who are tolerant to morphine will be less likely to traverse the apparatus which would result in lower number of crosses and more time spent in the bright chamber, but mice who are not tolerant will be more likely to cross, yielding higher number of crosses and less time spent in the bright chamber.

3.2.2 Differences Between EU93-108 and Previous GluN2B-selective NAMs

EU93-108 has properties that distinguish it from previously published GluN2B-selective NAMs. The first of which is that EU93-108 demonstrated efficacy in nociceptive tests in the absence of morphine, whereas ifenprodil and Ro25-6981 do not have efficacy in antinociceptive tests in our hands. One potential explanation of this could be that the acute analgesic effects of EU93-108 could be mediated through inhibition of another receptor. In our off-target data, we showed that EU93-108 has a higher affinity for 5-HT$_{2A}$, Alpha$_{1A}$, D$_3$, H$_1$, and sigma$_1$ receptors compared to the GluN2B-containing NMDAR. Evidence has shown that inhibition of 5-HT$_{2A}$,

Alpha$_{1A}$, H$_1$, and sigma$_1$ receptors all produce antinociceptive effects[534–537], so the antinociceptive properties seen in EU93-108 could be due to interaction with any of these receptors as opposed to negative modulation of the GluN2B subunit.

The second difference is that EU93-108 did not have any effect on tolerance development, whereas ifenprodil and Ro25-6981 have demonstrated efficacy in inhibiting tolerance. One potential explanation could be differences in experimental design set-up. Ko *et al.* demonstrated that Ro25-6981 can decrease tolerance when chronically co-administered with morphine[442]. One difference between the experiment in that study and the one we conducted was that Ko took latency measurements each day during the co-administration, whereas we only looked once at the beginning of co-administration and again at the end. Ko's beginning and end data looked very similar to ours: by the end of the experiment Ro25-6981 no longer improved latency. Perhaps the effect of EU93-108 is similarly short-lived and only able to be observed during the intermediate days of the experiment. A future study should take latency measurements each day to provide more information about any effects EU93-108 might elicit, but at present we cannot conclude that EU93-108 does not have efficacy in decreasing tolerance.

3.2.3 Off-Target Effects

A significant limitation of EU93-108 is the prevalence of many off-target interactions among which alpha-1 adrenergic, 5-HT, dopamine D3, sigma 1 and histamine 1 receptors were the strongest.

One strategy to improve the clinical utility of EU93-108 and similar compounds could be to decrease the histamine 1 receptor interaction, which would decrease the likelihood of sedation. EU93-108 functions as a histamine 1 receptor antagonist, giving it antihistamine properties like

that of allergy medications such as fexofenadine (Allegra®) or cetirizine (Zyrtec®) **(Figure 19)**. Upon studying these chemical structures, nitrogen-containing heterocycles and oxygens inserted into an acyl chain are featured in all structures. Focusing on modifying these moieties while maintaining efficacy could allow for a class of compounds with significantly decreased histamine receptor interactions.

Alpha-1-adrenergic receptor interactions are among the strongest off-target effects seen in EU93-108 and in GluN2B-selective NAMs in general. Substitutions on the phenyl ring and the presence of secondary amines are two structural similarities between much of the 93 series and many common alpha-1 agonists as seen in Figure 19. These structural motifs could be good focal points to drive down alpha-1 activity; however, maintaining potency and selectivity will most likely be an ongoing challenge.
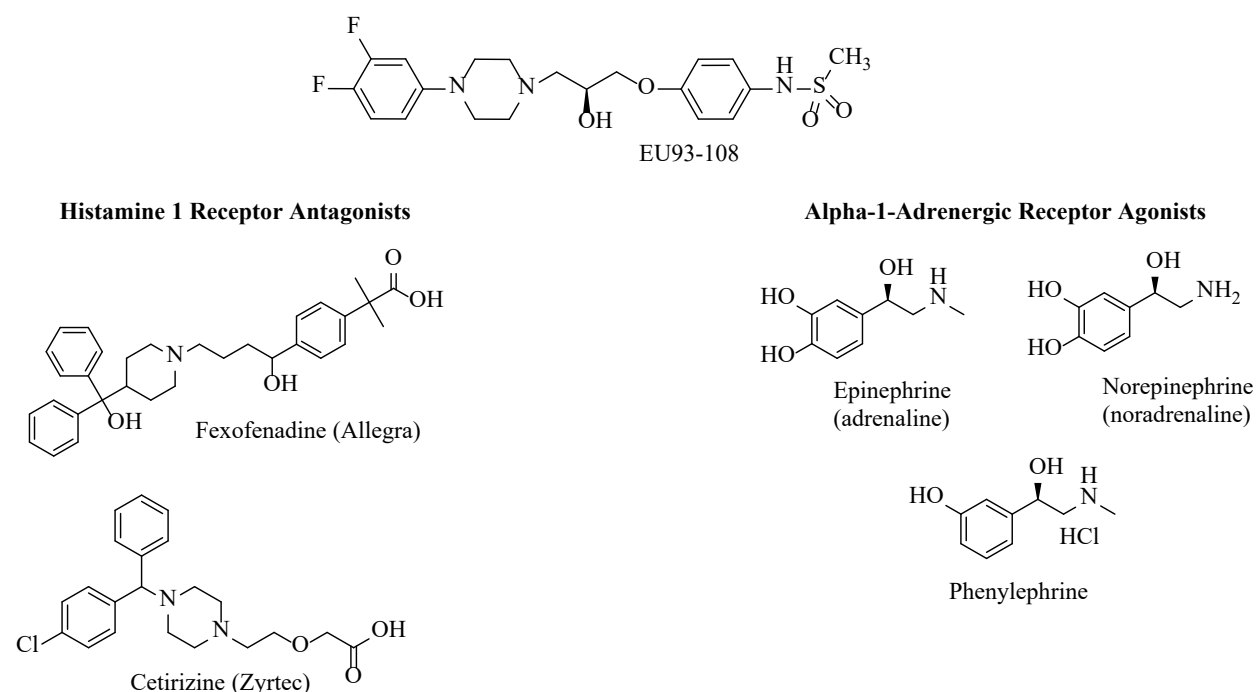
Figure 20. Structural considerations for improving off-target effects of EU93-108 and similar GluN2B-selective NAMs.

3.2.4 Sex differences

As discussed in Chapter 2, we observed differences in potency of EU93-108 between males and females, where males required lower doses of the compound than females to achieve the same increase in tail flick latency. The following section is a more detailed discussion of the basis of sexual dimorphism in animal research as it relates to differences in stress hormone levels, metabolic enzyme expression and pain sensitivity.

Stress Hormones

The stress response is how living organisms respond to environmental changes. Stress helps to alert our bodies to potentially harmful stimuli and is an important survival mechanism[538]. The mechanisms underlying stress differ between males and females[539]. In females, the different phases of the estrus cycle and the associated changes in estradiol and progesterone are known to impact the stress response[540]. In fact, fluctuations in gonadal steroids such as progesterone are thought to be the main contributor to differences in stress response between sexes[538]. The pituitary gland functions to reestablish homeostasis following stress[541]. The female pituitary gland releases more adrenocorticotropic hormone compared to males in response to stress[542] which suggests that females have a stronger response to stress than males. In the adrenal gland, females also release more corticosterone compared to males following stress[543].

To contextualize this to my work with EU93-108, it is known that the estrus cycle significantly impacts stress response in female mice. The late diestrus stage is characterized by a decline in progesterone, and this is the phase where female mice are most easily stressed[544]. Future work could involve determining which stage of the estrus cycle the female mice are in prior to

experimentation and avoiding conducting experiments during the late diestrus stage to mitigate the stress response as much as possible.

Rodents are heavily predated animals, so any behavioral experiment will elicit a stress response. Therefore, minimizing stress before, during, and after experimentation should be prioritized. Methods of mitigating stress include handling the animal prior to experimentation, reducing the time spent in the experiment, reducing time spent either upside-down or on the side, reducing light and sound in the room, and avoiding temperature fluctuations.

CYP Expression

As mentioned in the Chapter 2 discussion, CYP metabolic enzyme expression differs between males and females. Kato and Kamataki[545] were the first to report on sex-specific and sex-dominant CYPs in the liver in 1982. CYP2C11 is known to be regulated by growth hormones. This isoform is suppressed by female growth hormones and stimulated by male growth hormones, making it male-specific. Conversely, CYP2C12 is female-specific[546]. The most male-dominant CYPs are 3A2, 2A2, 2C13, and 2C22. These isoforms have 10- to 20-fold higher expression in males compared to females. CYPs 2B1, 2B2, and 3A1 are slightly less male-dominated, having 2- to 5-fold higher expression in males. Female dominant CYPs are 2A1, 2C7, 2E1, and 1A2, and are 2-fold higher in females than males. CYP 2C6 and 1A1 expression has no significant sex difference[547].

Metabolic analysis of compounds of interest is very useful because it provides more information on how quickly the compound is metabolized and by which enzyme(s). CYP analysis also helps to determine whether any enzymes are being suppressed by the compound and could help to explain any differences in efficacy in *in vivo* experiments. For example, if EU93-108 is

found to be primarily metabolized by a female-dominant CYP isoform, then that might suggest that the compound is cleared more rapidly in females and therefore more frequent dosing might be required to see comparable effects compared to male mice.

Pain Sensitivity

Pain threshold and pain sensitivity are known to be lower in females than males, as shown in a series of studies[182,513,548–550]. Additionally, frequency, severity, and duration of pain is higher in females[182,551]. In fact, in humans some types of chronic pain are more common in women including migraine, irritable bowel syndrome, fibromyalgia, temporomandibular disorder, and rheumatoid arthritis[550,552,553]. For female mice, the estrus cycle can also impact pain sensitivity[554–556]. In the context of EU93-108, if pain threshold is lower in female mice, then a higher dose would be required to elicit the same level of analgesia observed in male mice. This might also potentially explain the lower potency of EU93-108 in female mice. In general, differences in pain threshold should be taken into account when performing animal research as this can affect efficacy of analgesic therapies.

3.3 Future Directions

In light of the useful information gained from EU93-108, many additional research questions can be asked to further probe the compound's utility and to deepen our understanding of GluN2B negative modulation as it relates to pain and analgesia, such as:

1. What are the effects of EU93-108 in a mouse model where 2B is overexpressed, such as Tg-GluN2B$^{2A(CT)}$?

2. What is the effect of EU93-108 in combination with biased agonists like oliceridine (TRV130) in context of analgesic tolerance and pain?

3. Does EU93-108 have an effect on physical dependence?

4. Does EU93-108 have any addiction liability?

The Tg-GluN2B$^{2A(CT)}$ transgenic mouse has been genetically modified to overexpress the GluN2B subunit in the forebrain. Several studies have used this mouse line to show that overexpression of GluN2A in forebrain leads to impaired memory function while overexpression of GluN2B leads to enhanced memory[557,558]. As discussed in the ***NMDAR Role in Tolerance*** section, there is significant overlap between the mechanisms that allow for learning and memory and those that bring about central sensitization and chronic pain. Therefore, evaluating the effects of EU3-108 in this mouse line would be advantageous. Because EU93-108 is GluN2B-selective and the GluN2B subunit is overexpressed in this model, I would expect a significant increase in potency. Less drug would be needed to see favorable effects because there are more receptors to bind to. I would also expect to see less off-target effects due to the lower dose.

As discussed in the ***Strategies to Develop Safer Analgesics*** section, biased agonism or functional selectivity is at the forefront of analgesic research. Biased agonists like oliceridine are considered the next generation of opioids and the actions of these compounds require further evaluation. EU93-108 could be co-administered with oliceridine in analgesia and tolerance experiments. Because oliceridine is Gα-biased like morphine[204], I would expect to see similar enhancement effects. Additionally, EU93-108 could be evaluated for oral bioavailability then used in combination with opioids such as oxycodone or hydrocodone which are commonly prescribed and orally administrated. Oral dosing is more clinically relevant and is therefore the next logical step in testing the efficacy of EU93-108 and subsequent compounds.

Physical dependence is manifested by withdrawal symptoms following cessation of drug use. Rasmussen and other groups have reported that these withdrawal symptoms are primarily

brought about by increased excitation due to increased glutamate release in the locus coeruleus (LC)[559–562]. To that end, negatively modulating NMDAR activity in the LC has previously been shown to mitigate or completely inhibit withdrawal symptoms, as seen in the channel blockers dextromethorphan[563], ketamine[563], and MK-801[564,565]. Additionally, the GluN2B-selective NAM con-T has recently demonstrated efficacy in inhibiting physical dependence to morphine[566]. This suggests a role for GluN2B in mitigating physical dependence as well as tolerance to opioids. As such, EU93-108 would be expected to have some efficacy in naloxone-precipitated withdrawal experiments. I would expect to see decreases in wet dog shakes, escape jumps and weight loss among other withdrawal symptoms commonly seen in rodents.

Finally, in addition to tolerance evaluation, the conditioned place preference (CPP) paradigm is also useful for assessing addiction liability of compounds[567]. This paradigm, along with self-administration paradigms, evaluates how likely an animal is to repeatedly seek out the test compound. NMDAR antagonists are commonly subjected to these types of experiments alongside PCP, a channel blocker with profound psychotomimetic and addictive effects[568]. In an effort to gain a more complete understanding of the favorable and unfavorable effects of EU93-108, this compound could be subjected to CPP. I do not expect that EU93-108 would have significant psychotomimetic effects because I did not observe any abnormal behavior in treated animals, however it is still a worthwhile experiment and would provide useful information.

3.4 Broader Implications for GluN2B Negative Modulation

The goal of this dissertation was to learn more about the effects of GluN2B negative modulation in the context of pain and opioid use. My work highlighted analgesic tolerance which is one of many substrates of opioid misuse and addiction. I also briefly discussed how GluN2B negative modulation has efficacy in inhibiting physical dependence[566].

It is promising to see that GluN2B negative modulation has positive effects on physiological aspects of drug misuse like tolerance and dependence, but the potential utility of this negative modulation does not stop there. A growing body of evidence supports the idea that GluN2B negative modulation can also have utility in treating chronic pain itself[356]. This would mean that future GluN2B NAMs might not have to be used in combination with an opioid, but could function as effective analgesics alone.

Additionally, a relatively small body of evidence suggests that GluN2B negative modulation has further implications in treating addiction[569]. Shen *et al.* demonstrated that LTP mediated by GluN2B-containing NMDARs is required for heroin relapse in rats. Negatively modulating these receptors could therefore inhibit drug relapse and, potentially, addiction as well. Somatoform pain disorder is a form of idiopathic chronic pain characterized by hyper-fixation on symptoms like pain or fatigue[570] and is a common comorbidity in chronic pain patients[571]. GluN2B negative modulation could have applications in treating this disorder as well.

Further research is needed to explore all of the ideas discussed above, but there is much promise and much to be explored in the future. The work presented in this dissertation is yet another step forward in broadening and deepening our understanding of the potential therapeutic impact of GluN2B negative modulation.

3.5 References

1. Raja, S. N. *et al.* The revised International Association for the Study of Pain definition of pain: concepts, challenges, and compromises. *Pain* **161**, 1976–1982 (2020).

2. Melzack, R. & Wall, P. D. *The Challenge of Pain*. (Penguin Science, 1996).

3. Garland, E. L. Pain Processing in the Human Nervous System: A Selective Review of Nociceptive and Biobehavioral Pathways. *Prim Care* **39**, 561 (2012).

4. Schembri, E. Are Opioids Effective in Relieving Neuropathic Pain? doi:10.1007/s42399-018-0009-4.

5. Peirs, C. & Seal, R. P. Neural circuits for pain: Recent advances and current views. *Science* **354**, 578–584 (2016).

6. Martinac, B., Adler, J. & Kung, C. Mechanosensitive ion channels of E. coli activated by amphipaths. *Nature* **348**, 261–263 (1990).

7. Nilius, B. & Honoré, E. Sensing pressure with ion channels. *Trends in neurosciences* **35**, 477–486 (2012).

8. Osterweis, M., Kleinman, A. & Mechanic, D. The Anatomy and Physiology of Pain. in *Pain and Disability: Clinical, Behavioral, and Public Policy Perspectives* (National Academic Press, 1987).

9. Wu, L. J., Sweet, T. B. & Clapham, D. E. International Union of Basic and Clinical Pharmacology. LXXVI. Current progress in the mammalian TRP ion channel family. *Pharmacological reviews* **62**, 381–404 (2010).

10. Nilius, B. & Owsianik, G. The transient receptor potential family of ion channels. *Genome Biology* **12**, 1–11 (2011).

11. Zheng, J. Molecular Mechanism of TRP Channels. (2013) doi:10.1002/cphy.c120001.

12. Dhakal, S. & Lee, Y. Molecules and Cells Minireview Transient Receptor Potential Channels and Metabolism. *Mol. Cells* **42**, 569 (2019).

13. McEntire, D. M. *et al.* Pain transduction: a pharmacologic perspective. *Expert review of clinical pharmacology* **9**, 1069–1080 (2016).

14. Brederson, J. D., Kym, P. R. & Szallasi, A. Targeting TRP channels for pain relief. *European journal of pharmacology* **716**, 61–76 (2013).

15. Caterina, M. J. *et al.* The capsaicin receptor: a heat-activated ion channel in the pain pathway. *Nature 1997 389:6653* **389**, 816–824 (1997).

16. Spicarova, D. & Palecek, J. The role of the TRPV1 endogenous agonist N-Oleoyldopamine in modulation of nociceptive signaling at the spinal cord level. *Journal of neurophysiology* **102**, 234–243 (2009).

17. Moore, C., Gupta, R., Jordt, S. E., Chen, Y. & Liedtke, W. B. Regulation of Pain and Itch by TRP Channels. *Neuroscience bulletin* **34**, 120–142 (2018).

18. Li, Y. *et al.* Enhanced function of TRPV1 via up-regulation by insulin-like growth factor-1 in a rat model of bone cancer pain. *European journal of pain (London, England)* **18**, 774–784 (2014).

19. Dinh, Q. T. *et al.* Substance P expression in TRPV1 and trkA-positive dorsal root ganglion neurons innervating the mouse lung. *Respiratory physiology & neurobiology* **144**, 15–24 (2004).

20. De Logu, F., Patacchini, R., Fontana, G. & Geppetti, P. TRP functions in the broncho-pulmonary system. *Seminars in immunopathology* **38**, 321–329 (2016).

21. Smith, G. D. *et al.* TRPV3 is a temperature-sensitive vanilloid receptor-like protein. *Nature* **418**, 186–190 (2002).

22. Peier, A. M. *et al.* A heat-sensitive TRP channel expressed in keratinocytes. *Science (New York, N.Y.)* **296**, 2046–2049 (2002).

23. Xu, H. *et al.* TRPV3 is a calcium-permeable temperature-sensitive cation channel. *Nature* **418**, 181–186 (2002).

24. Macpherson, L. J. *et al.* Noxious compounds activate TRPA1 ion channels through covalent modification of cysteines. *Nature* **445**, 541–545 (2007).

25. Kremeyer, B. *et al.* A gain-of-function mutation in TRPA1 causes familial episodic pain syndrome. *Neuron* **66**, 671–680 (2010).

26. Clapham, D. E. TRP channels as cellular sensors. *Nature* **426**, 517–524 (2003).

27. Bautista, D. M. *et al.* The menthol receptor TRPM8 is the principal detector of environmental cold. *Nature* **448**, 204–208 (2007).

28. Colburn, R. W. *et al.* Attenuated cold sensitivity in TRPM8 null mice. *Neuron* **54**, 379–386 (2007).

29. Wemmie, J. A., Price, M. P. & Welsh, M. J. Acid-sensing ion channels: advances, questions and therapeutic opportunities. *Trends in neurosciences* **29**, 578–586 (2006).

30. Price, M. P. *et al.* The DRASIC cation channel contributes to the detection of cutaneous touch and acid stimuli in mice. *Neuron* **32**, 1071–1083 (2001).

31. Cheng, Y. *et al.* The Role of ASIC1a in Epilepsy: A Potential Therapeutic Target. *Current Neuropharmacology* **19**, 1855–1864 (2021).

32. Karsan, N., Gonzales, E. B. & Dussor, G. Targeted Acid-Sensing Ion Channel Therapies for Migraine. *Neurotherapeutics* **15**, 402–414 (2018).

33. Coryell, M. W. *et al.* Acid-Sensing Ion Channel-1a in the Amygdala, a Novel Therapeutic Target in Depression-Related Behavior. *Journal of Neuroscience* **29**, 5381–5388 (2009).

34. Kung, C.-C. *et al.* Deletion of Acid-Sensing Ion Channel 3 Relieves the Late Phase of Neuropathic Pain by Preventing Neuron Degeneration and Promoting Neuron Repair. *Cells* **9**, 2355 (2020).

35. Nagaeva, E. I., Potapieva, N. N. & Tikhonov, D. B. The Effect of Hydrophobic Monoamines on Acid-Sensing Ion Channels ASIC1B. *Acta Naturae* **7**, 95 (2015).

36. Shields, S. D. *et al.* Sodium channel Na(v)1.7 is essential for lowering heat pain threshold after burn injury. *The Journal of neuroscience : the official journal of the Society for Neuroscience* **32**, 10819–10832 (2012).

37. Catterall, W. A., Goldin, A. L. & Waxman, S. G. International Union of Pharmacology. XLVII. Nomenclature and structure-function relationships of voltage-gated sodium channels. *Pharmacological reviews* **57**, 397–409 (2005).

38. Ho, C. & O'Leary, M. E. Single-cell analysis of sodium channel expression in dorsal root ganglion neurons. *Molecular and cellular neurosciences* **46**, 159 (2011).

39. Persson, A. K. *et al.* Sodium-calcium exchanger and multiple sodium channel isoforms in intra-epidermal nerve terminals. *Molecular pain* **6**, (2010).

40. Maksimovic, S. *et al.* Epidermal Merkel cells are mechanosensory cells that tune mammalian touch receptors. *Nature* **509**, 617–621 (2014).

41. Pang, Z. *et al.* Selective keratinocyte stimulation is sufficient to evoke nociception in mice. *Pain* **156**, 656–665 (2015).

42. Baumbauer, K. M. *et al.* Keratinocytes can modulate and directly initiate nociceptive responses. *eLife* **4**, (2015).

43. Stein, C. *et al.* Opioids from immunocytes interact with receptors on sensory nerves to inhibit nociception in inflammation. *Proceedings of the National Academy of Sciences of the United States of America* **87**, 5935–5939 (1990).

44. Stein, C. & Machelska, H. Modulation of peripheral sensory neurons by the immune system: implications for pain therapy. *Pharmacological reviews* **63**, 860–881 (2011).

45. Rittner, H. L., Brack, A. & Stein, C. Pain and the immune system. *British journal of anaesthesia* **101**, 40–44 (2008).

46. Yoshimura, M. & North, R. A. Substantia gelatinosa neurones hyperpolarized in vitro by enkephalin. *Nature* **305**, 529–530 (1983).

47. Kaneko, S. *et al.* Ca2+ channel inhibition by kappa opioid receptors expressed in Xenopus oocytes. *Neuroreport* **5**, 2506–2508 (1994).

48. Piros, E. T. *et al.* Ca2+ channel and adenylyl cyclase modulation by cloned mu-opioid receptors in GH3 cells. *Molecular Pharmacology* **47**, (1995).

49. Herz, A., Millan, M. J. & Stein, C. Arthritic inflammation in rats as a model of chronic pain: role of opioid systems. *NIDA research monograph* **95**, 110–115 (1989).

50. Cheng, H. Y. M. *et al.* DREAM is a critical transcriptional repressor for pain modulation. *Cell* **108**, 31–43 (2002).

51. Todd, A. J. Neuronal circuitry for pain processing in the dorsal horn. *Nature Reviews Neuroscience* (2010) doi:10.1038/nrn2947.

52. Duan, B., Cheng, L. & Ma, Q. Spinal Circuits Transmitting Mechanical Pain and Itch. *Neuroscience Bulletin* **34**, 186 (2018).

53. Woolf, C. J. Pain modulation in the spinal cord. *Frontiers in pain research (Lausanne, Switzerland)* **3**, (2022).

54. Gatto, G. *et al.* A Functional Topographic Map for Spinal Sensorimotor Reflexes. *Neuron* **109**, 91-104.e5 (2021).

55. Barik, A., Thompson, J. H., Seltzer, M., Ghitani, N. & Chesler, A. T. A Brainstem-Spinal Circuit Controlling Nocifensive Behavior. *Neuron* **100**, 1491-1503.e3 (2018).

56. Lindsay, N. M., Chen, C., Gilam, G., Mackey, S. & Scherrer, G. Brain circuits for pain and its treatment. *Science translational medicine* **13**, (2021).

57. Ingvar, M. Pain and functional imaging. *Philosophical transactions of the Royal Society of London. Series B, Biological sciences* **354**, 1347–1358 (1999).

58. Moulton, E. A., Schmahmann, J. D., Becerra, L. & Borsook, D. The cerebellum and pain: passive integrator or active participator? *Brain research reviews* **65**, 14–27 (2010).

59. Peyron, R., Laurent, B. & García-Larrea, L. Functional imaging of brain responses to pain. A review and meta-analysis (2000). *Neurophysiologie clinique = Clinical neurophysiology* **30**, 263–288 (2000).

60. Stein, C. Opioid Receptors. *Annual review of medicine* **67**, 433–451 (2016).

61. Schweinhardt, P. & Bushnell, M. C. Pain imaging in health and disease--how far have we come? *The Journal of clinical investigation* **120**, 3788–3797 (2010).

62. Apkarian, A. V. *et al.* Persistent pain inhibits contralateral somatosensory cortical activity in humans. *Neuroscience letters* **140**, 141–147 (1992).

63. Jones, A. K. P., Brown, W. D., Friston, K. J., Qi, L. Y. & Frackowiak, R. S. J. Cortical and subcortical localization of response to pain in man using positron emission tomography. *Proceedings. Biological sciences* **244**, 39–44 (1991).

64. Iannetti, G. D. & Mouraux, A. From the neuromatrix to the pain matrix (and back). *Experimental brain research* **205**, 1–12 (2010).

65. Davis, K. D. *et al.* Brain imaging tests for chronic pain: medical, legal and ethical issues and recommendations. *Nature reviews. Neurology* **13**, 624–638 (2017).

66. Kucyi, A. & Davis, K. D. The dynamic pain connectome. *Trends in neurosciences* **38**, 86–95 (2015).

67. Martucci, K. T. & MacKey, S. C. Neuroimaging of Pain: Human Evidence and Clinical Relevance of Central Nervous System Processes and Modulation. *Anesthesiology* **128**, 1241–1254 (2018).

68. Turk, D. C. & Melzack, R. The measurement of pain and the assessment of people experiencing pain. in *Handbook of Pain Assessment* 3–16 (The Guilford Press, 2011).

69. Pain, I. A. for the S. of. *Classification of Chronic Pain*. (IASP Press, 1986).

70. Hylands-White, N., Duarte, R. V. & Raphael, J. H. An overview of treatment approaches for chronic pain management. *Rheumatology international* **37**, 29–42 (2017).

71. S, S. The role of physical therapy in chronic pain. in *Clinical Pain Management Chronic Pain* 313–324 (2003).

72. Hayden, J., van Tulder, M. W., Malmivaara, A. & Koes, B. W. Exercise therapy for treatment of non-specific low back pain. *The Cochrane database of systematic reviews* (2005) doi:10.1002/14651858.CD000335.PUB2.

73. McHugh Pendleton, H. & Schultz-Krohn, W. *Pedretti's Occupational Therapy: Practice Skills for Physical Dysfunction*.

74. Claxton, A. J., Cramer, J. & Pierce, C. A systematic review of the associations between dose regimens and medication compliance. *Clinical therapeutics* **23**, 1296–1310 (2001).

75. Eccleston, C. Role of psychology in pain management. *British journal of anaesthesia* **87**, 144–152 (2001).

76. Beck, A., Rush, A., Shaw, B. & Emery, G. *Cognitive Therapy of Depression*. (Guilford Press, 1979).

77. Moore, R. K. *et al.* Health related quality of life of patients with refractory angina before and one year after enrolment onto a refractory angina program. *European journal of pain (London, England)* **9**, 305 (2005).

78. Moore, R. K. G. *et al.* A brief cognitive-behavioral intervention reduces hospital admissions in refractory angina patients. *Journal of pain and symptom management* **33**, 310–316 (2007).

79. Hayes, S., Follette, V. & Linehan, M. Acceptance and commitment therapy and the new behaviour therapies. in *Mindfulness and acceptance: expanding the cognitive–behavioral tradition.* 1–29 (Guilford Press, 2004).

80. Sturgeon, J. A. Psychological therapies for the management of chronic pain. *Psychology research and behavior management* **7**, 115–124 (2014).

81. Ventafridda, V., Saita, L., Ripamonti, C. & De Conno, F. WHO guidelines for the use of analgesics in cancer pain. *International Journal of Tissue Reactions* **7**, 93–96 (1985).

82. Williams, J. T. *et al.* Regulation of m-Opioid Receptors: Desensitization, Phosphorylation, Internalization, and Tolerance. (2013) doi:10.1124/pr.112.005942.

83. Koehl, A. *et al.* Structure of the μ Opioid Receptor-Gi Protein Complex. *Nature* **558**, 547 (2018).

84. Trescot, A. M., Datta, S., Lee, M. & Hans, H. Opioid pharmacology. *Pain physician* **11**, (2008).

85. Kieffer, B. L., Befort, K., Gaveriaux-Ruff, C. & Hirth, C. G. The delta-opioid receptor: isolation of a cDNA by expression cloning and pharmacological characterization. *Proceedings of the National Academy of Sciences of the United States of America* **89**, 12048–12052 (1992).

86. Evans, C. J., Keith, D. E., Morrison, H., Magendzo, K. & Edwards, R. H. Cloning of a delta opioid receptor by functional expression. *Science (New York, N.Y.)* **258**, 1952–1955 (1992).

87. Hughes, J. *et al.* Identification of two related pentapeptides from the brain with potent opiate agonist activity. *Nature* **258**, 577–579 (1975).

88. Zöllner, C. & Stein, C. Opioids. *Handbook of experimental pharmacology* **177**, 31–63 (2007).

89. Filliol, D. *et al.* Mice deficient for delta- and mu-opioid receptors exhibit opposing alterations of emotional responses. *Nature genetics* **25**, 195–200 (2000).

90. Pradhan, A. A., Befort, K., Nozaki, C., Gavériaux-Ruff, C. & Kieffer, B. L. The delta opioid receptor: an evolving target for the treatment of brain disorders. *Trends in pharmacological sciences* **32**, 581–590 (2011).

91. Kieffer, B. L. & Gavériaux-Ruff, C. Exploring the opioid system by gene knockout. *Progress in Neurobiology* **66**, 285–306 (2002).

92. Pasternak, G. W. Incomplete cross tolerance and multiple mu opioid peptide receptors. *Trends in pharmacological sciences* **22**, 67–70 (2001).

93. Bolan, E. A., Pan, Y. X. & Pasternak, G. W. Functional analysis of MOR-1 splice variants of the mouse mu opioid receptor gene Oprm. *Synapse (New York, N.Y.)* **51**, 11–18 (2004).

94. Pan, L. *et al.* Identification and characterization of six new alternatively spliced variants of the human mu opioid receptor gene, Oprm. *Neuroscience* **133**, 209–220 (2005).

95. Deng, H. B. *et al.* Role for the C-terminus in agonist-induced mu opioid receptor phosphorylation and desensitization. *Biochemistry* **39**, 5492–5499 (2000).

96. Staahl, C. *et al.* Differential effect of opioids in patients with chronic pancreatitis: an experimental pain study. *Scandinavian journal of gastroenterology* **42**, 383–390 (2007).

97. Drewes, A. M. *et al.* Differences between opioids: pharmacological, experimental, clinical and economical perspectives. *British Journal of Clinical Pharmacology* **75**, 60 (2013).

98. Gretton, S. K. & Droney, J. Splice variation of the mu-opioid receptor and its effect on the action of opioids. *British journal of pain* **8**, 133–138 (2014).

99. Pan, Y. X. *et al.* Generation of the mu opioid receptor (MOR-1) protein by three new splice variants of the Oprm gene. *Proceedings of the National Academy of Sciences of the United States of America* **98**, 14084–14089 (2001).

100. Xu, J. *et al.* Isolating and characterizing three alternatively spliced mu opioid receptor variants: mMOR-1A, mMOR-1O, and mMOR-1P. *Synapse (New York, N.Y.)* **68**, 144–152 (2014).

101. Pang, G. S. Y. *et al.* A non-synonymous single nucleotide polymorphism in an OPRM1 splice variant is associated with fentanyl-induced emesis in women undergoing minor gynaecological surgery. *PloS one* **7**, (2012).

102. Liu, X. Y. *et al.* Unidirectional cross-activation of GRPR by MOR1D uncouples itch and analgesia induced by opioids. *Cell* **147**, 447–458 (2011).

103. Tedford, H. W. & Zamponi, G. W. Direct G protein modulation of Cav2 calcium channels. *Pharmacological reviews* **58**, 837–862 (2006).

104. Lüscher, C. & Slesinger, P. A. Emerging roles for G protein-gated inwardly rectifying potassium (GIRK) channels in health and disease. *Nature reviews. Neuroscience* **11**, 301–315 (2010).

105. Corder, G., Castro, D. C., Bruchas, M. R. & Scherrer, G. Endogenous and Exogenous Opioids in Pain. *Annual review of neuroscience* **41**, 453–473 (2018).

106. Mitrovic, I. *et al.* Contribution of GIRK2-mediated postsynaptic signaling to opiate and alpha 2-adrenergic analgesia and analgesic sex differences. *Proceedings of the National Academy of Sciences of the United States of America* **100**, 271–276 (2003).

107. Marker, C. L., Stoffel, M. & Wickman, K. Spinal G-protein-gated K+ channels formed by GIRK1 and GIRK2 subunits modulate thermal nociception and contribute to morphine analgesia. *The Journal of neuroscience : the official journal of the Society for Neuroscience* **24**, 2806–2812 (2004).

108. Blednov, Y. A., Stoffel, M., Alva, H. & Harris, R. A. A pervasive mechanism for analgesia: activation of GIRK2 channels. *Proceedings of the National Academy of Sciences of the United States of America* **100**, 277–282 (2003).

109. Gold, M. S. & Levine, J. D. DAMGO inhibits prostaglandin E2-induced potentiation of a TTX-resistant Na+ current in rat sensory neurons in vitro. *Neuroscience Letters* **212**, 83–86 (1996).

110. Ingram, S. L. & Williams, J. T. Opioid inhibition of Ih via adenylyl cyclase. *Neuron* **13**, 179–186 (1994).

111. Endres-Becker, J. *et al.* Mu-opioid receptor activation modulates transient receptor potential vanilloid 1 (TRPV1) currents in sensory neurons in a model of inflammatory pain. *Molecular pharmacology* **71**, 12–18 (2007).

112. Spahn, V. *et al.* Opioid withdrawal increases transient receptor potential vanilloid 1 activity in a protein kinase A-dependent manner. *Pain* **154**, 598–608 (2013).

113. Cai, Q. *et al.* Morphine inhibits acid-sensing ion channel currents in rat dorsal root ganglion neurons. *Brain research* **1554**, 12–20 (2014).

114. Pathan, H. & Williams, J. Basic opioid pharmacology: an update. *British Journal of Pain* **6**, 11 (2012).

115. Jensen, T. S. & Yaksh, T. L. Comparison of antinociceptive action of morphine in the periaqueductal gray, medial and paramedial medulla in rat. *Brain research* **363**, 99–113 (1986).

116. Gebhart, G. F., Sandkuhler, J., Thalhammer, J. G. & Zimmermann, M. Inhibition in spinal cord of nociceptive information by electrical stimulation and morphine microinjection at identical sites in midbrain of the cat. *Journal of neurophysiology* **51**, 75–89 (1984).

117. Gebhart, G. F. & Jones, S. L. Effects of morphine given in the brain stem on the activity of dorsal horn nociceptive neurons. *Progress in brain research* **77**, 229–243 (1988).

118. Carman, C. V. & Benovic, J. L. G-protein-coupled receptors: Turn-ons and turn-offs. *Current Opinion in Neurobiology* **8**, 335–344 (1998).

119. Krupnick, J. G. & Benovic, J. L. The role of receptor kinases and arrestins in G protein-coupled receptor regulation. *Annual review of pharmacology and toxicology* **38**, 289–319 (1998).

120. Gurevich, V. V. & Gurevich, E. V. GPCR signaling regulation: The role of GRKs and arrestins. *Frontiers in Pharmacology* **10**, (2019).

121. Wang, H. L. A cluster of Ser/Thr residues at the C-terminus of μ-opioid receptor is required for G protein-coupled receptor kinase 2-mediated desensitization. *Neuropharmacology* **39**, 353–363 (2000).

122. Li, A. H. & Wang, H. L. G protein-coupled receptor kinase 2 mediates mu-opioid receptor desensitization in GABAergic neurons of the nucleus raphe magnus. *Journal of neurochemistry* **77**, 435–444 (2001).

123. Kovoor, A., Celver, J. P., Wu, A. & Chavkin, C. Agonist induced homologous desensitization of mu-opioid receptors mediated by G protein-coupled receptor kinases is dependent on agonist efficacy. *Molecular pharmacology* **54**, 704–711 (1998).

124. Cheng, Z. J., Yu, Q. M., Wu, Y. L., Ma, L. & Pei, G. Selective interference of beta-arrestin 1 with kappa and delta but not mu opioid receptor/G protein coupling. *The Journal of biological chemistry* **273**, 24328–24333 (1998).

125. KÜHn, H. & Wilden, U. Deactivation of Photoactivated Rhodopsin by Rhodopsin-Kinase and Arrestin. *Journal of Receptor Research* **7**, 283–298 (1987).

126. Benovic, J. L. *et al.* Functional desensitization of the isolated beta-adrenergic receptor by the beta-adrenergic receptor kinase: potential role of an analog of the retinal protein arrestin (48-kDa protein). *Proceedings of the National Academy of Sciences* **84**, 8879–8882 (1987).

127. Lohse, M. J., Benovic, J. L., Codina, J., Caron, M. G. & Lefkowitz, R. J. beta-Arrestin: a protein that regulates beta-adrenergic receptor function. *Science (New York, N.Y.)* **248**, 1547–1550 (1990).

128. Attramadal, H. *et al.* Beta-arrestin2, a novel member of the arrestin/beta-arrestin gene family. *The Journal of biological chemistry* **267**, 17882–17890 (1992).

129. Gainetdinov, R. R., Premont, R. T., Bohn, L. M., Lefkowitz, R. J. & Caron, M. G. Desensitization of G protein-coupled receptors and neuronal functions. *Annual review of neuroscience* **27**, 107–144 (2004).

130. Everitt, B. J. & Robbins, T. W. Neural systems of reinforcement for drug addiction: from actions to habits to compulsion. *Nature neuroscience* **8**, 1481–1489 (2005).

131. Salamone, J. D. Functions of mesolimbic dopamine: changing concepts and shifting paradigms. *Psychopharmacology* **191**, 389 (2007).

132. Volkow, N. D., Michaelides, M. & Baler, R. The Neuroscience of Drug Reward and Addiction. *Physiological reviews* **99**, 2115–2140 (2019).

133. Fields, H. L. & Margolis, E. B. Understanding opioid reward. *Trends in neurosciences* **38**, 217–225 (2015).

134. Trigo, J. M., Martin-García, E., Berrendero, F., Robledo, P. & Maldonado, R. The endogenous opioid system: a common substrate in drug addiction. *Drug and alcohol dependence* **108**, 183–194 (2010).

135. Laurent, V., Morse, A. K. & Balleine, B. W. The role of opioid processes in reward and decision-making. *British journal of pharmacology* **172**, 449–459 (2015).

136. Gourley, S. L. & Taylor, J. R. Going and stopping: Dichotomies in behavioral control by the prefrontal cortex. *Nature neuroscience* **19**, 656–664 (2016).

137. Wise, R. A. The neurobiology of craving: implications for the understanding and treatment of addiction. *Journal of abnormal psychology* **97**, 118–132 (1988).

138. Balleine, B. W. Neural bases of food-seeking: affect, arousal and reward in corticostriatolimbic circuits. *Physiology & behavior* **86**, 717–730 (2005).

139. Cardinal, R. N., Parkinson, J. A., Hall, J. & Everitt, B. J. Emotion and motivation: The role of the amygdala, ventral striatum, and prefrontal cortex. *Neuroscience and Biobehavioral Reviews* **26**, 321–352 (2002).

140. Hyman, S. E., Malenka, R. C. & Nestler, E. J. Neural mechanisms of addiction: the role of reward-related learning and memory. *Annual review of neuroscience* **29**, 565–598 (2006).

141. Koob, G. F. & Le Moal, M. Drug addiction, dysregulation of reward, and allostasis. *Neuropsychopharmacology : official publication of the American College of Neuropsychopharmacology* **24**, 97–129 (2001).

142. Davis, M. & Whalen, P. J. The amygdala: vigilance and emotion. *Molecular psychiatry* **6**, 13–34 (2001).

143. Kelley, A. E. & Berridge, K. C. The neuroscience of natural rewards: relevance to addictive drugs. *The Journal of neuroscience : the official journal of the Society for Neuroscience* **22**, 3306–3311 (2002).

144. Bozarth, M. A. & Wise, R. A. Intracranial self-administration of morphine into the ventral tegmental area in rats. *Life sciences* **28**, 551–555 (1981).

145. Phillips, A. G. & LePiane, F. G. Reinforcing effects of morphine microinjection into the ventral tegmental area. *Pharmacology, biochemistry, and behavior* **12**, 965–968 (1980).

146. Phillips, A. G., LePiane, F. G. & Fibiger, H. C. Dopaminergic mediation of reward produced by direct injection of enkephalin into the ventral tegmental area of the rat. *Life sciences* **33**, 2505–2511 (1983).

147. Johnson, S. W. & North, R. A. Opioids excite dopamine neurons by hyperpolarization of local interneurons. *Journal of Neuroscience* **12**, 483–488 (1992).

148. Everitt, B. J. & Robbins, T. W. Drug Addiction: Updating Actions to Habits to Compulsions Ten Years On. *Annual review of psychology* **67**, 23–50 (2016).

149. Mitchell, M. R., Berridge, K. C. & Mahler, S. V. Endocannabinoid-Enhanced 'Liking' in Nucleus Accumbens Shell Hedonic Hotspot Requires Endogenous Opioid Signals. *Cannabis and cannabinoid research* **3**, 166–170 (2018).

150. Castro, D. C. & Berridge, K. C. Opioid hedonic hotspot in nucleus accumbens shell: mu, delta, and kappa maps for enhancement of sweetness 'liking' and 'wanting'. *The Journal of neuroscience : the official journal of the Society for Neuroscience* **34**, 4239–4250 (2014).

151. Grueter, B. A., Rothwell, P. E. & Malenka, R. C. Integrating synaptic plasticity and striatal circuit function in addiction. *Current opinion in neurobiology* **22**, 545–551 (2012).

152. Koob, G. F. Neurobiology of addiction. Toward the development of new therapies. *Annals of the New York Academy of Sciences* **909**, 170–185 (2000).

153. Peciña, S. & Berridge, K. C. Hedonic hot spot in nucleus accumbens shell: where do mu-opioids cause increased hedonic impact of sweetness? *The Journal of neuroscience : the official journal of the Society for Neuroscience* **25**, 11777–11786 (2005).

154. Smith, K. S. & Berridge, K. C. The ventral pallidum and hedonic reward: neurochemical maps of sucrose 'liking' and food intake. *The Journal of neuroscience : the official journal of the Society for Neuroscience* **25**, 8637–8649 (2005).

155. Smith, K. S. & Berridge, K. C. Opioid limbic circuit for reward: interaction between hedonic hotspots of nucleus accumbens and ventral pallidum. *The Journal of neuroscience : the official journal of the Society for Neuroscience* **27**, 1594–1605 (2007).

156. Jewett, K. A., Lee, K. Y., Eagleman, D. E., Soriano, S. & Tsai, N. P. Dysregulation and restoration of homeostatic network plasticity in fragile X syndrome mice. *Neuropharmacology* **138**, 182–192 (2018).

157. Dautan, D. *et al.* Segregated cholinergic transmission modulates dopamine neurons integrated in distinct functional circuits. *Nature neuroscience* **19**, 1025–1033 (2016).

158. Lim, S. A. O., Kang, U. J. & McGehee, D. S. Striatal cholinergic interneuron regulation and circuit effects. *Frontiers in synaptic neuroscience* **6**, (2014).

159. Fitzgerald, P. J. Elevated Norepinephrine may be a Unifying Etiological Factor in the Abuse of a Broad Range of Substances: Alcohol, Nicotine, Marijuana, Heroin, Cocaine, and Caffeine. *Substance abuse : research and treatment* **7**, 171–183 (2013).

160. Borroto-Escuela, D. O. *et al.* Disturbances in the FGFR1-5-HT1A Heteroreceptor Complexes in the Raphe-Hippocampal 5-HT System Develop in a Genetic Rat Model of Depression. *Frontiers in cellular neuroscience* **11**, (2017).

161. Macoveanu, J. Serotonergic modulation of reward and punishment: evidence from pharmacological fMRI studies. *Brain research* **1556**, 19–27 (2014).

162. Scheefhals, N. & MacGillavry, H. D. Functional organization of postsynaptic glutamate receptors. *Molecular and cellular neurosciences* **91**, 82–94 (2018).

163. Kauer, J. A. & Malenka, R. C. Synaptic plasticity and addiction. *Nature reviews. Neuroscience* **8**, 844–858 (2007).

164. Scofield, M. D. *et al.* The Nucleus Accumbens: Mechanisms of Addiction across Drug Classes Reflect the Importance of Glutamate Homeostasis. *Pharmacological reviews* **68**, 816–871 (2016).

165. Wolf, M. E. Synaptic mechanisms underlying persistent cocaine craving. *Nature reviews. Neuroscience* **17**, 351–365 (2016).

166. Golden, S. A. & Russo, S. J. Mechanisms of psychostimulant-induced structural plasticity. *Cold Spring Harbor perspectives in medicine* **2**, (2012).

167.   Pignatelli, M. & Bonci, A. Role of Dopamine Neurons in Reward and Aversion: A Synaptic Plasticity Perspective. *Neuron* **86**, 1145–1157 (2015).

168.   Shan, Q., Ge, M., Christie, M. J. & Balleine, B. W. The acquisition of goal-directed actions generates opposing plasticity in direct and indirect pathways in dorsomedial striatum. *The Journal of neuroscience : the official journal of the Society for Neuroscience* **34**, 9196–9201 (2014).

169.   Opioid Overdose | Drug Overdose | CDC Injury Center. https://www.cdc.gov/drugoverdose/index.html.

170.   Rudd, R. A., Seth, P., David, F. & Scholl, L. Increases in drug and opioid-involved overdose deaths — United States, 2010-2015. *Morbidity and Mortality Weekly Report* (2016) doi:10.15585/mmwr.mm655051e1.

171.   Mattson, C. L. *et al.* Trends and Geographic Patterns in Drug and Synthetic Opioid Overdose Deaths — United States, 2013–2019. *MMWR. Morbidity and Mortality Weekly Report* **70**, 202–207 (2022).

172.   Zelaya, C. E., Dahlhamer, J. M., Lucas, J. W. & Connor, E. M. Chronic Pain and High-impact Chronic Pain Among U.S. Adults, 2019. *NCHS data brief* 1–8 (2020).

173.   Duca, L. M. *et al.* A Review of Potential National Chronic Pain Surveillance Systems in the United States. *Journal of Pain* **23**, 1492–1509 (2022).

174.   Yong, R. J., Mullins, P. M. & Bhattacharyya, N. Prevalence of chronic pain among adults in the United States. *Pain* **163**, E328–E332 (2022).

175.   Goldberg, D. S. & McGee, S. J. Pain as a global public health priority. *BMC public health* **11**, (2011).

176.   Cohen, S. P., Vase, L. & Hooten, W. M. Chronic pain: an update on burden, best practices, and new advances. *The Lancet* **397**, 2082–2097 (2021).

177.   Clarke, J. L., Skoufalos, A. & Scranton, R. The American Opioid Epidemic: Population health implications and potential solutions. Report from the national stakeholder panel. *Population Health Management* **19**, S1–S10 (2016).

178.   Policy SLoD. Harrison Narcotics Tax Act, 1914. http://www.druglibrary.org/schaffer/history/e1910/ harrisonact.htm.

179.   Vadivelu, N., Kai, A. M., Kodumudi, V., Sramcik, J. & Kaye, A. D. The Opioid Crisis: a Comprehensive Overview. *Current pain and headache reports* **22**, (2018).

180.   Pain, I. P. S. of the I. A. for the S. of. Declaration of Montréal: Declaration That Access to Pain Management Is a Fundamental Human Right. *http://dx.doi.org/10.3109/15360288.2010.547560* **25**, 29–31 (2011).

181.   Unruh, A. M. Gender variations in clinical pain experience. *Pain* **65**, 123–167 (1996).

182.   Berkley, K. Sex Differences in Pain. *Behavioural Brain Science* **20**, 371–80 (1997).

183. Ren, X., Amick, B. & Williams, D. Racial/ethnic disparities in health: the interplay between discrimination and socioeconomic status. *Ethnicity & Disease* **9**, 151–65 (1999).

184. Todd, K. H., Samaroo, N. & Hoffman, J. R. Ethnicity as a Risk Factor for Inadequate Emergency Department Analgesia. *JAMA* **269**, 1537–1539 (1993).

185. Elliott, T. E. Principles of Analgesic Use in the Treatment of Acute Pain and Cancer Pain, 4th EditionThe American Pain Society: Principles of Analgesic Use in the Treatment of Acute Pain and Cancer Pain. 4th edition. Glenview, IL: American Pain Society, 1999. $7.00. *Journal of Palliative Medicine* **3**, 98–99 (2000).

186. Frasco, P. E., Sprung, J. & Trentman, T. L. The impact of the joint commission for accreditation of healthcare organizations pain initiative on perioperative opiate consumption and recovery room length of stay. *Anesthesia and analgesia* **100**, 162–168 (2005).

187. Van Zee, A. The promotion and marketing of oxycontin: commercial triumph, public health tragedy. *American journal of public health* **99**, 221–227 (2009).

188. CDC Grand Rounds: Prescription Drug Overdoses — a U.S. Epidemic. https://www.cdc.gov/mmwr/preview/mmwrhtml/mm6101a3.htm.

189. Lipton, B. & Colon, D. WORKERS COMPENSATION AND PRESCRIPTION DRUGS — 2018 UPDATE. https://www.ncci.com/Articles/Documents/Insights_ResearchBrief_WC_Prescription_Drugs-2018.pdf (2019).

190. Matthes, H. W. D. *et al.* Loss of morphine-induced analgesia, reward effect and withdrawal symptoms in mice lacking the mu-opioid-receptor gene. *Nature* **383**, 822–823 (1996).

191. Contet, C., Kieffer, B. L. & Befort, K. Mu opioid receptor: A gateway to drug addiction. *Current Opinion in Neurobiology* **14**, 370–378 (2004).

192. Roberts, A. J. *et al.* Opioid Receptor Knockout Mice Do Not Self-Administer Alcohol 1,2. *THE JOURNAL OF PHARMACOLOGY AND EXPERIMENTAL THERAPEUTICS* **293**, (2000).

193. Ghozland, S. *et al.* Motivational effects of cannabinoids are mediated by mu-opioid and kappa-opioid receptors. *The Journal of neuroscience : the official journal of the Society for Neuroscience* **22**, 1146–1154 (2002).

194. Berrendero, F., Kieffer, B. L. & Maldonado, R. Attenuation of nicotine-induced antinociception, rewarding effects, and dependence in mu-opioid receptor knock-out mice. *The Journal of neuroscience : the official journal of the Society for Neuroscience* **22**, 10935–10940 (2002).

195. Papaleo, F., Kieffer, B. L., Tabarin, A. & Contarino, A. Decreased motivation to eat in mu-opioid receptor-deficient mice. *The European journal of neuroscience* **25**, 3398–3405 (2007).

196. Moles, A., Kieffer, B. L. & D'Amato, F. R. Deficit in attachment behavior in mice lacking the mu-opioid receptor gene. *Science (New York, N.Y.)* **304**, 1983–1986 (2004).

197. Becker, J. A. *et al.* Autistic-like syndrome in mu opioid receptor null mice is relieved by facilitated mGluR4 activity. *Neuropsychopharmacology : official publication of the American College of Neuropsychopharmacology* **39**, 2049–2060 (2014).

198. Bohn, L. M. *et al.* Enhanced morphine analgesia in mice lacking beta-arrestin 2. *Science (New York, N.Y.)* **286**, 2495–2498 (1999).

199. Raehal, K. M., Walker, J. K. L. & Bohn, L. M. Morphine side effects in beta-arrestin 2 knockout mice. *The Journal of pharmacology and experimental therapeutics* **314**, 1195–1201 (2005).

200. Olson, K. M., Lei, W., Keresztes, A., Lavigne, J. & Streicher, J. M. Focus: Drug Development: Novel Molecular Strategies and Targets for Opioid Drug Discovery for the Treatment of Chronic Pain. *The Yale Journal of Biology and Medicine* **90**, 97 (2017).

201. Siuda, E. R., Carr, R., Rominger, D. H. & Violin, J. D. Biased mu-opioid receptor ligands: a promising new generation of pain therapeutics. *Current opinion in pharmacology* **32**, 77–84 (2017).

202. Schmid, C. L. *et al.* Bias Factor and Therapeutic Window Correlate to Predict Safer Opioid Analgesics. *Cell* **171**, 1165.e13-1175.e13 (2017).

203. DeWire, S. M. *et al.* A G protein-biased ligand at the μ-opioid receptor is potently analgesic with reduced gastrointestinal and respiratory dysfunction compared with morphine. *The Journal of pharmacology and experimental therapeutics* **344**, 708–717 (2013).

204. Lambert, D. & Calo, G. Approval of oliceridine (TRV130) for intravenous use in moderate to severe pain in adults. *British journal of anaesthesia* **125**, e473–e474 (2020).

205. Manglik, A. *et al.* Structure-based discovery of opioid analgesics with reduced side effects. *Nature* **537**, 185–190 (2016).

206. Spahn, V. *et al.* A nontoxic pain killer designed by modeling of pathological receptor conformations. *Science (New York, N.Y.)* **355**, 966–969 (2017).

207. Burford, N. T. *et al.* Discovery of positive allosteric modulators and silent allosteric modulators of the μ-opioid receptor. *Proceedings of the National Academy of Sciences of the United States of America* **110**, 10830–10835 (2013).

208. Noble, F. & Roques, B. P. [Selective opioid agonists and inhibitors of enkephalin degradation enzymes: pharmacological and clinical values]. *Comptes rendus des seances de la Societe de biologie et de ses filiales* **186**, 37–60 (1992).

209. Khroyan, T. V. *et al.* The first universal opioid ligand, (2S)-2-[(5R,6R,7R,14S)-N-cyclopropylmethyl-4,5-epoxy-6,14-ethano-3-hydroxy-6-methoxymorphinan-7-yl]-3,3-dimethylpentan-2-ol (BU08028): characterization of the in vitro profile and in vivo behavioral effects in mouse models of acute pain and cocaine-induced reward. *The Journal of pharmacology and experimental therapeutics* **336**, 952–961 (2011).

210. Gomes, I. *et al.* Identification of a μ-δ opioid receptor heteromerbiased agonist with antinociceptive activity. *Proceedings of the National Academy of Sciences of the United States of America* **110**, 12072–12077 (2013).

211. Woolfe, G. & Macdonald, A. D. The Evaluation of the Analgesic Action of Pethidine hydrochloride (Demerol). *Journal of Pharmacology and Experimental Therapeutics* **80**, (1944).

212. Bernardi, M., Bertolini, A., Szczawinska, K. & Genedani, S. Blockade of the polyamine site of NMDA receptors produces antinociception and enhances the effect of morphine, in mice. *European Journal of Pharmacology* **298**, 51–55 (1996).

213. D'amour, F. E. & Smith, D. L. *A METhOD FOR DETERMINING LOSS OF PAIN SENSATION*.

214. Wong, C. S., Cherng, C. H., Luk, H. N., Ho, S. T. & Tung, C. S. Effects of NMDA receptor antagonists on inhibition of morphine tolerance in rats: binding at mu-opioid receptors. *European journal of pharmacology* **297**, 27–33 (1996).

215. Pantouli, F. *et al.* Comparison of morphine, oxycodone and the biased MOR agonist SR-17018 for tolerance and efficacy in mouse models of pain. *Neuropharmacology* **185**, (2021).

216. Hargreaves, K., Dubner, R., Brown, F., Flores, C. & Joris, J. A new and sensitive method for measuring thermal nociception in cutaneous hyperalgesia. *Pain* **32**, 77–88 (1988).

217. Harvey, V. L. & Dickenson, A. H. Behavioural and electrophysiological characterisation of experimentally induced osteoarthritis and neuropathy in C57Bl/6 mice. *Molecular pain* **5**, (2009).

218. O'Brien, D. E., Brenner, D. S., Gutmann, D. H. & Gereau IV, R. W. Assessment of pain and itch behavior in a mouse model of neurofibromatosis type 1. *The journal of pain* **14**, 628–637 (2013).

219. Chaplan, S. R., Bach, F. W., Pogrel, J. W., Chung, J. M. & Yaksh, T. L. Quantitative assessment of tactile allodynia in the rat paw. *Journal of neuroscience methods* **53**, 55–63 (1994).

220. Scholz, J. *et al.* Blocking caspase activity prevents transsynaptic neuronal apoptosis and the loss of inhibition in lamina II of the dorsal horn after peripheral nerve injury. *The Journal of neuroscience : the official journal of the Society for Neuroscience* **25**, 7317–7323 (2005).

221. Minett, M. S., Quick, K. & Wood, J. N. Behavioral Measures of Pain Thresholds. *Current protocols in mouse biology* **1**, 383–412 (2011).

222. RANDALL, L. O. & SELITTO, J. J. A method for measurement of analgesic activity on inflamed tissue. *Archives internationales de pharmacodynamie et de therapie* **111**, 409–419 (1957).

223. Santos-Nogueira, E., Redondo Castro, E., Mancuso, R. & Navarro, X. Randall-Selitto test: a new approach for the detection of neuropathic pain after spinal cord injury. *Journal of neurotrauma* **29**, 898–904 (2012).

224. Dubuisson, D. & Dennis, S. G. The formalin test: a quantitative study of the analgesic effects of morphine, meperidine, and brain stem stimulation in rats and cats. *Pain* **4**, 161–174 (1977).

225. Hunskaar, S. & Hole, K. The formalin test in mice: dissociation between inflammatory and non-inflammatory pain. *Pain* **30**, 103–114 (1987).

226. Hoffmann, T. *et al.* The formalin test does not probe inflammatory pain but excitotoxicity in rodent skin. *Physiological reports* **10**, (2022).

227. López-Cano, M., Fernández-Dueñas, V., Llebaria, A. & Ciruela, F. Formalin Murine Model of Pain. *Bio-protocol* **7**, (2017).

228. Brittain, R. T., Lehrer, D. N. & Spencer, P. S. J. Phenylquinone Writhing Test: Interpretation of Data. *Nature* **200**, 895–896 (1963).

229. Mogilski, S. *et al.* Antinociceptive, anti-inflammatory and smooth muscle relaxant activities of the pyrrolo[3,4-d]pyridazinone derivatives: Possible mechanisms of action. *Pharmacology, biochemistry, and behavior* **133**, 99–110 (2015).

230. Ren, K., Hylden, J. L. K., Williams, G. M., Ruda, M. A. & Dubner, R. The effects of a non-competitive NMDA receptor antagonist, MK-801, on behavioral hyperalgesia and dorsal horn neuronal activity in rats with unilateral inflammation. *Pain* **50**, 331–344 (1992).

231. Gu, Y. *et al.* Electroacupuncture Attenuates CFA-Induced Inflammatory Pain by Regulating CaMKII. *Neural plasticity* **2020**, (2020).

232. Boyce, S. *et al.* Selective NMDA NR2B antagonists induce antinociception without motor dysfunction: Correlation with restricted localisation of NR2B subunit in dorsal horn. *Neuropharmacology* (1999) doi:10.1016/S0028-3908(98)00218-4.

233. Taniguchi, K. *et al.* Antinociceptive activity of CP-101,606, an NMDA receptor NR2B subunit antagonist. *British journal of pharmacology* **122**, 809–812 (1997).

234. Buisseret, B., Guillemot-Legris, O., Muccioli, G. G. & Alhouayek, M. Prostaglandin D2-glycerol ester decreases carrageenan-induced inflammation and hyperalgesia in mice. *Biochimica et biophysica acta. Molecular and cell biology of lipids* **1864**, 609–618 (2019).

235. Alsalem, M. *et al.* Anti-nociceptive and desensitizing effects of olvanil on capsaicin-induced thermal hyperalgesia in the rat. *BMC pharmacology & toxicology* **17**, (2016).

236. Sakurada, T., Katsumata, K., Tan-No, K., Sakurada, S. & Kisara, K. The capsaicin test in mice for evaluating tachykinin antagonists in the spinal cord. *Neuropharmacology* **31**, 1279–1285 (1992).

237. Jancsó, N., Jancsó-Gábor, A. & Szolcsányi, J. Direct evidence for neurogenic inflammation and its prevention by denervation and by pretreatment with capsaicin. *British journal of pharmacology and chemotherapy* **31**, 138–151 (1967).

238. Zhang, L., Stuber, F., Lippuner, C., Schiff, M. & Stamer, U. M. Phorbol-12-myristate-13-acetate induces nociceptin in human Mono Mac 6 cells via multiple transduction signalling pathways. *British journal of anaesthesia* **117**, 250–257 (2016).

239. Chang, S. N. *et al.* Phorbol 12-Myristate 13-Acetate Induced Toxicity Study and the Role of Tangeretin in Abrogating HIF-1α-NF-κB Crosstalk In Vitro and In Vivo. *International journal of molecular sciences* **21**, 1–22 (2020).

240. Tsuchiya, M., Sakakibara, A. & Yamamoto, M. A tachykinin NK1 receptor antagonist attenuates the 4 beta-phorbol-12-myristate-13-acetate-induced nociceptive behaviour in the rat. *European journal of pharmacology* **507**, 29–34 (2005).

241. Ho Kim, S. & Mo Chung, J. An experimental model for peripheral neuropathy produced by segmental spinal nerve ligation in the rat. *Pain* **50**, 355–363 (1992).

242. Korah, H. E. *et al.* Partial Sciatic Nerve Ligation: A Mouse Model of Chronic Neuropathic Pain to Study the Antinociceptive Effect of Novel Therapies. *Journal of visualized experiments : JoVE* (2022) doi:10.3791/64555.

243. Kosten, T. R. & George, T. P. The Neurobiology of Opioid Dependence: Implications for Treatment.

244. Buntin-Mushock, C., Phillip, L., Moriyama, K. & Palmer, P. P. Age-dependent opioid escalation in chronic pain patients. *Anesthesia and Analgesia* Preprint at https://doi.org/10.1213/01.ANE.0000152191.29311.9B (2005).

245. Morgan, M. M. & Christie, M. J. Analysis of opioid efficacy, tolerance, addiction and dependence from cell culture to human. *British Journal of Pharmacology* Preprint at https://doi.org/10.1111/j.1476-5381.2011.01335.x (2011).

246. Ling, G. S. F., Paul, D., Simantov, R. & Pasternak, G. W. Differential development of acute tolerance to analgesia, respiratory depression, gastrointestinal transit and hormone release in a morphine infusion model. *Life Sciences* (1989) doi:10.1016/0024-3205(89)90272-5.

247. Tomek, S. E., LaCrosse, A. L., Nemirovsky, N. E. & Foster Olive, M. NMDA receptor modulators in the treatment of drug addiction. *Pharmaceuticals* Preprint at https://doi.org/10.3390/ph6020251 (2013).

248. Gulur, P., Williams, L., Chaudhary, S., Koury, K. & Jaff, M. Opioid tolerance--a predictor of increased length of stay and higher readmission rates. *Pain Physician* **17**, 503–7 (2014).

249. Tortorici, V., Morgan, M. M. & Vanegas, H. Tolerance to repeated microinjection of morphine into the periaqueductal gray is associated with changes in the behavior of off- and on-cells in the rostral ventromedial medulla of rats. *Pain* **89**, 237–244 (2001).

250. Morgan, M. M., Fossum, E. N., Levine, C. S. & Ingram, S. L. Antinociceptive tolerance revealed by cumulative intracranial microinjections of morphine into the periaqueductal gray in the rat. *Pharmacology, biochemistry, and behavior* **85**, 214–219 (2006).

251. Lueptow, L. M., Fakira, A. K. & Bobeck, E. N. The Contribution of the Descending Pain Modulatory Pathway in Opioid Tolerance. *Frontiers in neuroscience* **12**, (2018).

252. Morgan, M. M., Whittier, K. L., Hegarty, D. M. & Aicher, S. A. Periaqueductal gray neurons project to spinally projecting GABAergic neurons in the rostral ventromedial medulla. *Pain* **140**, 376–386 (2008).

253. Stiller, C. O., Bergquist, J., Beck, O., Ekman, R. & Brodin, E. Local administration of morphine decreases the extracellular level of GABA in the periaqueductal gray matter of freely moving rats. *Neuroscience Letters* **209**, 165–168 (1996).

254. Bobeck, E. N., Chen, Q., Morgan, M. M. & Ingram, S. L. Contribution of adenylyl cyclase modulation of pre- and postsynaptic GABA neurotransmission to morphine antinociception and tolerance. *Neuropsychopharmacology : official publication of the American College of Neuropsychopharmacology* **39**, 2142–2152 (2014).

255. Wierenga, C. J. & Wadman, W. J. Miniature inhibitory postsynaptic currents in CA1 pyramidal neurons after kindling epileptogenesis. *Journal of Neurophysiology* **82**, 1352–1362 (1999).

256. El Kouhen, R. *et al.* Phosphorylation of Ser363, Thr370, and Ser375 residues within the carboxyl tail differentially regulates mu-opioid receptor internalization. *The Journal of biological chemistry* **276**, 12774–12780 (2001).

257. Allouche, S., Noble, F. & Marie, N. Opioid receptor desensitization: mechanisms and its link to tolerance. *Frontiers in pharmacology* **5**, (2014).

258. Chiu, Y. T., Chen, C., Yu, D., Schulz, S. & Liu-Chen, L. Y. Correction: Agonist-dependent and-independent k opioid receptor phosphorylation: Distinct phosphorylation patterns and different cellular outcomes(Mol. Pharmacol (2018) 92: 5 (588-600) DOI: 10.1124/mol.117.108555). *Molecular Pharmacology* **94**, 895 (2018).

259. Doll, C. *et al.* Deciphering μ-opioid receptor phosphorylation and dephosphorylation in HEK293 cells. *British Journal of Pharmacology* **167**, 1259 (2012).

260. Goodman, O. B. *et al.* Role of arrestins in G-protein-coupled receptor endocytosis. *Advances in pharmacology (San Diego, Calif.)* **42**, 429–433 (1998).

261. Quillinan, N., Lau, E. K., Virk, M., Von Zastrow, M. & Williams, J. T. Recovery from mu-opioid receptor desensitization after chronic treatment with morphine and methadone. *The Journal of neuroscience : the official journal of the Society for Neuroscience* **31**, 4434–4443 (2011).

262. Trafton, J. A. & Basbaum, A. I. [D-Ala2,N-MePhe4,Gly-ol5]enkephalin-induced internalization of the μ opioid receptor in the spinal cord of morphine tolerant rats. *Neuroscience* **125**, 541–543 (2004).

263. Dang, V. C. & Williams, J. T. Chronic morphine treatment reduces recovery from opioid desensitization. *The Journal of neuroscience : the official journal of the Society for Neuroscience* **24**, 7699–7706 (2004).

264. Ingram, S. L., Macey, T. A., Fossum, E. N. & Morgan, M. M. Tolerance to repeated morphine administration is associated with increased potency of opioid agonists. *Neuropsychopharmacology : official publication of the American College of Neuropsychopharmacology* **33**, 2494–2504 (2008).

265. Gold, S. J. *et al.* Regulation of RGS proteins by chronic morphine in rat locus coeruleus. *The European journal of neuroscience* **17**, 971–980 (2003).

266. Charlton, J. J. *et al.* Multiple actions of spinophilin regulate mu opioid receptor function. *Neuron* **58**, 238–247 (2008).

267. Koch, T., Wu, D. F., Yang, L. Q., Brandenburg, L. O. & Höllt, V. Role of phospholipase D2 in the agonist-induced and constitutive endocytosis of G-protein coupled receptors. *Journal of neurochemistry* **97**, 365–372 (2006).

268. Dang, V. C. & Williams, J. T. Chronic morphine treatment reduces recovery from opioid desensitization. *The Journal of neuroscience : the official journal of the Society for Neuroscience* **24**, 7699–7706 (2004).

269. Dang, V. C., Chieng, B., Azriel, Y. & Christie, M. J. Cellular morphine tolerance produced by βarrestin-2-dependent impairment of μ-opioid receptor resensitization. *The Journal of neuroscience : the official journal of the Society for Neuroscience* **31**, 7122–7130 (2011).

270. Bohn, L. M., Gainetdinov, R. R., Lin, F. T., Lefkowitz, R. J. & Caron, M. G. Mu-opioid receptor desensitization by beta-arrestin-2 determines morphine tolerance but not dependence. *Nature* **408**, 720–723 (2000).

271. Bohn, L. M., Lefkowitz, R. J. & Caron, M. G. Differential mechanisms of morphine antinociceptive tolerance revealed in (beta)arrestin-2 knock-out mice. *The Journal of neuroscience : the official journal of the Society for Neuroscience* **22**, 10494–10500 (2002).

272. Raehal, K. M. & Bohn, L. M. The role of beta-arrestin2 in the severity of antinociceptive tolerance and physical dependence induced by different opioid pain therapeutics. *Neuropharmacology* **60**, 58–65 (2011).

273. Ammon-Treiber, S. & Höllt, V. Morphine-induced changes of gene expression in the brain. *Addiction biology* **10**, 81–89 (2005).

274. Terwilliger, R. Z., Ortiz, J., Guitart, X. & Nestler, E. J. Chronic morphine administration increases beta-adrenergic receptor kinase (beta ARK) levels in the rat locus coeruleus. *Journal of neurochemistry* **63**, 1983–1986 (1994).

275. Whistler, J. L. & Von Zastrow, M. Morphine-activated opioid receptors elude desensitization by beta-arrestin. *Proceedings of the National Academy of Sciences of the United States of America* **95**, 9914–9919 (1998).

276. Smith, F. L., Javed, R. R., Elzey, M. J. & Dewey, W. L. The expression of a high level of morphine antinociceptive tolerance in mice involves both PKC and PKA. *Brain Research* **985**, 78–88 (2003).

277. Zeitz, K. P., Malmberg, A. B., Gilbert, H. & Basbaum, A. I. Reduced development of tolerance to the analgesic effects of morphine and clonidine in PKC gamma mutant mice. *Pain* **94**, 245–253 (2001).

278. Newton, P. M. *et al.* Increased response to morphine in mice lacking protein kinase C epsilon. *Genes, brain, and behavior* **6**, 329–338 (2007).

279. Granados-Soto, V., Kalcheva, I., Hua, X. Y., Newton, A. & Yaksh, T. L. Spinal PKC activity and expression: role in tolerance produced by continuous spinal morphine infusion. *Pain* **85**, 395–404 (2000).

280. Melief, E. J., Miyatake, M., Bruchas, M. R. & Chavkin, C. Ligand-directed c-Jun N-terminal kinase activation disrupts opioid receptor signaling. *Proceedings of the National Academy of Sciences of the United States of America* **107**, 11608–11613 (2010).

281. Polakiewicz, R. D., Schieferl, S. M., Dorner, L. F., Kansra, V. & Comb, M. J. A mitogen-activated protein kinase pathway is required for mu-opioid receptor desensitization. *The Journal of biological chemistry* **273**, 12402–12406 (1998).

282. Schmidt, H. *et al.* Involvement of mitogen-activated protein kinase in agonist-induced phosphorylation of the mu-opioid receptor in HEK 293 cells. *Journal of neurochemistry* **74**, 414–422 (2000).

283. West, S. J., Bannister, K., Dickenson, A. H. & Bennett, D. L. Circuitry and plasticity of the dorsal horn – Toward a better understanding of neuropathic pain. *Neuroscience* **300**, 254–275 (2015).

284. Traynelis, S. F. *et al.* Glutamate receptor ion channels: Structure, regulation, and function. *Pharmacological Reviews* Preprint at https://doi.org/10.1124/pr.109.002451 (2010).

285. Karakas, E. & Furukawa, H. Crystal structure of a heterotetrameric NMDA receptor ion channel. *Science* **344**, 992–997 (2014).

286. Lee, C. H. *et al.* NMDA receptor structures reveal subunit arrangement and pore architecture. *Nature* **511**, 191–197 (2014).

287. Rachline, J., Perin-Dureau, F., Le Goff, A., Neyton, J. & Paoletti, P. The micromolar zinc-binding domain on the NMDA receptor subunit NR2B. *The Journal of neuroscience : the official journal of the Society for Neuroscience* **25**, 308–317 (2005).

288. Hansen, K. B., Furukawa, H. & Traynelis, S. F. Control of assembly and function of glutamate receptors by the amino-terminal domain. *Molecular pharmacology* **78**, 535–549 (2010).

289. Furukawa, H. & Gouaux, E. Mechanisms of activation, inhibition and specificity: crystal structures of the NMDA receptor NR1 ligand-binding core. *The EMBO journal* **22**, 2873–2885 (2003).

290. Karakas, E., Simorowski, N. & Furukawa, H. Structure of the zinc-bound amino-terminal domain of the NMDA receptor NR2B subunit. *The EMBO journal* **28**, 3910–3920 (2009).

291. Stern-Bach, Y. *et al.* Agonist selectivity of glutamate receptors is specified by two domains structurally related to bacterial amino acid-binding proteins. *Neuron* **13**, 1345–1357 (1994).

292. Erreger, K. *et al.* Subunit-specific agonist activity at NR2A-, NR2B-, NR2C-, and NR2D-containing N-methyl-D-aspartate glutamate receptors. *Molecular pharmacology* **72**, 907–920 (2007).

293. Laube, B., Schemm, R. & Betz, H. Molecular determinants of ligand discrimination in the glutamate-binding pocket of the NMDA receptor. *Neuropharmacology* **47**, 994–1007 (2004).

294. Kinarsky, L. *et al.* Identification of subunit- and antagonist-specific amino acid residues in the N-Methyl-D-aspartate receptor glutamate-binding pocket. *The Journal of pharmacology and experimental therapeutics* **313**, 1066–1074 (2005).

295. Anson, L. C., Chen, P. E., Wyllie, D. J. A., Colquhoun, D. & Schoepfer, R. Identification of amino acid residues of the NR2A subunit that control glutamate potency in recombinant NR1/NR2A NMDA receptors. *The Journal of neuroscience : the official journal of the Society for Neuroscience* **18**, 581–589 (1998).

296. Hansen, K. B. *et al.* Tweaking agonist efficacy at N-methyl-D-aspartate receptors by site-directed mutagenesis. *Molecular pharmacology* **68**, 1510–1523 (2005).

297. Erreger, K., Chen, P. E., Wyllie, D. J. A. & Traynelis, S. F. Glutamate receptor gating. *Critical reviews in neurobiology* **16**, 187–224 (2004).

298. Hansen, K. B., Yuan, H. & Traynelis, S. F. Structural aspects of AMPA receptor activation, desensitization and deactivation. *Current opinion in neurobiology* **17**, 281–288 (2007).

299. Mayer, M. L. Glutamate receptors at atomic resolution. *Nature* **440**, 456–462 (2006).

300. Furukawa, H., Singh, S. K., Mancusso, R. & Gouaux, E. Subunit arrangement and function in NMDA receptors. *Nature* **438**, 185–192 (2005).

301. Olney, J. W., Newcomer, J. W. & Farber, N. B. NMDA receptor hypofunction model of schizophrenia. *Journal of psychiatric research* **33**, 523–533 (1999).

302. Hansen, K. B., Ogden, K. K. & Traynelis, S. F. Subunit-selective allosteric inhibition of glycine binding to NMDA receptors. *The Journal of neuroscience : the official journal of the Society for Neuroscience* **32**, 6197–6208 (2012).

303. Galen Wo, Z. & Oswald, R. E. Unraveling the modular design of glutamate-gated ion channels. *Trends in Neurosciences* **18**, 161–168 (1995).

304. Wood, M. W., Vandongen, H. M. A. & Vandongen, A. M. J. Structural conservation of ion conduction pathways in K channels and glutamate receptors. *Proceedings of the National Academy of Sciences of the United States of America* **92**, 4882–4886 (1995).

305. Okabe, S. *et al.* Hippocampal synaptic plasticity in mice overexpressing an embryonic subunit of the NMDA receptor. *The Journal of neuroscience : the official journal of the Society for Neuroscience* **18**, 4177–4188 (1998).

306. Bliss, T. V. P. & Collingridge, G. L. A synaptic model of memory: long-term potentiation in the hippocampus. *Nature* **361**, 31–39 (1993).

307. Tang, Y. P. *et al.* Genetic enhancement of learning and memory in mice. *Nature* **401**, 63–69 (1999).

308. Collingridge, G. L. *et al.* The NMDA receptor as a target for cognitive enhancement. *Neuropharmacology* **64**, 13–26 (2013).

309. Rezvani, A. H. Involvement of the NMDA System in Learning and Memory. *Animal Models of Cognitive Impairment* 37–48 (2006) doi:10.1201/9781420004335.ch4.

310. Cotman, C. W., Monaghan, D. T. & Ganong, A. H. Excitatory amino acid neurotransmission: NMDA receptors and Hebb-type synaptic plasticity. *Annual review of neuroscience* **11**, 61–80 (1988).

311. Macdermott, A. B., Mayer, M. L., Westbrook, G. L., Smith, S. J. & Barker, J. L. NMDA-receptor activation increases cytoplasmic calcium concentration in cultured spinal cord neurones. *Nature* **321**, 519–522 (1986).

312. Mayer, M. L. & Westbrook, G. L. Permeation and block of N-methyl-D-aspartic acid receptor channels by divalent cations in mouse cultured central neurones. *The Journal of physiology* **394**, 501–527 (1987).

313. Ascher, P. & Nowak, L. The role of divalent cations in the N-methyl-D-aspartate responses of mouse central neurones in culture. *The Journal of physiology* **399**, 247–266 (1988).

314. Ghosh, A. & Greenberg, M. E. Calcium signaling in neurons: molecular mechanisms and cellular consequences. *Science (New York, N.Y.)* **268**, 239–247 (1995).

315. Lisman, J., Yasuda, R. & Raghavachari, S. Mechanisms of CaMKII action in long-term potentiation. *Nature reviews. Neuroscience* **13**, 169–182 (2012).

316. Johnson, J. W. & Ascher, P. Glycine potentiates the NMDA response in cultured mouse brain neurons. *Nature* **325**, 529–531 (1987).

317. Kleckner, N. W. & Dingledine, R. Requirement for glycine in activation of NMDA-receptors expressed in Xenopus oocytes. *Science (New York, N.Y.)* **241**, 835–837 (1988).

318. Laube, B., Hirai, H., Sturgess, M., Betz, H. & Kuhse, J. Molecular determinants of agonist discrimination by NMDA receptor subunits: analysis of the glutamate binding site on the NR2B subunit. *Neuron* **18**, 493–503 (1997).

319. Malenka, R. C. & Nicoll, R. A. Long-term potentiation--a decade of progress? *Science (New York, N.Y.)* **285**, 1870–1874 (1999).

320. Evans, R. H., Francis, A. A. & Watkins, J. C. Selective antagonism by Mg2+ of amino acid-induced depolarization of spinal neurones. *Experientia* **33**, 489–491 (1977).

321. Ault, B., Evans, R. H., Francis, A. A., Oakes, D. J. & Watkins, J. C. Selective depression of excitatory amino acid induced depolarizations by magnesium ions in isolated spinal cord preparations. *The Journal of physiology* **307**, 413–428 (1980).

322. Mayer, M. L., Westbrook, G. L. & Guthrie, P. B. Voltage-dependent block by Mg2+ of NMDA responses in spinal cord neurones. *Nature* **309**, 261–263 (1984).

323. Nowak, L., Bregestovski, P., Ascher, P., Herbet, A. & Prochiantz, A. Magnesium gates glutamate-activated channels in mouse central neurones. *Nature* **307**, 462–465 (1984).

324. Monyer, H., Burnashev, N., Laurie, D. J., Sakmann, B. & Seeburg, P. H. Developmental and regional expression in the rat brain and functional properties of four NMDA receptors. *Neuron* **12**, 529–540 (1994).

325. Vicini, S. *et al.* Functional and pharmacological differences between recombinant N-methyl-D-aspartate receptors. *Journal of neurophysiology* **79**, 555–566 (1998).

326. Paoletti, P., Bellone, C. & Zhou, Q. *NMDA receptor subunit diversity: Impact on receptor properties, synaptic plasticity and disease*. *Nature Reviews Neuroscience* vol. 14 383–400 (Nat Rev Neurosci, 2013).

327. Monyer, H. *et al.* Heteromeric NMDA receptors: molecular and functional distinction of subtypes. *Science (New York, N.Y.)* **256**, 1217–1221 (1992).

328. Schorge, S. & Colquhoun, D. Studies of NMDA receptor function and stoichiometry with truncated and tandem subunits. *The Journal of neuroscience : the official journal of the Society for Neuroscience* **23**, 1151–1158 (2003).

329. Ulbrich, M. H. & Isacoff, E. Y. Rules of engagement for NMDA receptor subunits. *Proceedings of the National Academy of Sciences of the United States of America* **105**, 14163–14168 (2008).

330. Ulbrich, M. H. & Isacoff, E. Y. Subunit counting in membrane-bound proteins. *Nature methods* **4**, 319–321 (2007).

331. Ikeda, K. *et al.* Cloning and expression of the epsilon 4 subunit of the NMDA receptor channel. *FEBS letters* **313**, 34–38 (1992).

332. Kutsuwada, T. *et al.* Molecular diversity of the NMDA receptor channel. *Nature* **358**, 36–41 (1992).

333. Meguro, H. *et al.* Functional characterization of a heteromeric NMDA receptor channel expressed from cloned cDNAs. *Nature* **357**, 70–74 (1992).

334. Ishii, T. *et al.* Molecular characterization of the family of the N-methyl-D-aspartate receptor subunits. *The Journal of biological chemistry* **268**, 2836–2843 (1993).

335. Ciabarra, A. M. *et al.* Cloning and characterization of chi-1: a developmentally regulated member of a novel class of the ionotropic glutamate receptor family. *The Journal of neuroscience : the official journal of the Society for Neuroscience* **15**, 6498–6508 (1995).

336. Sucher, N. J. *et al.* Developmental and regional expression pattern of a novel NMDA receptor-like subunit (NMDAR-L) in the rodent brain. *The Journal of neuroscience : the official journal of the Society for Neuroscience* **15**, 6509–6520 (1995).

337. Low, C. M. & Wee, K. S. L. New insights into the not-so-new NR3 subunits of N-methyl-D-aspartate receptor: localization, structure, and function. *Molecular pharmacology* **78**, 1–11 (2010).

338. Sheng, M., Cummings, J., Roldan, L. A., Jan, Y. N. & Jan, L. Y. Changing subunit composition of heteromeric NMDA receptors during development of rat cortex. *Nature* **368**, 144–147 (1994).

339. Chazot, P. L., Coleman, S. K., Cik, M. & Stephenson, F. A. Molecular characterization of N-methyl-D-aspartate receptors expressed in mammalian cells yields evidence for the coexistence of three subunit types within a discrete receptor molecule. *Journal of Biological Chemistry* **269**, 24403–24409 (1994).

340. Erreger, K., Dravid, S. M., Banke, T. G., Wyllie, D. J. A. & Traynelis, S. F. Subunit-specific gating controls rat NR1/NR2A and NR1/NR2B NMDA channel kinetics and synaptic signalling profiles. *The Journal of physiology* **563**, 345–358 (2005).

341. Dravid, S. M., Prakash, A. & Traynelis, S. F. Activation of recombinant NR1/NR2C NMDA receptors. *The Journal of physiology* **586**, 4425–4439 (2008).

342. Wyllie, D. J. A., Béhé, P. & Colquhoun, D. Single-channel activations and concentration jumps: comparison of recombinant NR1a/NR2A and NR1a/NR2D NMDA receptors. *The Journal of physiology* **510 (Pt 1)**, 1–18 (1998).

343. Vance, K. M., Hansen, K. B. & Traynelis, S. F. GluN1 splice variant control of GluN1/GluN2D NMDA receptors. *The Journal of physiology* **590**, 3857–3875 (2012).

344. Cull-Candy, S. G. & Leszkiewicz, D. N. Role of distinct NMDA receptor subtypes at central synapses. *Science's STKE : signal transduction knowledge environment* **2004**, (2004).

345. Paoletti, P. Molecular basis of NMDA receptor functional diversity. *European Journal of Neuroscience* Preprint at https://doi.org/10.1111/j.1460-9568.2011.07628.x (2011).

346. Chen, P. E. *et al.* Modulation of glycine potency in rat recombinant NMDA receptors containing chimeric NR2A/2D subunits expressed in Xenopus laevis oocytes. *The Journal of physiology* **586**, 227–245 (2008).

347. Akazawa, C., Shigemoto, R., Bessho, Y., Nakanishi, S. & Mizuno, N. Differential expression of five N-methyl-D-aspartate receptor subunit mRNAs in the cerebellum of developing and adult rats. *The Journal of comparative neurology* **347**, 150–160 (1994).

348. Sheng, M., Cummings, J., Roldan, L. A., Jan, Y. N. & Jan, L. Y. Changing subunit composition of heteromeric NMDA receptors during development of rat cortex. *Nature* **368**, 144–147 (1994).

349. Henson, M. A., Roberts, A. C., Pérez-Otaño, I. & Philpot, B. D. Influence of the NR3A subunit on NMDA receptor functions. *Progress in neurobiology* **91**, 23–37 (2010).

350. Watanabe, M., Inoue, Y., Sakimura, K. & Mishina, M. Developmental changes in distribution of NMDA receptor channel subunit mRNAs. *Neuroreport* **3**, 1138–1140 (1992).

351. Brown, K. M., Wrathall, J. R., Yasuda, R. P. & Wolfe, B. B. Quantitative measurement of glutamate receptor subunit protein expression in the postnatal rat spinal cord. *Developmental Brain Research* **137**, 127–133 (2002).

352. de Geus, T. J., Patijn, J. & Joosten, E. A. J. Qualitative review on N-methyl-D-aspartate receptor expression in rat spinal cord during the postnatal development: Implications for central sensitization and pain. *Dev Neurobiol* **80**, 443 (2020).

353. Simon, R. P., Swan, J. H., Griffiths, T. & Meldrum, B. S. Blockade of N-methyl-D-aspartate receptors may protect against ischemic damage in the brain. *Science (New York, N.Y.)* **226**, 850–852 (1984).

354. Khatri, N. *et al.* Oxidative Stress: Major Threat in Traumatic Brain Injury. *CNS & Neurological Disorders - Drug Targets* **17**, 689–695 (2018).

355. Gabrieli, D., Schumm, S. N., Vigilante, N. F. & Meaney, D. F. NMDA Receptor Alterations After Mild Traumatic Brain Injury Induce Deficits in Memory Acquisition and Recall. *Neural Computation* **33**, 67–95 (2021).

356. Wu, L.-J. J. & Zhuo, M. Targeting the NMDA receptor subunit NR2B for the treatment of neuropathic pain. *Neurotherapeutics : the journal of the American Society for Experimental NeuroTherapeutics* **6**, 693–702 (2009).

357. Matsumura, S. *et al.* Impairment of CaMKII activation and attenuation of neuropathic pain in mice lacking NR2B phosphorylated at Tyr1472. *The European journal of neuroscience* **32**, 798–810 (2010).

358. Reisberg, B. *et al.* Memantine in moderate-to-severe Alzheimer's disease. *The New England journal of medicine* **348**, 1333–1341 (2003).

359. Milnerwood, A. J. & Raymond, L. A. Early synaptic pathophysiology in neurodegeneration: insights from Huntington's disease. **33**, 513–523 (2010).

360. Hallett, P. J. & Standaert, D. G. Rationale for and use of NMDA receptor antagonists in Parkinson's disease. **102**, 155–174 (2004).

361. Berman, R. M. *et al.* Antidepressant effects of ketamine in depressed patients. **47**, 351–354 (2000).

362. Ahmed, H., Haider, A. & Ametamey, S. M. N-Methyl-D-Aspartate (NMDA) receptor modulators: a patent review (2015-present). *Expert opinion on therapeutic patents* **30**, 743–767 (2020).

363. Won, H. *et al.* Autistic-like social behaviour in Shank2-mutant mice improved by restoring NMDA receptor function. *Nature* **486**, 261–265 (2012).

364. Schmeisser, M. J. *et al.* Autistic-like behaviours and hyperactivity in mice lacking ProSAP1/Shank2. *Nature* **486**, 256–260 (2012).

365. Coyle, J. T. NMDA receptor and schizophrenia: a brief history. *Schizophrenia bulletin* **38**, 920–926 (2012).

366. Olney, J. W., Newcomer, J. W. & Farber, N. B. NMDA receptor hypofunction model of schizophrenia. *Journal of psychiatric research* **33**, 523–533 (1999).

367. Huettner, J. E. & Bean, B. P. Block of N-methyl-D-aspartate-activated current by the anticonvulsant MK-801: selective binding to open channels. *Proceedings of the National Academy of Sciences of the United States of America* **85**, 1307–1311 (1988).

368. Taylor, C. P., Traynelis, S. F., Siffert, J., Pope, L. E. & Matsumoto, R. R. Pharmacology of dextromethorphan: Relevance to dextromethorphan/quinidine (Nuedexta®) clinical use. *Pharmacology & therapeutics* **164**, 170–182 (2016).

369. Pioro, E. P. Review of Dextromethorphan 20 mg/Quinidine 10 mg (NUEDEXTA(®)) for Pseudobulbar Affect. *Neurology and therapy* **3**, 15–28 (2014).

370. Roth, B. L. *et al.* The ketamine analogue methoxetamine and 3- and 4-methoxy analogues of phencyclidine are high affinity and selective ligands for the glutamate NMDA receptor. *PloS one* **8**, (2013).

371. Zanos, P. *et al.* NMDAR inhibition-independent antidepressant actions of ketamine metabolites. *Nature* **533**, 481–486 (2016).

372. Zanos, P. & Gould, T. D. Mechanisms of ketamine action as an antidepressant. *Molecular psychiatry* **23**, 801–811 (2018).

373. Wilkinson, S. T. *et al.* The Effect of a Single Dose of Intravenous Ketamine on Suicidal Ideation: A Systematic Review and Individual Participant Data Meta-Analysis. *The American journal of psychiatry* **175**, 150–158 (2018).

374. Kurdi, M., Theerth, K. & Deva, R. Ketamine: Current applications in anesthesia, pain, and critical care. *Anesthesia, essays and researches* **8**, 283 (2014).

375. Brinck, E. C. V. *et al.* Perioperative intravenous ketamine for acute postoperative pain in adults. *Cochrane Database Syst Rev* **12**, (2018).

376. Pickering, G. *et al.* Ketamine and Magnesium for Refractory Neuropathic Pain: A Randomized, Double-blind, Crossover Trial. *Anesthesiology* **133**, 154–164 (2020).

377. Feder, A. *et al.* Efficacy of intravenous ketamine for treatment of chronic posttraumatic stress disorder: a randomized clinical trial. *JAMA psychiatry* **71**, 681–688 (2014).

378. Rodriguez, C. I. *et al.* Randomized controlled crossover trial of ketamine in obsessive-compulsive disorder: proof-of-concept. *Neuropsychopharmacology : official publication of the American College of Neuropsychopharmacology* **38**, 2475–2483 (2013).

379. Wu, Y. N. & Johnson, S. W. Memantine selectively blocks extrasynaptic NMDA receptors in rat substantia nigra dopamine neurons. *Brain research* **1603**, 1–7 (2015).

380. Xia, P., Chen, H. S. V., Zhang, D. & Lipton, S. A. Memantine preferentially blocks extrasynaptic over synaptic NMDA receptor currents in hippocampal autapses. *The Journal of neuroscience : the official journal of the Society for Neuroscience* **30**, 11246–11250 (2010).

381. Crosby, N. J., Deane, K. & Clarke, C. E. Amantadine for dyskinesia in Parkinson's disease. *The Cochrane database of systematic reviews* **2003**, (2003).

382. Varela, J. A. *et al.* Single nanoparticle tracking of [Formula: see text]-methyl-d-aspartate receptors in cultured and intact brain tissue. *Neurophotonics* **3**, 041808 (2016).

383. Hardingham, G. E. & Bading, H. Synaptic versus extrasynaptic NMDA receptor signalling: implications for neurodegenerative disorders. *Nature reviews. Neuroscience* **11**, 682–696 (2010).

384. Gladding, C. M. & Raymond, L. A. Mechanisms underlying NMDA receptor synaptic/extrasynaptic distribution and function. *Molecular and cellular neurosciences* **48**, 308–320 (2011).

385. Lai, T. W., Zhang, S. & Wang, Y. T. Excitotoxicity and stroke: identifying novel targets for neuroprotection. *Progress in neurobiology* **115**, 157–188 (2014).

386. Martel, M. A. *et al.* The subtype of GluN2 C-terminal domain determines the response to excitotoxic insults. *Neuron* **74**, 543–556 (2012).

387. Hardingham, G. E. Coupling of the NMDA receptor to neuroprotective and neurodestructive events. *Biochemical Society transactions* **37**, 1147–1160 (2009).

388. Kemp, J. A. & McKernan, R. M. NMDA receptor pathways as drug targets. *Nature neuroscience* **5 Suppl**, 1039–1042 (2002).

389. Hess, S. D. *et al.* Cloning and functional characterization of human heteromeric N-methyl-D-aspartate receptors. *The Journal of pharmacology and experimental therapeutics* **278**, 808–816 (1996).

390. Williams, K. Ifenprodil discriminates subtypes of the N-methyl-D-aspartate receptor: selectivity and mechanisms at recombinant heteromeric receptors. *Molecular pharmacology* **44**, 851–859 (1993).

391. Masuko, T. *et al.* A regulatory domain (R1-R2) in the amino terminus of the N-methyl-D-aspartate receptor: effects of spermine, protons, and ifenprodil, and structural similarity to bacterial leucine/isoleucine/valine binding protein. *Molecular pharmacology* **55**, 957–969 (1999).

392. Karakas, E., Simorowski, N. & Furukawa, H. Subunit arrangement and phenylethanolamine binding in GluN1/GluN2B NMDA receptors. *Nature* **475**, (2011).

393. Romero-Hernandez, A., Simorowski, N., Karakas, E. & Furukawa, H. Molecular Basis for Subtype Specificity and High-Affinity Zinc Inhibition in the GluN1-GluN2A NMDA Receptor Amino-Terminal Domain. *Neuron* **92**, 1324–1336 (2016).

394. Kew, J. N. C., Trube, G. & Kemp, J. A. A novel mechanism of activity-dependent NMDA receptor antagonism describes the effect of ifenprodil in rat cultured cortical neurones. *The Journal of physiology* **497 (Pt 3)**, 761–772 (1996).

395. Pahk, A. J. & Williams, K. Influence of extracellular pH on inhibition by ifenprodil at N-methyl-D-aspartate receptors in Xenopus oocytes. *Neuroscience letters* **225**, 29–32 (1997).

396. Mott, D. D. *et al.* Phenylethanolamines inhibit NMDA receptors by enhancing proton inhibition. *Nature Neuroscience* **1**, 659–667 (1998).

397. Traynelis, S. F., Hartley, M. & Heinemann, S. F. Control of proton sensitivity of the NMDA receptor by RNA splicing and polyamines. *Science* **268**, 873–876 (1995).

398. Yuan, H. *et al.* Context-Dependent GluN2B-Selective Inhibitors of NMDA Receptor Function are Neuroprotective with Minimal Side Effects. *Neuron* **85**, 1305 (2015).

399. Fischer, G. *et al.* Ro 25-6981, a highly potent and selective blocker of N-methyl-D- aspartate receptors containing the NR2B subunit. Characterization in vitro. *Journal of Pharmacology and Experimental Therapeutics* (1997).

400. Gotti, B. *et al.* Ifenprodil and SL 82.0715 as cerebral anti-ischemic agents. I. Evidence for efficacy in models of focal cerebral ischemia. *Journal of Pharmacology and Experimental Therapeutics* **247**, (1988).

401. Yurkewicz, L., Weaver, J., Bullock, M. R. & Marshall, L. F. The effect of the selective NMDA receptor antagonist traxoprodil in the treatment of traumatic brain injury. *Journal of neurotrauma* **22**, 1428–1443 (2005).

402. Preskorn, S. H. *et al.* An innovative design to establish proof of concept of the antidepressant effects of the NR2B subunit selective N-methyl-D-aspartate antagonist, CP-101,606, in patients with treatment-refractory major depressive disorder. *Journal of clinical psychopharmacology* **28**, 631–637 (2008).

403. Chizh, B. A., Headley, P. M. & Tzschentke, T. M. NMDA receptor antagonists as analgesics: Focus on the NR2B subtype. *Trends in Pharmacological Sciences* Preprint at https://doi.org/10.1016/S0165-6147(00)01863-0 (2001).

404. Mony, L., Kew, J. N. C., Gunthorpe, M. J. & Paoletti, P. Allosteric modulators of NR2B-containing NMDA receptors: molecular mechanisms and therapeutic potential. *British journal of pharmacology* **157**, 1301–1317 (2009).

405. Addy, C. *et al.* Single-dose administration of MK-0657, an NR2B-selective NMDA antagonist, does not result in clinically meaningful improvement in motor function in patients with moderate Parkinson's disease. *Journal of clinical pharmacology* **49**, 856–864 (2009).

406. Sasaki, T. *et al.* Ifenprodil for the treatment of flashbacks in adolescent female posttraumatic stress disorder patients with a history of abuse. *Psychotherapy and psychosomatics* **82**, 344–345 (2013).

407. Nutt, J. G. *et al.* Effects of a NR2B selective NMDA glutamate antagonist, CP-101,606, on dyskinesia and Parkinsonism. *Movement disorders : official journal of the Movement Disorder Society* **23**, 1860–1866 (2008).

408. Machado-Vieira, R., Henter, I. D. & Zarate, C. A. New targets for rapid antidepressant action. *Progress in neurobiology* **152**, 21–37 (2017).

409. Auvin, S. *et al.* Radiprodil, a NR2B negative allosteric modulator, from bench to bedside in infantile spasm syndrome. *Annals of clinical and translational neurology* **7**, 343–352 (2020).

410. Myers, S. J. *et al.* A Glutamate N-Methyl-d-Aspartate (NMDA) Receptor Subunit 2B-Selective Inhibitor of NMDA Receptor Function with Enhanced Potency at Acidic pH and Oral Bioavailability for Clinical Use. *The Journal of pharmacology and experimental therapeutics* **379**, 41–52 (2021).

411. Coderre, T. J., Katz, J., Vaccarino, A. L. & Melzack, R. Contribution of central neuroplasticity to pathological pain: review of clinical and experimental evidence. *Pain* **52**, 259–285 (1993).

412. Dubner, R. Three decades of pain research and its control. *Journal of dental research* **76**, 730–733 (1997).

413. Fleming, K. C. & Volcheck, M. M. Central sensitization syndrome and the initial evaluation of a patient with fibromyalgia: a review. *Rambam Maimonides medical journal* **6**, e0020 (2015).

414. Lenz, F. A., Gracely, R. H., Rowland, L. H. & Dougherty, P. M. A population of cells in the human thalamic principal sensory nucleus respond to painful mechanical stimuli. *Neuroscience letters* **180**, 46–50 (1994).

415. Willis, W. D., Sluka, K. A., Rees, H. & Westlund, K. N. Cooperative mechanisms of neurotransmitter action in central nervous sensitization. *Progress in brain research* **110**, 151–166 (1996).

416. Eide, P. K. Wind-up and the NMDA receptor complex from a clinical perspective. *European journal of pain (London, England)* **4**, 5–15 (2000).

417. Mendell, L. M. & Wall, P. D. Responses of Single Dorsal Cord Cells to Peripheral Cutaneous Unmyelinated Fibers. *Nature* **206**, 97–99 (1965).

418. Mendell, L. M. Physiological properties of unmyelinated fiber projection to the spinal cord. *Experimental neurology* **16**, 316–332 (1966).

419. Price, D. D., Hull, C. D. & Buchwald, N. A. Intracellular responses of dorsal horn cells to cutaneous and sural nerve A and C fiber stimuli. *Experimental neurology* **33**, 291–309 (1971).

420. Davies, S. N. & Lodge, D. Evidence for involvement of N-methylaspartate receptors in 'wind-up' of class 2 neurones in the dorsal horn of the rat. *Brain research* **424**, 402–406 (1987).

421. Dickenson, A. H. & Sullivan, A. F. Evidence for a role of the NMDA receptor in the frequency dependent potentiation of deep rat dorsal horn nociceptive neurones following C fibre stimulation. *Neuropharmacology* **26**, 1235–1238 (1987).

422. Bliss, T. V. P. & Lømo, T. Long-lasting potentiation of synaptic transmission in the dentate area of the anaesthetized rabbit following stimulation of the perforant path. *The Journal of physiology* **232**, 331–356 (1973).

423. Svendsen, F., Tjolsen, A. & Hole, K. AMPA and NMDA receptor-dependent spinal LTP after nociceptive tetanic stimulation. *Neuroreport* **9**, 1185–1190 (1998).

424. Svendsen, F., Tjølsen, A., Jørgen Rygh, L. & Hole, K. Expression of long-term potentiation in single wide dynamic range neurons in the rat is sensitive to blockade of glutamate receptors. *Neuroscience Letters* **259**, 25–28 (1999).

425. Zhao, Y. L., Chen, S. R., Chen, H. & Pan, H. L. Chronic opioid potentiates presynaptic but impairs postsynaptic N-methyl-D-aspartic acid receptor activity in spinal cords: implications for opioid hyperalgesia and tolerance. *The Journal of biological chemistry* **287**, 25073–25085 (2012).

426. Rodríguez-Mũoz, M., Sánchez-Blázquez, P., Vicente-Sánchez, A., Berrocoso, E. & Garzón, J. The mu-opioid receptor and the NMDA receptor associate in PAG neurons: implications in pain control. *Neuropsychopharmacology : official publication of the American College of Neuropsychopharmacology* **37**, 338–349 (2012).

427. Commons, K. G., Van Bockstaele, E. J. & Pfaff, D. W. Frequent colocalization of mu opioid and NMDA-type glutamate receptors at postsynaptic sites in periaqueductal gray neurons. *Journal of Comparative Neurology* **408**, 549–559 (1999).

428. Aicher, S. A., Goldberg, A. & Sharma, S. Co-localization of mu opioid receptor and N-methyl-D-aspartate receptor in the trigeminal dorsal horn. *The journal of pain* **3**, 203–10 (2002).

429. Garzón, J., Rodríguez-Muñoz, M. & Sánchez-Blázquez, P. Direct association of Mu-opioid and NMDA glutamate receptors supports their cross-regulation: molecular implications for opioid tolerance. *Current drug abuse reviews* **5**, 199–226 (2012).

430. Chen, B. S. & Roche, K. W. Regulation of NMDA receptors by phosphorylation. *Neuropharmacology* vol. 53 362–368 Preprint at https://doi.org/10.1016/j.neuropharm.2007.05.018 (2007).

431. Xu, L. *et al.* Arcuate Src activation-induced phosphorylation of NR2B NMDA subunit contributes to inflammatory pain in rats. *Journal of Neurophysiology* **108**, 3024–3033 (2012).

432. Trujillo, K. A. & Akil, H. Inhibition of morphine tolerance and dependence by the NMDA receptor antagonist MK-801. *Science* **251**, 85–87 (1991).

433. Mao, J., Price, D. D., Caruso, F. S. & Mayer, D. J. Oral administration of dextromethorphan prevents the development of morphine tolerance and dependence in rats. *Pain* (1996) doi:10.1016/0304-3959(96)03120-X.

434. Parsons, C. G. NMDA receptors as targets for drug action in neuropathic pain. *European journal of pharmacology* **429**, 71–78 (2001).

435. Ma, Q. P., Tian, L. & Woolf, C. J. Resection of sciatic nerve re-triggers central sprouting of A-fibre primary afferents in the rat. *Neuroscience Letters* **288**, 215–218 (2000).

436. Mutel, V. *et al.* In vitro binding properties in rat brain of [3H]Ro 25-6981, a potent and selective antagonist of NMDA receptors containing NR2B subunits. *Journal of neurochemistry* **70**, 2147–2155 (1998).

437. Wei, F. *et al.* Genetic enhancement of inflammatory pain by forebrain NR2B overexpression. *Nature neuroscience* **4**, 164–169 (2001).

438. Gong, K., Bhargava, A. & Jasmin, L. GluN2B N-methyl-D-aspartate receptor and excitatory amino acid transporter 3 are upregulated in primary sensory neurons after 7 days of morphine administration in rats: implication for opiate-induced hyperalgesia. *Pain* **157**, 147–158 (2016).

439. Temi, S. *et al.* Differential expression of GluN2 NMDA receptor subunits in the dorsal horn of male and female rats. (2021) doi:10.1080/19336950.2020.1871205.

440. Guo, W. *et al.* Tyrosine phosphorylation of the NR2B subunit of the NMDA receptor in the spinal cord during the development and maintenance of inflammatory hyperalgesia. *The Journal of neuroscience : the official journal of the Society for Neuroscience* **22**, 6208–6217 (2002).

441. Bayer, K. U., De Koninck, P., Leonard, A. S., Hell, J. W. & Schulman, H. Interaction with the NMDA receptor locks CaMKII in an active conformation. *Nature* **411**, 801–805 (2001).

442. Ko, S. W., Wu, L. J., Shum, F., Quan, J. & Zhuo, M. Cingulate NMDA NR2B receptors contribute to morphine-induced analgesic tolerance. *Mol Brain* (2008) doi:10.1186/1756-6606-1-2.

443.   Ren, B. *et al.* Con-T[M8Q] potently attenuates the expression and development of morphine tolerance in mice. *Neurosci Lett* **597**, 38–42 (2015).

444.   Allen, R. M. & Dykstra, L. A. The competitive NMDA receptor antagonist LY235959 modulates the progression of morphine tolerance in rats. *Psychopharmacologia* **142**, 209–214 (1999).

445.   Barta-Szalai, G. *et al.* Oxamides as novel NR2B selective NMDA receptor antagonists. *Bioorganic and Medicinal Chemistry Letters* **14**, 3953–3956 (2004).

446.   Curtis, N. R. *et al.* Novel N1-(benzyl)cinnamamidine derived NR2B subtype-selective NMDA receptor antagonists. *Bioorganic and Medicinal Chemistry Letters* **13**, 693–696 (2003).

447.   Mccauley, J. A. *et al.* NR2B-Selective N-Methyl-D-aspartate Antagonists: Synthesis and Evaluation of 5-Substituted Benzimidazoles. (2004) doi:10.1021/jm030483s.

448.   Tricklebank, M. D., Singh, L., Oles, R. J., Preston, C. & Iversen, S. D. The behavioural effects of MK-801: a comparison with antagonists acting non-competitively and competitively at the NMDA receptor. *European journal of pharmacology* **167**, 127–135 (1989).

449.   Masayuki Hiramatsu, Cho, A. K. & Toshitaka, N. Comparison of the behavioral and biochemical effects of the NMDA receptor antagonists, MK-801 and phencyclidine. *European journal of pharmacology* **166**, 359–366 (1989).

450.   Tahirovic, Y. A. *et al.* Enantiomeric propanolamines as selective N-methyl-D-aspartate 2B receptor antagonists. *Journal of Medicinal Chemistry* **51**, 5506–5521 (2008).

451.   Regan, M. C. *et al.* Structural elements of a pH-sensitive inhibitor binding site in NMDA receptors. *Nature communications* **10**, (2019).

452.   Rudolph, K. E. *et al.* The Relative Economy and Drug Overdose Deaths. *Epidemiology (Cambridge, Mass.)* **31**, 551 (2020).

453.   Rudd, R. A., Seth, P., David, F. & Scholl, L. Increases in drug and opioid-involved overdose deaths — United States, 2010-2015. *Morbidity and Mortality Weekly Report* (2016) doi:10.15585/mmwr.mm655051e1.

454.   Niles, J. K., Gudin, J., Radcliff, J. & Kaufman, H. W. The Opioid Epidemic Within the COVID-19 Pandemic: Drug Testing in 2020. *Population health management* **24**, S43–S51 (2021).

455.   Dahlhamer, J. *et al.* Prevalence of Chronic Pain and High-Impact Chronic Pain Among Adults — United States, 2016. *MMWR. Morbidity and Mortality Weekly Report* **67**, 1001–1006 (2018).

456.   Dahlhamer, J. *et al.* Prevalence of Chronic Pain and High-Impact Chronic Pain Among Adults — United States, 2016. *MMWR. Morbidity and Mortality Weekly Report* **67**, 1001–1006 (2018).

457.   Kennedy, J., Roll, J. M., Schraudner, T., Murphy, S. & McPherson, S. Prevalence of Persistent Pain in the U.S. Adult Population: New Data From the 2010 National Health Interview Survey. *The Journal of Pain* **15**, 979–984 (2014).

458.   Goldberg, D. S. & McGee, S. J. Pain as a global public health priority. *BMC Public Health* **11**, 770 (2011).

459. Lawrence, A., Kaul, A. & Seaver, M. Chronic Pain. *The 5-Minute Clinical Consult Standard 2016: Twenty Fourth Edition* (2021) doi:10.1542/9781581109689-part01-ch40.

460. Schiller, E. Y., Goyal, A. & Mechanic, O. J. Opioid Overdose. *Challenging Cases and Complication Management in Pain Medicine* 3–7 (2022) doi:10.1007/978-3-319-60072-7_1.

461. White, J. M. & Irvine, R. J. Mechanisms of fatal opioid overdose. *Addiction* **94**, 961–972 (1999).

462. Wilson-Poe, A. R., Jeong, H. J. & Vaughan, C. W. Chronic morphine reduces the readily releasable pool of GABA, a presynaptic mechanism of opioid tolerance. *Journal of Physiology* (2017) doi:10.1113/JP274157.

463. Chapman, V., Haley, J. E. & Dickenson, A. H. Electrophysiologic analysis of preemptive effects of spinal opioids on N-methyl-D-aspartate receptor-mediated events. *Anesthesiology* **81**, 1429–1435 (1994).

464. Sigtermans, M. J. *et al.* Ketamine produces effective and long-term pain relief in patients with Complex Regional Pain Syndrome Type 1. *Pain* **145**, 304–311 (2009).

465. Collingridge, G. The role of NMDA receptors in learning and memory. *Nature* (1987) doi:10.1038/330604a0.

466. Macdermott, A. B., Mayer, M. L., Westbrook, G. L., Smith, S. J. & Barker, J. L. NMDA-receptor activation increases cytoplasmic calcium concentration in cultured spinal cord neurones. *Nature* **321**, 519–522 (1986).

467. XiangWei, W., Jiang, Y. & Yuan, H. De Novo Mutations and Rare Variants Occurring in NMDA Receptors. *Current opinion in physiology* **2**, 27 (2018).

468. Park, C. K., Nehls, D. G., Graham, D. I., Teasdale, G. M. & McCulloch, J. The glutamate antagonist MK-801 reduces focal ischemic brain damage in the rat. *Annals of neurology* **24**, 543–551 (1988).

469. Morikawa, E. *et al.* Attenuation of focal ischemic brain injury in mice deficient in the epsilon1 (NR2A) subunit of NMDA receptor. *The Journal of neuroscience : the official journal of the Society for Neuroscience* **18**, 9727–9732 (1998).

470. aan het Rot, M. *et al.* Safety and Efficacy of Repeated-Dose Intravenous Ketamine for Treatment-Resistant Depression. *Biological Psychiatry* **67**, 139–145 (2010).

471. Moon, I. S., Apperson, M. L. & Kennedy, M. B. The major tyrosine-phosphorylated protein in the postsynaptic density fraction is N-methyl-D-aspartate receptor subunit 2B. *Proceedings of the National Academy of Sciences of the United States of America* **91**, 3954 (1994).

472. Salter, M. W. & Kalia, L. V. Src kinases: a hub for NMDA receptor regulation. *Nature Reviews Neuroscience 2004 5:4* **5**, 317–328 (2004).

473. Ali, D. W. & Salter, M. W. NMDA receptor regulation by Src kinase signalling in excitatory synaptic transmission and plasticity. *Current opinion in neurobiology* **11**, 336–342 (2001).

474.   Dawson, V. L., Dawson, T. M., London, E. D., Bredt, D. S. & Snyder, S. H. Nitric oxide mediates glutamate neurotoxicity in primary cortical cultures. *Proceedings of the National Academy of Sciences of the United States of America* **88**, 6368–6371 (1991).

475.   He, L., Fong, J., Von Zastrow, M. & Whistler, J. L. Regulation of opioid receptor trafficking and morphine tolerance by receptor oligomerization. *Cell* **108**, 271–282 (2002).

476.   Wang, Z., Arden, J. & Sadée, W. Basal phosphorylation of mu opioid receptor is agonist modulated and Ca2+-dependent. *FEBS letters* **387**, 53–57 (1996).

477.   Fedele, E. & Raiteri, M. In vivo studies of the cerebral glutamate receptor/NO/cGMP pathway. *Progress in neurobiology* **58**, 89–120 (1999).

478.   Petrenko, A. B., Yamakura, T., Baba, H. & Shimoji, K. The Role of N-Methyl-d-Aspartate (NMDA) Receptors in Pain: A Review. *Anesthesia & Analgesia* 1108–1116 (2003) doi:10.1213/01.ANE.0000081061.12235.55.

479.   Brown, A. G. The dorsal horn of the spinal cord. *Quarterly journal of experimental physiology (Cambridge, England)* (1982).

480.   Sun, Y. Y. *et al.* Surface expression of hippocampal NMDA GluN2B receptors regulated by fear conditioning determines its contribution to memory consolidation in adult rats. *Scientific Reports* (2016) doi:10.1038/srep30743.

481.   Ruppa, K. B., King, D. & Olson, R. E. NMDA Antagonists of GluN2B Subtype and Modulators of GluN2A, GluN2C, and GluN2D Subtypes-Recent Results and Developments. in *Annual Reports in Medicinal Chemistry* (2012). doi:10.1016/B978-0-12-396492-2.00007-2.

482.   Wang, H. *et al.* PH-Sensitive NMDA inhibitors improve outcome in a murine model of SAH. *Neurocritical Care* **20**, 119–131 (2014).

483.   Tahirovic, Y. A. *et al.* Enantiomeric propanolamines as selective N-methyl-D-aspartate 2B receptor antagonists. *Journal of Medicinal Chemistry* **51**, 5506–5521 (2008).

484.   Stroebel, D. *et al.* A Novel Binding Mode Reveals Two Distinct Classes of NMDA Receptor GluN2B-selective Antagonists. *Molecular pharmacology* **89**, 541–551 (2016).

485.   Hansen, K. B., Ogden, K. K., Yuan, H. & Traynelis, S. F. Distinct functional and pharmacological properties of Triheteromeric GluN1/GluN2A/GluN2B NMDA receptors. *Neuron* **81**, 1084–1096 (2014).

486.   Chou, T.-H. *et al.* Structural insights into binding of therapeutic channel blockers in NMDA receptors. *Nature Structural & Molecular Biology* **29**, 507–518 (2022).

487.   Chou, T.-H., Tajima, N., Romero-Hernandez, A. & Furukawa, H. Structural Basis of Functional Transitions in Mammalian NMDA Receptors. *Cell* **182**, 357-371.e13 (2020).

488.   Tajima, N. *et al.* Activation of NMDA receptors and the mechanism of inhibition by ifenprodil. *Nature* **534**, 63–68 (2016).

489. Sewell, R. D. E. & Spencer, P. S. J. Antinociceptive activitiy of narcotic agonist and partial agonist analgesics and other agents in the tail-immersion test in mice and rats. *Neuropharmacology* **15**, 683–688 (1976).

490. Luttinger, D. Determination of antinociceptive efficacy of drugs in mice using different water temperatures in a tail-immersion test. *Journal of pharmacological methods* **13**, 351–357 (1985).

491. Matthews, E. A. & Dickenson, A. H. A Combination of Gabapentin and Morphine Mediates Enhanced Inhibitory Effects on Dorsal Horn Neuronal Responses in a Rat Model of Neuropathy. *Anesthesiology* **96**, 633–673 (2002).

492. HU, C. Y. & ZHAO, Y.-T. Analgesic effects of naringenin in rats with spinal nerve ligation-induced neuropathic pain. *Biomedical Reports* **2**, 569 (2014).

493. Clifford, J. L., Mares, A., Hansen, J. & Averitt, D. L. Preemptive perineural bupivacaine attenuates the maintenance of mechanical and cold allodynia in a rat spinal nerve ligation model. *BMC Anesthesiology* **15**, 1–9 (2015).

494. Gao, X., Hee, K. K., Jin, M. C. & Chung, K. Enhancement of NMDA receptor phosphorylation of the spinal dorsal horn and nucleus gracilis neurons in neuropathic rats. *Pain* **116**, 62–72 (2005).

495. Geng, S.-J. *et al.* Contribution of the spinal cord BDNF to the development of neuropathic pain by activation of the NR2B-containing NMDA receptors in rats with spinal nerve ligation. (2010) doi:10.1016/j.expneurol.2010.01.003.

496. Yan, X., Jiang, E., Gao, M., Weng, H.-R. & Weng, R. Endogenous activation of presynaptic NMDA receptors enhances glutamate release from the primary afferents in the spinal dorsal horn in a rat model of neuropathic pain. *The Journal of Physiology Neuroscience C* **591**, 2001–2019 (2013).

497. Inquimbert, P. *et al.* NMDA Receptor Activation Underlies the Loss of Spinal Dorsal Horn Neurons and the Transition to Persistent Pain after Peripheral Nerve Injury. *Cell Reports* **23**, 2678–2689 (2018).

498. Ellison, G. The N-methyl-d-aspartate antagonists phencyclidine, ketamine and dizocilpine as both behavioral and anatomical models of the dementias. *Brain Research Reviews* **20**, 250–267 (1995).

499. Andiné, P. *et al.* Characterization of MK-801-Induced Behavior as a Putative Rat Model of Psychosis 1. (1999).

500. Oliveira, S. M. *et al.* Antinociceptive effect of a novel armed spider peptide Tx3-5 in pathological pain models in mice. *Pflugers Archiv : European journal of physiology* **468**, 881–894 (2016).

501. Rigo, F. K. *et al.* Spider peptide Phα1β induces analgesic effect in a model of cancer pain. *Cancer science* **104**, 1226–1230 (2013).

502. Marshall, I. & Weinstock, M. Quantitative method for assessing one symptom of the withdrawal syndrome in mice after chronic morphine administration. *Nature* **234**, 223–224 (1971).

503. Mccool, B. A. & Lovinger, D. M. Ifenprodil inhibition of the 5-Hydroxytryptamine3 receptor. *Neuropharmacology* **34**, 621–629 (1995).

504.   Chenard, B. L. *et al. Separation of alpha 1 adrenergic and N-methyl-D-aspartate antagonist activity in a series of ifenprodil compounds*. *J. Med. Chem* vol. 34 (1991).

505.   Renaud, H. J., Cui, J. Y., Khan, M. & Klaassen, C. D. Tissue Distribution and Gender-Divergent Expression of 78 Cytochrome P450 mRNAs in Mice. *TOXICOLOGICAL SCIENCES* **124**, 261–277 (2011).

506.   Hrycay, E. G. & Bandiera, S. M. Expression, function and regulation of mouse cytochrome P450 enzymes: comparison with human P450 enzymes. *Current drug metabolism* **10**, 1151–1183 (2009).

507.   Waxman, D. J. & Holloway, M. G. Sex Differences in the Expression of Hepatic Drug Metabolizing Enzymes. *Molecular Pharmacology* **76**, 215 (2009).

508.   Kobayashi, K. *et al.* Gender Difference of Hepatic and Intestinal CYP3A4 in CYP3AHumanized Mice Generated by a Human Chromosome-engineering Technique. *Drug metabolism letters* **11**, (2017).

509.   Smith, J. C. A Review of Strain and Sex Differences in Response to Pain and Analgesia in Mice. *Comparative Medicine* **69**, 490 (2019).

510.   Dahan, A., Kest, B., Waxman, A. R. & Sarton, E. Sex-specific responses to opiates: animal and human studies. *Anesthesia and analgesia* **107**, 83–95 (2008).

511.   Cicero, T. J., Nock, B. & Meyer, E. R. Gender-related differences in the antinociceptive properties of morphine. *Journal of Pharmacology and Experimental Therapeutics* **279**, (1996).

512.   Cook, C. D., Barrett, A. C., Roach, E. L., Bowman, J. R. & Picker, M. J. Sex-related differences in the antinociceptive effects of opioids: importance of rat genotype, nociceptive stimulus intensity, and efficacy at the μ opioid receptor. *Psychopharmacology 2000 150:4* **150**, 430–442 (2000).

513.   Wiesenfeld-Hallin, Z. Sex differences in pain perception. *Gender Medicine* **2**, 137–145 (2005).

514.   Craft, R. M. & Lee, D. A. NMDA antagonist modulation of morphine antinociception in female vs. male rats. *Pharmacology Biochemistry and Behavior* **80**, 639–649 (2005).

515.   Gabel, F., Hovhannisyan, V., Andry, V. & Goumon, Y. Central metabolism as a potential origin of sex differences in morphine antinociception but not induction of antinociceptive tolerance in mice. *British Journal of Pharmacology* (2022) doi:10.1111/BPH.15792.

516.   Smith, H. S. *Opioid Metabolism REVIEW*. *Mayo Clin Proc* vol. 84 (2009).

517.   De Gregori, S. *et al.* Morphine metabolism, transport and brain disposition. *Metabolic Brain Disease* **27**, 1 (2012).

518.   Buckley, D. B. & Klaassen, C. D. Tissue- and Gender-Specific mRNA Expression of UDP-Glucuronosyltransferases (UGTs) in Mice. *Drug Metabolism and Disposition* **35**, 121–127 (2007).

519.   Kitaori, K., Furukawa, Y., Yoshimoto, H. & Otera, J. CsF in organic synthesis. Regioselective nucleophilic reactions of phenols with oxiranes leading to enantiopure β-blockers. *Tetrahedron* (1999) doi:10.1016/S0040-4020(99)00896-0.

520. Sajiki, H., Hattori, K. & Hirota, K. Highly chemoselective hydrogenation with retention of the epoxide function using a heterogeneous Pd/C - Ethylenediamine catalyst and THF. *Chemistry - A European Journal* (2000) doi:10.1002/1521-3765(20000616)6:12<2200::AID-CHEM2200>3.0.CO;2-3.

521. Traynelis, S. F., Burgess, M. F., Zheng, F., Lyuboslavsky, P. & Powers, J. L. Control of voltage-independent Zinc inhibition of NMDA receptors by the NR1 subunit. *Journal of Neuroscience* (1998) doi:10.1523/jneurosci.18-16-06163.1998.

522. Jackson, M. R., Nilsson, T. & Peterson, P. A. Retrieval of transmembrane proteins to the endoplasmic reticulum. *The Journal of cell biology* **121**, 317–333 (1993).

523. Jackson, M. R., Nilsson, T. & Peterson, P. A. Identification of a consensus motif for retention of transmembrane proteins in the endoplasmic reticulum. *The EMBO journal* **9**, 3153–3162 (1990).

524. Zerangue, N. *et al.* Analysis of endoplasmic reticulum trafficking signals by combinatorial screening in mammalian cells. *Proceedings of the National Academy of Sciences of the United States of America* **98**, 2431–2436 (2001).

525. D'amour, F. E. & Smith, D. L. *A METhOD FOR DETERMINING LOSS OF PAIN SENSATION*.

526. BEN-BASSAT, J., PERETZ, E. & SULMAN, F. G. Analgesimetry and ranking of analgesic drugs by the receptacle method. *Archives internationales de pharmacodynamie et de therapie* **122**, 434–47 (1959).

527. JANSSEN, P. A., NIEMEGEERS, C. J. & DONY, J. G. The inhibitory effect of fentanyl and other morphine-like analgesics on the warm water induced tail withdrawl reflex in rats. *Arzneimittel-Forschung* **13**, 502–507 (1963).

528. Grotto, M. & Sulman, F. G. Modified receptacle method for animal analgesimetry. *Archives internationales de pharmacodynamie et de therapie* **165**, 152–9 (1967).

529. Faul, F., Erdfelder, E., Lang, A. G. & Buchner, A. G*Power 3: a flexible statistical power analysis program for the social, behavioral, and biomedical sciences. *Behavior research methods* **39**, 175–191 (2007).

530. Besnard, J. *et al.* Automated design of ligands to polypharmacological profiles. *Nature* **492**, 215–220 (2012).

531. Cunningham, C. L., Gremel, C. M. & Groblewski, P. A. Drug-induced conditioned place preference and aversion in mice. *Nature protocols* **1**, 1662–1670 (2006).

532. Harte, S. E., Meyers, J. B., Donahue, R. R., Taylor, B. K. & Morrow, T. J. Mechanical Conflict System: A Novel Operant Method for the Assessment of Nociceptive Behavior. *PloS one* **11**, (2016).

533. Gaffney, C. M., Muwanga, G., Shen, H., Tawfik, V. L. & Shepherd, A. J. Mechanical Conflict-Avoidance Assay to Measure Pain Behavior in Mice. *Journal of visualized experiments : JoVE* **2022**, (2022).

534. Van Steenwinckel, J. *et al.* Role of spinal serotonin 5-HT2A receptor in 2',3'-dideoxycytidine-induced neuropathic pain in the rat and the mouse. *Pain* **137**, 66–80 (2008).

535. Matos, R. *et al.* Bladder pain induced by prolonged peripheral alpha 1A adrenoceptor stimulation involves the enhancement of transient receptor potential vanilloid 1 activity and an increase of urothelial adenosine triphosphate release. *Acta Physiologica* **218**, 265–275 (2016).

536. Wouters, M. M. *et al.* Histamine Receptor H1-Mediated Sensitization of TRPV1 Mediates Visceral Hypersensitivity and Symptoms in Patients With Irritable Bowel Syndrome. *Gastroenterology* **150**, 875-887.e9 (2016).

537. Puente, B. de la *et al.* Sigma-1 receptors regulate activity-induced spinal sensitization and neuropathic pain after peripheral nerve injury. *Pain* **145**, 294–303 (2009).

538. Oyola, M. G. & Handa, R. J. Hypothalamic-pituitary-adrenal and hypothalamic-pituitary-gonadal axes: sex differences in regulation of stress responsivity. *Stress (Amsterdam, Netherlands)* **20**, 476–494 (2017).

539. Bale, T. L. & Epperson, C. N. Sex differences and stress across the lifespan. *Nature neuroscience* **18**, 1413–1420 (2015).

540. Viau, V. & Meaney, M. J. Variations in the hypothalamic-pituitary-adrenal response to stress during the estrous cycle in the rat. *Endocrinology* **129**, 2503–2511 (1991).

541. Perez-Castro, C., Renner, U., Haedo, M. R., Stalla, G. K. & Arzt, E. Cellular and molecular specificity of pituitary gland physiology. *Physiological reviews* **92**, 1–38 (2012).

542. Young, E. A. Sex differences in response to exogenous corticosterone: a rat model of hypercortisolemia. *Molecular psychiatry* **1**, 313–319 (1996).

543. Figueiredo, H. F., Dolgas, C. M. & Herman, J. P. Stress activation of cortex and hippocampus is modulated by sex and stage of estrus. *Endocrinology* **143**, 2534–2540 (2002).

544. Lovick, T. A. & Zangrossi, H. Effect of Estrous Cycle on Behavior of Females in Rodent Tests of Anxiety. *Front Psychiatry* **12**, 1492 (2021).

545. Kato, R. & Kamataki, T. Cytochrome P-450 as a determinant of sex difference of drug metabolism in the rat. *Xenobiotica; the fate of foreign compounds in biological systems* **12**, 787–800 (1982).

546. Kato, R., Yamazoe, Y., Shimada, M., Murayama, N. & Kamataki, T. Effect of growth hormone and ectopic transplantation of pituitary gland on sex-specific forms of cytochrome P-450 and testosterone and drug oxidations in rat liver. *Journal of biochemistry* **100**, 895–902 (1986).

547. Kato, R. & Yamazoe, Y. Sex-specific cytochrome P450 as a cause of sex- and species-related differences in drug toxicity. *Toxicology letters* **64-65 Spec No**, 661–667 (1992).

548. Fillingim, R. B., Edwards, R. R. & Powell, T. The relationship of sex and clinical pain to experimental pain responses. *Pain* **83**, 419–425 (1999).

549. Mogil, J. S. Sex differences in pain and pain inhibition: multiple explanations of a controversial phenomenon. (2012) doi:10.1038/nrn3360.

550. Greenspan, J. D. *et al.* Studying sex and gender differences in pain and analgesia: a consensus report. *Pain* **132 Suppl 1**, (2007).

551. Hurley, R. W. & Adams, M. C. B. Sex, gender, and pain: an overview of a complex field. *Anesthesia and analgesia* **107**, 309–317 (2008).

552. Ektor-Andersen, J., Janzon, L. & Sjolund, B. Chronic pain and the sociodemographic environment: results from the Pain Clinic at Malmö General Hospital in Sweden. *The Clinical journal of pain* **9**, 183–188 (1993).

553. Craft, R. M., Mogil, J. S. & Maria Aloisi, A. Sex differences in pain and analgesia: The role of gonadal hormones. *European Journal of Pain* **8**, 397–411 (2004).

554. Tall, J. M. & Crisp, T. Effects of gender and gonadal hormones on nociceptive responses to intraplantar carrageenan in the rat. *Neuroscience Letters* **354**, 239–241 (2004).

555. Clemente, J. T., Parada, C. A., Veiga, M. C. A., Gear, R. W. & Tambeli, C. H. Sexual dimorphism in the antinociception mediated by kappa opioid receptors in the rat temporomandibular joint. *Neuroscience letters* **372**, 250–255 (2004).

556. Berglund, L. A., Derendorf, H. & Simpkin, J. W. Desensitization of brain opiate receptor mechanisms by gonadal steroid treatments that stimulate luteinizing hormone secretion. *Endocrinology* **122**, 2718–2726 (1988).

557. Cui, Y. *et al.* Forebrain NR2B overexpression facilitating the prefrontal cortex long-term potentiation and enhancing working memory function in mice. *PloS one* **6**, (2011).

558. Jacobs, S. A. & Tsien, J. Z. genetic overexpression of NR2B subunit enhances social recognition memory for different strains and species. *PloS one* **7**, (2012).

559. Rasmussen, K., Beitner-Johnson, D. B., Krystal, J. H., Aghajanian, G. K. & Nestler, E. J. Opiate withdrawal and the rat locus coeruleus: behavioral, electrophysiological, and biochemical correlates. *The Journal of neuroscience : the official journal of the Society for Neuroscience* **10**, 2308–2317 (1990).

560. Rasmussen, K. & Aghajanian, G. K. Withdrawal-induced activation of locus coeruleus neurons in opiate-dependent rats: attenuation by lesions of the nucleus paragigantocellularis. *Brain research* **505**, 346–350 (1989).

561. Aghajanian, G. K., Kogan, J. H. & Moghaddam, B. Opiate withdrawal increases glutamate and aspartate efflux in the locus coeruleus: an in vivo microdialysis study. *Brain research* **636**, 126–130 (1994).

562. Zhang, T., Feng, Y., Rockhold, R. W. & Ho, I. K. Naloxone-precipitated morphine withdrawal increases pontine glutamate levels in the rat. *Life sciences* **55**, (1994).

563. Koyuncuoğlu, H., Güngör, M., Sağduyu, H. & Aricioğlu, F. Suppression by ketamine and dextromethorphan of precipitated abstinence syndrome in rats. *Pharmacology, biochemistry, and behavior* **35**, 829–832 (1990).

564. Tokuyama, S., Wakabayashi, H. & Ho, I. K. Direct evidence for a role of glutamate in the expression of the opioid withdrawal syndrome. *European journal of pharmacology* **295**, 123–129 (1996).

565. Tanganelli, S., Antonelli, T., Morari, M., Bianchi, C. & Beani, L. Glutamate antagonists prevent morphine withdrawal in mice and guinea pigs. *Neuroscience letters* **122**, 270–272 (1991).

566. Liu, Z. *et al.* A Conantokin Peptide Con-T[M8Q] Inhibits Morphine Dependence with High Potency and Low Side Effects. *Marine drugs* **19**, (2021).

567. Bertino, M. *et al.* A small dose of morphine increases intake of and preference for isotonic saline among rats. *Pharmacology, biochemistry, and behavior* **29**, 617–623 (1988).

568. Alaghband, Y. & Marshall, J. F. Common influences of non-competitive NMDA receptor antagonists on the consolidation and reconsolidation of cocaine-cue memory. *Psychopharmacology* **226**, 707–719 (2013).

569. Shen, H., Moussawi, K., Zhou, W., Toda, S. & Kalivas, P. W. Heroin relapse requires long-term potentiation-like plasticity mediated by NMDA2b-containing receptors. *Proceedings of the National Academy of Sciences of the United States of America* **108**, 19407–19412 (2011).

570. Bai, Y., Ouyang, S.-L., Bai, Y.-J. & Wu, D.-H. Treatment for Persistent Somatoform Pain Disorder via Electroacupuncture and a Low Dosage of Fluoxetine Hydrochloride. *Integr Med* **16**, 28–31 (2017).

571. Ho, P. T., Li, C. F., Ng, Y. K., Tsui, S. L. & Ng, K. F. J. Prevalence of and factors associated with psychiatric morbidity in chronic pain patients. *Journal of psychosomatic research* **70**, 541–547 (2011).